THE *EX VIVO* ANALYSIS OF THE EFFECTS OF ENVIRONMENTAL METAL POLLUTANTS ON ERYTHROCYTES

CORNELIA PETRONELLA UYS

UNIVERSITEIT VAN PRETORIA
UNIVERSITY OF PRETORIA
YUNIBESITHI YA PRETORIA

THE *EX VIVO* ANALYSIS OF THE EFFECTS OF ENVIRONMENTAL METAL POLLUTANTS ON ERYTHROCYTES

by

CORNELIA PETRONELLA UYS

Submitted in partial fulfilment of the requirements for the degree

MASTER OF SCIENCE

in the

FACULTY OF HEALTH SCIENCES

Department of Anatomy

University of Pretoria

2016

THE *EX VIVO* ANALYSIS OF THE EFFECTS OF ENVIRONMENTAL METAL POLLUTANTS ON ERYTHROCYTES

by

Cornelia Petronella Uys

Supervisor: Prof MJ Bester
Co-supervisor: Dr HM Oberholzer
Department: Anatomy
Degree: MSc (Anatomy) with specialisation in Human Cell Biology

Abstract

Mining and energy generation, through the burning of coal, are the main anthropogenic activities in South Africa which leads to heavy metal pollution. Eight metals relevant to metal pollution in South Africa were identified. These metals are cadmium (Cd), cobalt (Co), chromium (Cr), copper (Cu), manganese (Mn), nickel (Ni), lead (Pb), and mercury (Hg). In the scientific literature, the effects and mechanisms of toxicity of single metals and several double metal combinations are well described. However there is a lack of information on the effects of triple metal combinations. The aim of this study was to determine the toxic effects of metal combinations related to direct toxicity and oxidative effects in *ex vivo* human erythrocytes.

The *ex vivo* haemolysis assay was used to determine the total toxicity of each metal alone and in double and triple combinations. It was found that from most to least toxic the metals can be ordered as follows: Hg >> Co > Cu > Pb > Mn > Cd > Ni. The effect of Cr could not be determined due to its inherent absorbance at 570 nm. Evaluated at a concentration that caused 10% haemolysis, the combination of Cd:Co:Hg had the highest model deviation ration (MDR) of

2.864 indicating a synergistic toxic effect. An antagonistic effect was observed for several metal combinations with the strongest effect found, with a MDR of 0.399, for Cd:Cu:Ni.

Toxicity can be a consequence of oxidative damage and therefore the ability of each metal alone and in double and triple combinations to cause reduced glutathione (GSH) depletion (via direct binding), catalyse the Fenton reaction (hydroxyl radical averting capacity (HORAC) assay), malondialdehyde formation (thiobarbituric acid reactive substances (TBARS) formation) and cause reactive oxygen species (ROS) formation (2',7'-Dichlorodihydrofluorescein diacetate (DCFH-DA) assay) was investigated.

Cu and Hg strongly bound GSH and effectively catalysed the Fenton reaction. For both assays, observed effects were not synergistic although some metal combinations showed an antagonistic effect.

Within a cellular environment, MDA formation and reactive oxygen species formation (DCFH-DA assay) in erythrocytes was the highest for Cu and Hg. Using the DCFH-DA assay a strong synergistic- and antagonistic effect was observed for the combination Ni:Mn:Hg (MDR = 2.964) and Co:Cr:Ni (MDR =-0.036) respectively. Regarding MDA formation, the synergistic effect was the highest for the Cu:Mn:Pb combination (MDR = 4.990) while for the combination Cd:Cr:Pb (MDR= 0.402) the observed effect was antagonistic.
Reduced glutathione depletion was found to be the highest after exposure to the combination of Cu:Pb:Hg. The combination of Co:Cu:Hg formed the most hydroxyl radicals according to the HORAC assay. Lastly the combination of Cu:Mn:Hg caused the most ROS formation of all combinations according to the DCFH-DA assay.

The metal combinations found in each assay as having one of the highest effect values did show some correlation between the different assays. Only one of these combinations, the combination of Cu:Mn:Pb did however have a high reading in four of the five assays used. It caused more than 15% haemolysis, more than 80% reduced glutathione depletion, high levels of lipid peroxidation as well as ROS formation.

Declaration

I, Cornelia Uys, declare that this research dissertation, which I hereby submit for the degree MSc Anatomy (with specialisation in Human Cell Biology) is my own work and has not previously been submitted for degree purposes at this or any other tertiary institution.

Signed……

Date……

Department of Anatomy, School of Medicine, Faculty of Health Sciences,
University of Pretoria

South Africa

Acknowledgements

"Nie aan ons, o HERE, nie aan ons nie, maar aan u Naam gee eer, om u goedertierenheid, om u trou ontwil." Psalms 115:1

I wish to express my gratitude to the Department of Anatomy for providing me with the necessary facilities for this study and for the support of the personnel with regards to this study.

I am grateful to my supervisor, Prof MJ Bester and co-supervisor, Dr HM Oberholzer, as well as the other personnel in the Department for sharing their expertise in research methodologies as well as laboratory techniques.

I would like to extend my gratitude to my mother, for her guidance and unwavering support and to my husband for his unceasing encouragement.

Lastly I would like to thank my family and friends for their continuous support.

Table of Contents

List of Tables

List of Figures

List of Abbreviations and Chemical Formulae

%	Percentage
µM	Micromolar
A	
ADME	Absorption, distribution, metabolism, and excretion
Ag	Silver
Al	Aluminium
As	Arsenic
B	
BPG	2,3-bisphosphoglycerate
C	
Ca	Calcium
Cd	Cadmium
Cd:Co	Cadmium and cobalt
Cd:Co:Cr	Cadmium, cobalt and chromium
Cd:Co:Cu	Cadmium, cobalt and copper
Cd:Co:Hg	Cadmium, cobalt and mercury
Cd:Co:Mn	Cadmium, cobalt and manganese
Cd:Co:Ni	Cadmium, cobalt and nickel
Cd:Co:Pb	Cadmium, cobalt and lead
Cd:Cr	Cadmium and chromium
Cd:Cr:Cu	Cadmium, chromium and copper
Cd:Cr:Hg	Cadmium, chromium and mercury
Cd:Cr:Mn	Cadmium, chromium and manganese
Cd:Cr:Ni	Cadmium, chromium and nickel
Cd:Cr:Pb	Cadmium, chromium and lead
Cd:Cu	Cadmium and copper
Cd:Cu:Hg	Cadmium, copper and mercury
Cd:Cu:Mn	Cadmium, copper and manganese
Cd:Cu:Ni	Cadmium, copper and nickel
Cd:Cu:Pb	Cadmium, copper and lead
Cd:Hg	Cadmium and mercury
Cd:Mn	Cadmium and manganese
Cd:Mn:Hg	Cadmium, manganese and mercury
Cd:Mn:Ni	Cadmium, manganese and nickel
Cd:Mn:Pb	Cadmium, manganese and lead
Cd:Ni	Cadmium and nickel
Cd:Ni:Hg	Cadmium, nickel and mercury
Cd:Ni:Pb	Cadmium, nickel and lead
Cd:Pb	Cadmium and lead
Cd:Pb:Hg	Cadmium, lead and mercury
Cd^{2+}	Cadmium ion
$CdCl_2$	Cadmium chloride
$(CH_3COO)_2Pb$	Lead acetate
Cl^-	Chloride ion
Co	Cobalt
Co:Cr	Cobalt and chromium
Co:Cr:Cu	Cobalt, chromium and copper

Co:Cr:Hg	Cobalt, chromium and mercury
Co:Cr:Mn	Cobalt, chromium and manganese
Co:Cr:Ni	Cobalt, chromium and nickel
Co:Cr:Pb	Cobalt, chromium and lead
Co:Cu	Cobalt and copper
Co:Cu:Hg	Cobalt, copper and mercury
Co:Cu:Mn	Cobalt, copper and manganese
Co:Cu:Ni	Cobalt, copper and nickel
Co:Cu:Pb	Cobalt, copper and lead
Co:Hg	Cobalt and mercury
Co:Mn	Cobalt and manganese
Co:Mn:Hg	Cobalt, manganese and mercury
Co:Mn:Ni	Cobalt, manganese and nickel
Co:Mn:Pb	Cobalt, manganese and lead
Co:Ni	Cobalt and nickel
Co:Ni:Hg	Cobalt, nickel and mercury
Co:Ni:Pb	Cobalt, nickel and lead
Co:Pb	Cobalt and lead
Co:Pb:Hg	Cobalt, lead and mercury
Co^{2+}	Cobalt ion
$CO_3^{\bullet -}$	Carbonate anion radical
$CoCl_2$	Cobalt(II) chloride
Cr	Chromium
Cr:Cu	Chromium and copper
Cr:Cu:Hg	Chromium, copper and mercury
Cr:Cu:Mn	Chromium, copper and manganese
Cr:Cu:Ni	Chromium, copper and nickel
Cr:Cu:Pb	Chromium, copper and lead
Cr:Hg	Chromium and mercury
Cr:Mn	Chromium and manganese
Cr:Mn:Hg	Chromium,manganese and mercury
Cr:Mn:Ni	Chromium, manganese and nickel
Cr:Mn:Pb	Chromium, manganese and lead
Cr:Ni	Chromium and nickel
Cr:Ni:Hg	Chromium, nickel and mercury
Cr:Ni:Pb	Chromium, nickel and lead
Cr:Pb	Chromium and lead
Cr:Pb:Hg	Chromium, lead and mercury
Cr^{3+}	Chromium ion
Cu	Copper
Cu:Hg	Copper and mercury
Cu:Mn	Copper and manganese
Cu:Mn:Hg	Copper, manganese and mercury
Cu:Mn:Ni	Copper, manganese and nickel
Cu:Mn:Pb	Copper, manganese and lead
Cu:Ni	Copper and nickel
Cu:Ni:Hg	Copper, nickel and mercury
Cu:Ni:Pb	Copper, nickel and lead
Cu:Pb	Copper and lead
Cu:Pb:Hg	Copper, lead and mercury
Cu^{2+}	Copper ion
$CuSO_4$	Copper(II) sulfate
Cys	Cysteine

D

DCF	Dichlorofluorescein
DCFH	Dichlorodihydrofluorescein
DCFH-DA	2',7'-Dichlorodihydrofluorescein diacetate / 2'7'-Dichlorofluorescin diacetate
DMT1	Divalent metal transporter 1
DNA	Deoxyribonucleic acid
DTNB	5.5-Dithiobis(2-nitrobenzoic acid) (Ellman's reagent)

F

Fe	Iron

G

GPx	Glutathione peroxidase
$GS^{\bullet}$	Glutathione-thiyl radical
GSH	Reduced glutathione
GSSG	Glutathione disulfide (oxidised)

H

H_2O	Water
H_2O_2	Hydrogen peroxide
Hb	Haemoglobin
HCl	Hydrochloric acid
Hg	Mercury
Hg^{2+}	Mercury ion
$HgCl_2$	Mercuric chloride
HOCl	Hypochlorous acid
HORAC	Hydroxyl radical averting capacity

I

IsoPBS	Isotonic phosphate buffered saline

K

K	Potassium
$K_3Fe^{3+}(CN)_6$	Potassium ferricyanide
$K_4Fe^{2+}(CN)_6$	Potassium ferrocyanide
KCl	Potassium chloride
KCN	Potassium cyanide
$KCr(SO_4)_2$	Chromium potassium sulfate

L

LASEC	Scientific Laboratory Equipment Company
LOOH	Lipid hydroperoxides

M

MDA	Malondialdehyde
MDR	Model deviation ratio
Min	Minute
mM	Millimolar
Mn	Manganese
Mn:Hg	Manganese and mercury
Mn:Ni	Manganese and nickel
Mn:Ni:Hg	Manganese, nickel and mercury

Mn:Ni:Pb	Manganese, nickel and lead
Mn:Pb	Manganese and lead
Mn:Pb:Hg	Manganese, lead and mercury
Mn^{2+}	Manganese ion
$MnCl_2$	Manganese(II) chloride
MnO_2	Manganese dioxide
Mn_3O_4	Manganese (II, III) oxide
MT	Metallothionein

N

NaCl	Sodium chloride
NADPH	Nicotinamide adenine dinucleotide phosphate
$Na_2HPO_4•2H_2O$	Sodium phosphate dibasic dehydrate
NaH_2PO_4	Sodium phosphate
$NaHCO_3$	Sodium bicarbonate
Ni	Nickel
Ni:Hg	Nickel and mercury
Ni:Pb	Nickel and lead
Ni:Pb:Hg	Nickel, lead and mercury
Ni^{2+}	Nickel ion
$NiCl_2$	Nickel(II) chloride
nm	Nanometre
nM	Nanomolar
$NO•$	Nitroxyl radical
$NO_2•$	Nitrogen dioxide radical

O

O_2	Oxygen
$O_2•^-$	Superoxide radical
$OH•$	Hydroxyl radical

P

Pb	Lead
Pb:Hg	Lead and mercury
Pb^{2+}	Lead ion
PGM	Platinum group metals

R

$R•$	Free radical
RBC	Red blood cell
RFU	Relevant fluorescent units
RH	Polyunsaturated fatty acid chain
$RO•$	Alkoxyl radical
$ROO•$	Peroxyl radicals
ROOH	Organic hydroperoxides
ROS	Reactive oxygen species
RSH	Thiol

S

SA	South Africa
SEM	Standard error of the mean
SH	Thiol

T

TBA	Thiobarbituric acid
TBARS	Thiobarbituric acid reactive substances
TWQR	Target Water Quality Range

U

U	Uranium

V

v/v	Volume to volume
vs.	Versus

W

WHO	World Health Organisation
w/v	Weight to volume

X

X•	Free radical
x g	Relative centrifugal force

Z

Zn	Zinc

Chapter 1: Introduction

Heavy metals occur naturally in soil and groundwater. Human activity has however led to an increase in these natural levels (Awofolu *et al*. 2005). South Africa (SA) is a highly industrialised country with increasing anthropogenic activity. The increase in heavy metal levels in certain areas that has resulted from this activity is reason for concern (Coetzee 2004). According to a study done by Coetzee (2004), the mean levels of heavy metals, including cobalt (Co), zinc (Zn), arsenic (As), cadmium (Cd) and uranium (U), but especially Cd and U in the Wonderfonteinspruit catchment are of concern, seeing that these levels are higher than the natural background concentrations, as well as regulatory levels. Herselman (2007) found that cadmium (Cd), cobalt (Co), chromium (Cr), copper (Cu), lead (Pb), zinc (Zn), and nickel (Ni) are of importance in South-Africa due to their natural geological occurrence.

Agriculture, transport, mining and related operations are the main anthropogenic sources increasing the heavy metal levels in SA (Al-Attar 2011). These increased levels of heavy metals have a direct effect on irrigated crops and hence an indirect effect on the rural people in the affected area via food intake. Heavy metals can be absorbed through the skin, orally or through inhalation, (Awofolu *et al*. 2005) from air, food, water, as well as medical devices such as hip and knee replacements and dental amalgam fillings (Nordberg *et al.* 2007). The degree of heavy metal toxicity depends on dose, duration, route of administration and other physiological factors, especially nutrition (Al-Attar 2011).

In SA heavy metal exposure of concern in the general environment is mostly through the ingestion of contaminated water; be it by drinking the water, preparing food in it or using it for irrigation of crops (Awofolu *et al*. 2005). The water in the Tyume River in the Eastern Cape Province, as well as the Wonderfontein catchment in South Africa is used for domestic as well as irrigative purposes and the effect on the people by the mixtures of metals they consume daily is unknown. Additional sources of heavy metal exposure include exhaust fumes, (Street *et al*. 2008) smoking, (Whitfield *et al*. 2010) and contamination of medicinal plants either deliberate (Singh *et al*. 2011; Ndhlala *et al*. 2011) or through contaminated water sources (Awofolu *et al*. 2005). Regarding the latter, a study done by Street *et al.* (2008) found that samples of top-selling medicinal bulbs obtained from street markets exceeded the World Health Organization's limits for As and Cd. Other plant samples showed relatively high concentrations of As, Co, Pb, Ni as well as Cd (Street *et al*. 2008).

Heavy metals have unique toxic effects. One of these effects is oxidative stress which can be caused by decreased levels of superoxide dismutase, catalase, and glutathione, as well as an increased production of reactive oxygen species (Kowalczyk *et al*. 2002). Calcium regulation can also be affected and this can lead to cell death activation and injury of biological systems (Awofolu *et al*. 2005).

Oxidative cellular damage is also induced by the Fenton reaction, whereby hydrogen peroxide (H_2O_2) is decomposed to form hydroxyl radicals. Cu, Cr, Co and Ni are known catalysts of the Fenton reaction (Benedet & Shibamoto 2008). Mercury (Hg), Pb and Cd cause oxidative stress by indirectly causing the formation of reactive radical species or by depleting the natural antioxidant mechanisms, particularly thiol-containing antioxidants and enzymes (Al-Attar 2011; Valko *et al*. 2005). This cellular damage is associated with diseases such as atherosclerosis, diabetes, rheumatoid arthritis, cardiovascular disease and coronary artery disease (Dalle-Donne *et al*. 2006).

The toxicity of individual metals is well described in literature and the biochemical effects found in cell, animal and human studies are presented in Table 1.1.

Humans are most likely exposed to a mixture of metals and the interaction/s between these mixtures of metals is important to consider. These interaction/s can cause additive, synergistic or antagonistic effects which can be manifested as e.g. cellular toxicity (Nordberg *et al*., 2007a). In a literature review done by Nordberg in 2007 it was found that there is a lack of direct primary data on the interactions among toxic or essential elements (Nordberg *et al*., 2007a). This dissertation attempts to address this lack of primary data on metal interactions and their effect at cellular level.

To be able to study these combinational effects a simple *ex vivo* model system that allows the rapid screening of many metal combinations was developed, used, and verified. For this purpose the human erythrocyte was used, seeing that these cells are readily available, many metals and metal combinations can be tested on a single sample, and several parameters can be measured and evaluated. The study presented entails both an investigation of the haemolytic effect of heavy metal combinations and an investigation of the oxidative effect of these combinations on erythrocytes.

Table 1.1: Single metal intracellular effects in cell, animal, and human studies.

	Cd	Co	Cr	Cu	Pb	Mn	Ni	Hg
Fenton reaction	-	√ [1]	√ [1]	√ [1]	-	-	√ [1]	-
Lipid peroxidation	√ [1 2]	-	√ [2]	√ [3]	√ [4]	√ [5]	√ [1]	√ [1]
Anaemia	√ [6]	-	√ [7]	√ [8]	√ [9]	-	√ [10]	√ [11]
Reduced glutathione	↓ [1]	-	↓ [1]	↓ [1]	↓ [4]	↓ [5]	↓ [1]	↓ [1]
Catalase	↓ [12]	-	↓ [13]	-	↓ [14]	↓ [5]	↓ [1]	↓ [1]
Superoxide dismutase	↕ [1, 12]	-	↓ [1]	-	↓ [14]	↓ [5]	↓ [15]	↓ [1]
GPx	↕ [12]	-	↓ [1]	-	↓ [14]	↓ [5]	↓ [1]	↓ [1]
Apoptosis	√ [12]	√ [16]	√ [16]	-	√ [17]	√ [18]	-	√ [19]
Blood coagulation	↑ [20]	↓ [21]	↓ [22]	-	↑ [23]	-	-	↑ [24]
WHO limit	3 µg/l [25]	40 µg/l [26]	50 µg/l [27]	2 mg/l [27]	10 µg/l [27]	500µg/l [27]	20 µg/l [27]	1 µg/l [27]
WHO limit (molarity)	0.03 µM	0.68 µM	0.96 µM	31.47µM	0.05 µM	9.1 µM	0.34 µM	0.004µM
SA limit	5 µg/l [28]		100µg/l [27]	1 mg/l [27]	20 µg/l [27]	100µg/l [27]	150µg/l [27]	1 µg/l [27]

1 - Valko *et al*., 2005
2 - Benedet & Shibamoto 2008
3 - Rana 2008
4 - Ahamed & Siddiqui 2007
5 - Chtourou *et al*., 2010
6 - Nordberg, Fowler, *et al*., 2007
7 - Wilbur, *et al*., 2008
8 - Dorsey *et al*., 2004
9 - Baranowska-Bosiacka & Hlynczak 2003
10 - Das *et al*., 2007
11 - Lessler & Walters 1973
12 - Bertin & Averbeck 2006
13 - Kalahasthi *et al*., 2006
14 - Hunaiti & Soud 2000
15 - Pari & Amudha 2011
16 - Catelas *et al*., 2007
17 - Yedjou *et al*., 2010
18 - Hirata 2002
19 - Eisele *et al*., 2006
20 - Koçak & Akçil 2006
21 - Smith & Smith 1984
22 - Kattlove & Spaet 1970
23 - Shin, *et al*., 2007
24 - Nakayama, *et al*., 2002
25 - Fawell J, *et al*,. 2011
26 - Kazi TG, *et al*., 2009
27 - Mamba *et al., 2008*
28 - Okonkwo & Mothiba 2005

Key: √ - does occur; ↕ - increases at low concentrations, but decreases at high concentrations; ↓- decrease; ↑-increase.

Chapter 2: Literature Review

2.1 Heavy metal industry in South Africa

South Africa (SA) is still one of the world's leading mining and mineral-processing countries. Mined metals and processed minerals include platinum, kyanite, chromium, palladium, vermiculite, aluminium, antimony, iron ore, as well as platinum group metals (PGM), which includes hafnium, zirconium, vanadium, manganese, rutile, fluorspar, phosphate rock, ilmenite, nickel, and gold (Yager 2008). The effects of mining on the environment include the release of many chemical contaminants into water resources. It can also cause environmental damage that can persist even after mine closure. These environmental effects often compromise the health and safety of nearby communities. The closure of gold mines leads to acid mine drainage, and the coal and platinum mining sectors also impose severe consumptive demands on available water resources (Hobbs 2010).

Different regions of SA contain specific metals and minerals. The Witwatersrand Basin contains considerable resources of uranium, silver, pyrite and osmiridium and yields approximately 94% of South Africa's gold output. Cu, Ni and Co mineralisation is associated with the platinum group metals in the Bushveld Complex. This Complex also contains Cr and vanadium-bearing titanium iron-ore formations as well as large deposits of industrial minerals, including fluorspar and andalusite. The Transvaal Supergroup contains manganese and iron ore. The Karoo Basin, extending through Mpumalanga, Kwazulu-Natal, Free State and Limpopo contains bituminous coal and anthracite resources. Deposits of Cu, phosphate, titanium, vermiculite, feldspar and zirconium ores are found in the Phalaborwa Igneous complex. Cu and silver associated lead-zinc ore deposits are found in the Northern Cape near Aggeneys (Burger 2010/11).

In SA, mining is the single industry sector with the largest water quality impact (by volume). The correlation between active mines, industrialised areas, and endangered freshwater ecosystems can clearly be seen in Figure 1. Almost all of South Africa's fresh water resources have been allocated for existing uses and the quality of most water resources are declining due to urbanization, acid mine drainage, inflows of treated and untreated sewage, deforestation, agricultural return flows, and energy use (Oberholster *et al*. 2010).

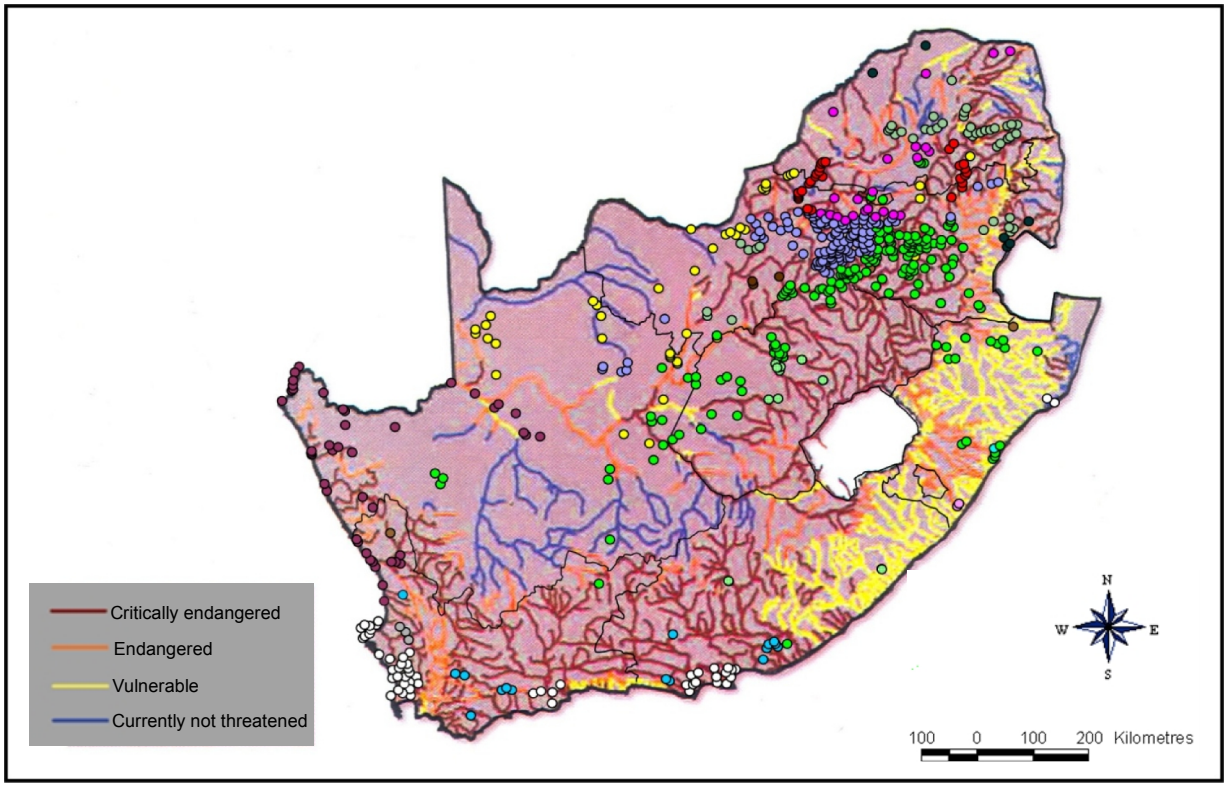

Figure 2.1: Conservation status of South Africa's freshwater ecosystems in relation to active mines and industrialised areas near the coast, in Gauteng, and Limpopo – different mine groups indicated with different coloured circles (Adapted from: Nel 2010; Vorster 2002).

As early as 1987 the US Environmental Protection Agency recognised that "…problems related to mining waste may be rated as second only to global warming and stratospheric ozone depletion in terms of ecological risk. True to this, the release to the environment of mining waste can result in profound, generally irreversible destruction of ecosystems" (Hobbs 2010). Decrease in water pH, increase in salinity, increase in metal content, and increase in sediment load, is some of the effects of mining. The polluted groundwater discharging into streams in the mining areas around Johannesburg contributes to 20% of the stream flow (Naicker *et al.* 2003). Naicker *et al*. (2003) found that the effects of the contaminated water from the mines can persist for more than 10 km beyond the source.

Industrial pollution contributes to decreased water quality due to pollution with poisonous and hazardous chemicals and -nutrients as well as increased salinity and sediments. This pollution mainly leads to salinisation - typical pollutants include heavy metals, dyes, chemicals, high organic compounds, brine and sewage sludge (Oelofse 2010). The burning of fossil fuels causes the release of metal particles such as Cr, Co, Ni, Cu, Zn and Pb into the air. Vapours and gases of metallic compounds are usually insoluble in water causing these compounds to

reach the alveoli and thus crossing the air-blood barrier of humans and animals via inhalation (Nordberg *et al.* 2007).

Lowering of pH over time due to human-induced acidification - from industrial effluents, mine drainage and acid rain - results in the deterioration of water quality (Oberholster *et al*. 2010), and the degradation of soil quality and aquatic habitats (Hobbs 2010). This also leads to the mobilization of elements due to increased solubility of trace metals in sediments (Oberholster 2010). These metals include iron (Fe), aluminium (Al), Cd, Co, Cu, Hg, manganese (Mn), Ni, Pb, and Zn which can accumulate in fruits and crops (Oberholster *et al*. 2010).

Toxicity is a function of dosage and duration of exposure. Infants and children are the most vulnerable to these toxic effects. It is important to note that children (up to the age of 12) have a higher rate of intake than adults: twofold for air, threefold for water and six fold for food (Nordberg *et al.* 2007). The symptoms related to direct toxicity due to over dosage are easily identifiable, but the effect of long term exposure to low levels of a mixture of heavy metals is unknown.

2.2 Metabolism of heavy metals

In order to evaluate the effect of heavy metals and heavy metal combinations on the human body, it is necessary to consider the possible reactions that might occur. Different metals bind to different proteins in the body, for example, Cd binds to metallothionein (MT). Metallothioneins are low molecular weight, cysteine (Cys) rich, intracellular proteins that can bind to metals, including Cd, Zn, Pb and Hg. It can however integrate more than one metal – 7 divalent metal atoms or 12 monovalent atoms – thereby playing an important role in the detoxification of toxic metals as well as the essential metal metabolism. The binding of Cd to MT makes the excretion of Cd through urine possible, but this excreted Cd is toxic to the renal tubules (Nordberg *et al.* 2007).

Up to 99% of Cd and Hg are bound to protein (Nordberg *et al*. 2007) whereas Pb and Cd are transported into erythrocytes through an anion exchanger. Transport proteins play a role in the uptake of nonessential metals seeing that these metals can act as molecular mimics due to the resemblance to essential metals (Nordberg *et al*. 2007). Transferrin is involved in the cellular uptake of Fe and can theoretically also transport nonessential metals resembling Fe. After receptor-mediated endocytosis of transferrin-bound-Fe, Fe is released and passes out of the

endosome through the divalent metal transporter 1 (DMT1). DMT1 is also involved in the transferrin receptor's independent transport of Fe but DMT1 isn't specific and also transports Ni, Mn, Co, Cu, and Zn and these metals can then compete with Fe for entry into the cell (Nordberg *et al*. 2007).

Zn is an essential metal for various cellular processes. Certain nonspecific Zn transporters have also been shown to transport Mn, Cd, and Cu. Zn, Cu, Cd, Cr, and Pb have been found to mimic glutathione and are then transported by glutathione transporters. Chromate resembles sulfate, leading to the displacement of sulfate in its' specific transporters. Pb, Cd, Ni and other toxic metals also mimics calcium (Ca), entering the cells through Ca channels. The transport of the nonessential metals in all of these cases can lead to abnormal cellular functioning (Nordberg *et al*. 2007).

2.3 Heavy metals under investigation

2.3.1. Mercury (Hg)

Mercury pollution is associated with gold mining as well as coal combustion. SA is second only to China with regards to gold mining and more than 90% of the electricity generated in SA is from coal-fired power plants. Comparing mercury emissions per capita from coal-fired power plants between SA, Canada, China, Europe, Mexico, Poland, Russia, and the USA; SA ranks second. SA also ranks second to China with regards to mercury emissions to the environment (Oosthuizen *et al*. 2010). Table 2.1 summarises the health impact of Hg.

Table 2.1: Characteristics and health risks of Hg.

Natural occurrence:	☙ Mainly as mercuric sulfide (cinnabar ore), metallic mercury, mercuric chloride, and methylmercury
Anthropogenic occurrence:	☙ Mpumalanga, Witwatersrand, Free State, North West, Limpopo, Barberton
Uses:	☙ Small-scale mining (illegal in SA) ☙ 50% - chlorine-caustic soda manufacture; 50% - dental amalgams, mercury electronic switches, fluorescent lamps and other electronic devices
Absorption:	☙ Inhalation: 80% ☙ Ingestion: 2% ☙ Dermal: 0.8%
Effects of: ☙ Chronic exposure	Mercury vapour: Central nervous system – critical organ ☙ Weakness, fatigue, anorexia, loss of weight, disturbance of

	gastrointestinal functions ᔓ At higher exposure levels: mercurial tremors (fine trembling of muscles interrupted by coarse shaking movements every few minutes); mercurial erethism (severe behavioural and personality changes, increased excitability, loss of memory, insomnia, may develop into depression; in severe cases – delirium and hallucination) ᔓ Inflammatory changes to the gums with ptyalism (excessive flow of saliva – up to several litres per day) ᔓ Reduced peripheral nerve conduction velocity ᔓ Reduced colour vision ᔓ Changes in coordination ability, tremor, concentration capability, mood ᔓ Effects on foetal nerve growth Mercury vapour and mercuric mercury: ᔓ Glomerular renal injury, necrosis and damage of distal and middle portion of proximal tubules ᔓ Erythema, contact dermatitis ᔓ Impaired thyroid function
ᔓ Acute exposure	Mercury vapour: ᔓ Erosive bronchitis, bronchiolitis with interstitial pneumonitis ᔓ Effects on central nervous system: tremor, increased excitability. Mercuric salts: ᔓ Corrosive effect on mucous membranes of gastrointestinal tract – extensive precipitation of proteins ᔓ Gastric pain, vomiting ᔓ Abdominal pain, bloody diarrhoea, necrosis of intestinal mucosa – can lead to circulatory collapse and death ᔓ Renal failure – necrosis of proximal tubular epithelium
Total biological half-time	ᔓ 80% - 42-60 days

Compiled from: Hobbs 2010; Nordberg, Fowler, *et al*., 2007; Risher & DeWoskin 1999; Oosthuizen *et al.,* 2010

Mercury is released into the environment during combustion of fossil fuels, due to waste disposal as well as other industrial activities (Nordberg *et al*. 2007). Mercury vapour as well as mercury ions (Hg^{2+}) are emitted from coal-fired power plants. All forms of Hg cause toxic effects in humans (Nordberg *et al*. 2007). Hg^{2+} binds to SH-groups on proteins which can lead to a change in the normal tertiary and quaternary structure of these proteins as well as changing the binding properties of certain enzymes. This binding of Hg^{2+} also leads to modification and blocking of receptor binding, alteration in potassium (K)- or Ca-ion flow through the cell membrane's pores, and ionic channels which can affect the cell membrane potentials and intracellular and intercellular signals (Nordberg *et al*. 2007). Glutathione and MT binds to Hg^{2+} and can neutralise it as well as transport it in order for it to be eliminated (Nordberg *et al*. 2007).

In erythrocytes, Hg binds to the sulfhydryl groups on haemoglobin as well as to glutathione (Nordberg *et al*. 2007).

Gold mining is associated with an increase in Hg levels in nearby water sources. Hg exposure levels are reflected in the blood and urine levels (Nordberg *et al*. 2007). Low-level Hg exposure has been shown to cause cardiovascular and renal diseases (Whitfield *et al*. 2010). The kidney takes up and accumulates most of the mercuric ions from the blood (Nordberg *et al*. 2007). During ongoing exposure the major part of Hg in the blood can be found in erythrocytes. Hg has an especially high affinity for ectodermal and endodermal epithelial cells and glands. The organs with the longest retention times for Hg are the brain, kidneys, and testicles but Hg is also accumulated in the epithelial lining of the intestinal tract; in the squamous epithelium of the skin and hair; in glandular tissues like the salivary glands, thyroid, liver, pancreas, and the sweat glands; as well as the prostate (Nordberg *et al*. 2007).

Oxidative damage contributes to the development of cardiovascular disease. Hg causes the haemolysis of erythrocytes; reduction in erythrocyte, and haemoglobin (Hb) levels; and lipid peroxidation - a marker of oxidative damage (Brandão *et al*. 2008). At a cellular level Hg is an apoptogen, as it causes the activation of caspase-3 via oxidative activation of the death signalling pathways (Rana 2008). This leads to the inhibition of superoxide dismutase, catalase, as well as glutathione peroxidase (Brandão *et al*. 2008).

Hg has an affinity for sulphur and sulfhydryl groups leading to the binding of Hg to proteins in membranes and enzymes. This sulfhydryl group binding leads to interference with normal membrane structure and function as well as enzyme activity (Nordberg *et al*. 2007). Due to its high affinity for sulfhydryl groups ionic Hg binds to glutathione, cysteine, homocysteine, *N*-acetylcysteine, MT, as well as albumin (Nordberg *et al*. 2007). It is clear that exposure to Hg can cause severe damage and that the risk of being exposed is high in SA as a result of prevalent mining activity and the dependence on coal for electricity generation.

2.3.2 Cadmium (Cd)

The health risks associated with Cd is summarised in Table 2.2.

Table 2.2: Characteristics and health risks of Cd.

Natural occurrence:	☙ Naturally with zinc and lead in sulfide ores ☙ In the Northern Cape near Aggeneys ☙ The Transvaal Supergroup

Anthropogenic occurrence:	☙ Mpumalanga, Western Bushveld, Eastern Bushveld, Limpopo, Barberton, Okiep
Uses:	☙ Ni-Cd batteries ☙ Anticorrosive ☙ Electroplated onto steel ☙ Pigments in plastics
Absorption:	☙ Inhalation: 10-50% ☙ Ingestion: 4-14%
Effects of: ☙ Chronic exposure	☙ Group 1 IARC carcinogen ☙ Inhalation: Chronic inflammation of the nose, pharynx, larynx; olfactory disturbances. ☙ Inhalation: chronic obstructive lung disease, impaired pulmonary function, lung cancer ☙ Inhalation and gastrointestinal: proximal renal tubular reabsorptive dysfunction, anaemia, ☙ Gastrointestinal alone or combined with other routes of exposure: disturbance of Ca metabolism, osteoporosis, osteomalacia, Itai-Itai disease.
☙ Acute exposure	☙ Inhalation: Irritation, dryness of nose and throat, coughing, headaches, chills, fevers, chest pains. ☙ Inhalation: Pulmonary oedema, chemical pneumonitis. ☙ Ingestion: Acute gastrointestinal effects: diarrhoea, vomiting, abdominal pain.
Total biological half-time	☙ 10-30 years

Compiled from: Hobbs 2010; Nordberg *et al*. 2007; Faroon *et al*. 2008

The primary Cd exposure in humans is via inhalation of Cd fume and ingestion of Cd-containing food. Vegetables are the main carrier of Cd compounds when compared to other foods, because it is exposed to the most pollution in the natural environment (Kowalczyk *et al*. 2002). In natural water Cd is found mainly in bottom sediments and suspended particles; the concentration in the water phase is low. Concentrations in non-polluted natural waters are usually lower than 0.001 mg/L (Nordberg *et al*. 2007). In a study done by Awofolu *et al.* (2005) of the Tyume River water in the Eastern Cape province of SA mean Cd concentrations ranged from 0.03±0.002 to 0.044±0.003 mg/L. These Cd concentrations are higher than the tentative South African Target Water Quality Range (TWQR) guideline of 0 – 0.005 mg/l in river water for domestic use as well as crop irrigation and livestock watering (Awofolu *et al*. 2005).

The gastrointestinal absorption rate of Cd in an individual with Fe deficiency can be as high as 20% (Nordberg *et al*. 2007). Women often accumulate more Cd than men primarily because the menstrual cycle causes a decrease in Fe (Nordberg *et al*. 2007). Hamilton *et al.* (1978) found that in mice fed a low Fe diet Cd caused impaired Zn uptake. Low protein content in the diet

also leads to higher absorption of Cd and more severe signs of toxicity (Nordberg *et al*. 2007a). Indications were found that low intakes of calcium and other minerals, vitamin D and protein were contributing factors for Itai-Itai disease, a disease caused by chronic uptake of high levels of Cd. Cd interferes with the normal Ca metabolism in both the kidneys and bones of people which may increase the risk for Itai-Itai disease, a disease associated with osteoporosis (Nordberg *et al*. 2007). Acidification of soils results in the elevation of Cd levels in crops. Rice, wheat and vegetables take up Cd readily from polluted soil and irrigation water (Nordberg *et al*. 2007).

In a study done by Shaikh *et al*. (1999) oxidative stress intensification was observed after Cd administration. Cd indirectly affects the generation of various radicals, including superoxide and hydroxyl radical. It also generates H_2O_2 which in its turn can be a source of free radicals in the Fenton reaction (Benedet & Shibamoto 2008). Cd leads to a decrease in antioxidative elements e.g. superoxide dismutase, catalase and glutathione content and due to this there is an increased production of reactive oxygen species (ROS) (Kowalczyk *et al*. 2002). It also interferes with Ca regulation and through this induces cell death and injury in biological systems (Awofolu *et al*. 2005).

2.3.3 Lead (Pb)

Lead compounds are either organic or inorganic but organic lead compounds are metabolized into inorganic compounds (Nordberg *et al*. 2007), in this review only the inorganic lead compounds will be discussed seeing that they are biologically relevant (See Table 2.3).

Table 2.3: Characteristics and health risks of Pb.

Natural occurrence:	☙ Lead ore ☙ Northern Cape near Aggeneys
Anthropogenic occurrence:	☙ Mpumalanga
Uses:	☙ Batteries, pigment, ammunition, cable sheeting, in solders, alloys, weights, crystal, and as stabilizer in polyvinyl chloride (PVC)
Absorption:	☙ Inhalation: particles 0.01-5µm – 10-60% ☙ Ingestion: 4-21% ☙ Skin: ~0.06%
Effects of: ☙ Chronic exposure	☙ Affect central nervous system – causes irritability, hostility, anxiety, fatigue, tension, difficulties in concentrating. ☙ May damage peripheral nervous system – peripheral motor neuropathy with paralysis (“wrist drop” and “ankle drop”), lower

	exposures cause mild distal weakness in the upper limb as well as other sensory effects including tingling or numbness in arms or legs. ᔓ Affect autonomous nervous system ᔓ Affect auditory and visual functions ᔓ Anaemia ᔓ Malignant neoplasms; ᔓ Cause renal dysfunction characterised by glomerular and tubulointerstitial changes – causing hypertension, hyperuricemia and gout; chronic renal failure ᔓ Increase risk of coronary heart and cerebrovascular disease as well as strokes ᔓ May cause an increase in blood pressure ᔓ Cause low skeletal growth ᔓ Mutagenic ᔓ Increase risk of neural tube defects in foetus ᔓ Reduce foetal growth ᔓ Induce toxic effects on central nervous system of foetus, infants and children – causes impaired cognitive functioning
ᔓ Acute exposure	ᔓ Acute encephalopathy ᔓ Lead colic - protracted constipation, indigestion, loss of appetite, occasionally diarrhoea is present; vomiting
Total biological half-time	ᔓ Decades

Compiled from: Hobbs 2010; Nordberg *et al*. 2007; Abdin *et al*. 2007

In a study done by Okonkwo & Mothiba (2005) on the surface waters from the Dzindi, Madanzhe, and Mvudi rivers in Thohoyandou, SA, it was found that the concentration of Pb was higher than international guidelines and acceptable concentrations for Pb in drinking water.

The use of leaded gasoline (tetraethyl lead) has decreased, but is still, although minimally, used in SA. It gives rise to air pollution forming Pb-containing aerosols which is specifically a problem in cities and along highways. Pb is also used in paint and was present in high concentrations in exterior as well as interior paint. Even on toys up to 40% of the dry paints consisted of lead (Nordberg *et al*. 2007). The use of Pb in paint is regulated, but due to the fact that older paints contained high concentrations of Pb it still poses a serious health risk, especially to children. In a study done by Mathee *et al.* (2009) in the Johannesburg, Tshwane and Ekurhuleni (SA) municipalities it was found that paint on playground equipment is still Pb-based. Some 48% of the Pb measurements taken on the equipment were found to have concentrations higher than the internationally accepted reference levels (Mathee *et al.,* 2009). In older houses lead was also used in water pipes and fitting for water pipes causing a continuous release of lead into the water (Nordberg *et al*. 2007).

Of inhaled Pb 30-40% is absorbed in the bloodstream, however the gastrointestinal absorption is affected by the nutritional status and age of an individual (Patrick 2006). Gastrointestinal Pb absorption in adults range between 5-20% but in fasting individuals absorption was found to be as high as 70% (Nordberg *et al*. 2007). Pb uptake is the greatest in infants. They can ingest up to 50% of Pb from food, water, contaminated dust, and soil (Nordberg *et al*. 2007).

Fe deficiency as well as a diet low in Ca leads to an increased Pb absorption (Patrick 2006; Nordberg *et al*. 2007), whereas supplementation with Ca, magnesium, phosphate and dietary fat decreases Pb uptake (Patrick 2006). Patrick (2006) reports that 99% of absorbed Pb binds to erythrocytes, with only 1% in the plasma, for approximately 30-35 days.

From blood, Pb is dispersed into the soft tissue – liver, renal cortex, aorta, brain as well as bone. In adults 80-95% of Pb is stored in bone whereas only 70% is stored in bone in children (Patrick 2006). The biological half-time for Pb in trabecular bone is approximately 1 year, but 69% of absorbed Pb is stored in cortical bone in which its biological half-time is decades (Nordberg *et al*. 2007). Bone Pb levels can cause elevated blood Pb levels long after environmental exposure isn't present anymore due to an increase in bone turnover due to e.g. pregnancy, hyperthyroidism, etc., (Patrick 2006).

A reduction in haeme production is one of the main consequences of chronic Pb exposure. Pb is a divalent cation with affinity to proteins with sulfhydryl groups. This leads to changes in the structure and function of certain proteins and interferes with enzyme activity. A zinc containing haeme enzyme, δ-aminolevulinic acid dehydratase, is especially sensitive to Pb (Patrick 2006; Rana 2008). Pb has a high affinity for δ-aminolevulinic acid dehydratase which is the enzyme in the haeme pathway responsible for the asymmetrical addition of two molecules of δ-aminolevulinic acid (Nordberg *et al*. 2007). δ-aminolevulinic acid dehydratase is present in all cells including erythrocytes (Nordberg *et al*. 2007). Inhibition of this enzyme leads to δ-aminolevulinic acid accumulation which can induce the generation of ROS by the substitution of Zn (Needleman 2004; Rana 2008).

During haeme metabolism Pb can also affect the Fe^{2+} transport into and in the mitochondria (Nordberg *et al*. 2007). Pb can mimic Ca as well as compete with Ca causing diverse effects on cells, including affecting neuronal signalling, and the mitochondria (Needleman 2004).

High Pb levels have been associated with hypertension, peripheral vascular disease as well as cognitive decline in older people. In a study done on the United States' population an increase in Pb concentration led to a 40-60% increase in adjusted mortality (Whitfield *et al*. 2010). Pb mimics calcium and thus may trigger apoptosis (Rana 2008). It also binds to glutathione and in this way decreases cellular glutathione levels (Rana 2008).

2.3.4 Manganese (Mn)

Mn is mainly found in its oxidised chemical forms MnO_2 or Mn_3O_4 in the environment. In the human body it exists primarily as Mn^{2+} and Mn^{3+}. Mn^{3+} species are bound to transferrin which forms a more stable complex. The liver, kidney, pancreas, bone and brain contain mostly Mn^{2+} species. However, both Mn^{2+} and Mn^{3+} enter the brain using different transport systems (O'Neal & Zheng 2015). The characteristics and health risks associated with Mn exposure is summarised in Table 2.4.

Table 2.4: Characteristics and health risks of Mn.

Natural occurrence:	☙ Found in more than 100 minerals, the most important being: pyrolusite, oxides, carbonates, and silicates ☙ The Transvaal Supergroup
Anthropogenic occurrence:	☙ Mpumalanga, KwaZulu-Natal, Waterberg, Mapungubwe, Pafuri, Free Sate, Witwatersrand, North West, Western Bushveld, Eastern Bushveld Limpopo, Phalaborwa, Barberton, Okiep
Uses:	☙ ~90% of total manganese is used in steel manufacture – deoxidizing and desulfurizing additive, as alloying constituent ☙ Component of welding consumables ☙ Methylcyclopentadienyl manganese tricarbonyl (MMT) is used in gasoline instead of tetraethyl lead
Absorption:	☙ Inhalation: 30-60% ☙ Ingestion: 3-5% ☙ Skin: minimal
Effects of: ☙ Chronic exposure	☙ Inhalation: chemical pneumonitis; acute respiratory diseases – bronchitis and pneumonia ☙ Inhalation: may result in neurological and neurobehavioral effects – manganism (similar to Parkinson's disease) ☙ Ingestion: Possible long-term effect on central nervous system
☙ Acute exposure	☙ Ingestion: methaemoglobinemia ☙ Inhalation: metal fume fever
Biological half-time	☙ 2-5 weeks

Compiled from: Hobbs 2010; Nordberg *et al*. 2007; Williams *et al*. 2008

Mn is essential nutritionally, acting as a co-factor of various enzymes and is required for normal development, maintenance and regulation of various cellular systems. However, overexposure can lead to toxicity to many organ systems and across different age groups (Higdon *et al*. 2010;

O'Neal & Zheng 2015). Unlike ingested Mn inhaled Mn is transported directly to the brain before it can be metabolised by the liver and this may result, in extreme cases, in manganism, a neurological disorder with symptoms similar to those of Parkinson's disease (Higdon *et al.* 2010). People with iron deficiency, chronic liver disease, infants, and children are more susceptible to manganese toxicity (Higdon *et al.* 2010).

More than 80% of the high-grade Mn ore internationally used is mined in SA, producing 17% of the total amount of Mn worldwide. Organo-manganese compounds are used instead of leaded gasoline in order to decrease the Pb exposure of the general population. However, this is likely to lead to increased Mn exposure (Nordberg *et al*. 2007).

Studies found limited evidence that high Mn intake from drinking water may be associated with manganism in adults (Higdon *et al.* 2010). However, studies found that children showing increased Mn concentrations had an increase in hyperactive behaviours, impaired cognitive development and an impairment of motor coordination, hand dexterity and odour identification. An increase in infant mortality was also found with Mn concentrations above the WHO (World Health Organisation) standard of 400 µg Mn/L (O'Neal & Zheng 2015).

2.3.5 Nickel (Ni)

The most important characteristics and health risks of Ni are given in Table 2.5.

Table 2.5: Characteristics and health risks of Ni.

Natural occurrence:	☙ Nickel sulphide or -oxide ores
Anthropogenic occurrence:	☙ Pafuri, Western- & Eastern Bushveld, Okiep
Uses:	☙ Steel and alloy production, electroplating, Ni-Cd battery production, chemical catalysis, used in the manufacture of electronic components ☙ Nickel alloys used in coins, jewellery, watches, eyeglass frames, clothing buttons & studs, household & cooking utensils, orthodontic appliances, dental tools, orthopaedic implants, circulatory stents
Absorption:	☙ Inhalation: 20% ☙ Ingestion: with food 1%; with water – 40%
Effects of: ☙ Chronic exposure	☙ Inhalation: Rhinitis, sinusitis, nasal septum perforations, asthma ☙ Dermal: Urticaria, eczema, erythema, pruritus ☙ Group 1 IARC carcinogen ☙ Genotoxic ☙ Hepatotoxic
☙ Acute exposure	☙ Ingestion or inhalation: headache, vertigo, nausea, vomiting,

	nephrotoxic effects, pneumonia followed by pulmonary fibrosis
Biological half-time	☙ 1-2 days

Compiled from: Hobbs 2010; Nordberg *et al*. 2007; Fay *et al*. 2005

Ni is a frequent cause of contact allergy with up to 30% of the general population showing sensitivity to Ni (Nordberg *et al*. 2007). Ni may substitute other metals, especially Zn thereby affecting Zn dependent enzymes (Rana 2008). It also results in an increase in intracellular Ca concentrations (Nordberg *et al*. 2007). Ni crosses cell membranes via the Ca channels and may bind to Ca specific receptors (Rana 2008). It also binds to MT forming a metalloprotein known as nickeloplasmin (Rana 2008). Ni accumulates in bone, the liver, and kidneys and is known to cause lipid peroxidation (Das *et al*. 2007). Das *et al.* (2007) found that Ni exposure resulted in significant decrease in erythrocyte content and Hb concentration.

Ni induces ROS production and reduces glutathione (Rana 2008; Das *et al*. 2007) and this increase in ROS and oxidative stress can result in apoptosis (Rana 2008). Ni, although essential to plants and animals, is not essential to humans. Its toxic effects in humans are related to dermal, lung, and nasal sinus cancers (Awofolu *et al*. 2005). Awofolu *et al*., (2005) found that Ni levels in the Tyume river (0.201 ± .003 to 1.777 ± 0.002 mg/L), SA, were higher than typical concentrations of Ni in unpolluted surface water (0.015-0.02 mg/L).

2.3.6 Chromium (Cr)

Refer to Table 2.6.

Table 2.6: Characteristics and health risks of Cr.

Natural occurrence:	☙ Primarily as chromite ore ☙ Bushveld complex
Anthropogenic occurrence:	☙ Western Bushveld, Eastern Bushveld
Uses:	☙ Used in the chemical and graphics industry – Artistic paints, anticorrosion paints, electroplating, steel alloys, stainless steel welding
Absorption:	☙ Ingestion: ~2%
Effects of: ☙ Chronic exposure	☙ Ulcerations on and perforations of the nasal septum ☙ Allergic eczematous dermatitis
☙ Acute exposure	☙ Skin: chrome ulcers, acute irritative dermatitis ☙ Ingestion and skin: tubular necrosis, liver necrosis, cardiovascular shock ☙ Inhalation: bronchial asthma
Total biological half-time	☙ 15-41 hours

Compiled from: Hobbs 2010; Nordberg *et al*. 2007; Wilbur *et al*. 2008

In a study done by Gzik *et al.,* (2003) it was found that the Cr contamination levels were high in soil samples taken in the Merensky Platina Belt, which stretches from the west of the Pilanesberg southwards through the Bafokeng area and Rustenburg towards Marikana, parallel to the Magaliesberg, SA.

Cr occurs almost always in the trivalent state in nature, mostly in combination with iron or other metal oxides (Ramzan *et al*. 2011). After intestinal absorption Cr is taken up by plasma protein fractions. Small physiological doses are almost entirely bound to the iron binding protein, transferrin (Ramzan *et al*. 2011). Occupational exposure to Cr leads to a decrease in Hb, total erythrocytes and glutathione (Ramzan *et al*. 2011). Cr^{3+} can produce free radicals from H_2O_2 and lipid hydroperoxides (LOOH) and this induction of ROS can lead to apoptosis as well as the activation of caspase-3 (Ścibior *et al*. 2010; Catelas *et al*. 2005; Rana 2008). Cr^{3+} can cause oxidative stress to cells due to its redox properties (Ścibior *et al*. 2010).

2.3.7 Cobalt (Co)

Co is an essential metabolic metal in humans; however when consumption levels are too high for a long period of time, toxicity does occur (Awofolu *et al*. 2005). The health risks associated with Co exposure is summarised in Table 2.7.

Table 2.7: Characteristics and health risks of Co.

Natural occurrence:	☙ In mineral form as arsenides, sulphides and oxides ☙ Bushveld complex
Anthropogenic occurrence:	☙ Mpumalanga
Uses:	☙ Used in the production of steel and alloys, in hip and knee replacement joints
Absorption:	☙ Ingestion: 5-45%
Effects of: ☙ Chronic exposure	☙ Inhalation: respiratory irritation, diminished pulmonary function, wheezing, asthma, pneumonia, and fibrosis ☙ Ingestion: cardiomyopathy, polycythemia, thyroid lesions, goiter, lung cancer ☙ Ingestion: increases erythrocytes, hypocoagulation
☙ Acute exposure	☙ Skin: erythematous and/or papular dermatitis
Total biological half-time	☙ 6, 60, 800 days

Compiled from: Hobbs 2010; Nordberg *et al*. 2007; Faroon *et al*. 2004

Iron deficiency leads to an increase in cobalt absorption (Faroon *et al.* 2004*).* Known toxic effects of Co include vasodilation, flushing and cardiomyopathy (Awofolu *et al*. 2005). Environmental or occupational exposure to Co causes a decrease in erythrocyte and Hb levels

(Swennen *et al*. 1993; Raffn *et al*. 1988; Lantin *et al*. 2011). Co is bound to Hb in the cytosol. During long-term exposure Co will be absorbed irreversibly by erythrocytes (Simonsen *et al*. 2011). Co is the 33rd most abundant element in the earth's crust and is often found in association with Ni, Ag, Pb, Cu and Fe ores (Faroon *et al.* 2004). Co mediates activation of caspase-3 through intracellular glutathione reactive oxidation (Catelas *et al*. 2005; Rana 2008).

The primary anthropogenic sources of Co in the environment are from the burning of fossil fuels, application of Co-containing sludge or phosphate fertilizers, mining and smelting of Co-containing ores, processing of Co-containing alloys, and industries that use or process Co compounds (Faroon *et al.* 2004). The general population will most likely be exposed to Co through the ingestion of contaminated water or food (Faroon *et al.* 2004). In a study done in the Olifants river, SA, by Jooste *et al.* (2015) it was found that amongst others Co accumulates in the muscle tissue of the sharptooth catfish, indicating that long term consumption of this fish may cause adverse health effects.

2.3.8 Copper (Cu)

A summary of the effect of Cu exposure is provided in Table 2.8.

Table 2.8: Characteristics and health risks of Cu.

Natural occurrence:	☙ In copper ores ☙ Bushveld complex ☙ Phalaborwa Igneous complex ☙ Northern Cape near Aggeneys
Anthropogenic occurrence:	☙ Mpumalanga, KwaZulu-Natal, Free State, Witwatersrand, North West, Limpopo, Phalaborwa, Barberton, Okiep
Uses:	☙ Electric wires and cables; compounds are used in wood preservatives, fungicides, fertilizers; alloying element.
Absorption:	☙ Ingestion: 12-56% depending on amount of Cu in diet
Effects of: ☙ Chronic exposure	☙ Inhalation: respiratory irritation, mucosal and atrophic changes in the mucous membranes of the nose, lung nodular changes
☙ Acute exposure	☙ Ingestion: gastrointestinal disturbances: vomiting, epigastric burns, diarrhea, nausea, increased urinary sucrose excretion; haemolysis; hepatotoxicity, gastrointestinal tract bleeding, acute renal failure, acute intravascular haemolysis ☙ Inhalation: metal fume fever
Total biological half-time	☙ 2-5 weeks

Compiled from: Hobbs 2010; Nordberg *et al*. 2007; Dorsey *et al*. 2004

Cu is essential due to the fact that it forms part of numerous enzymes, including superoxide dismutase (Nordberg *et al*. 2007). However, at high levels of exposure which occurs primarily

through ingestion, toxicity does occur. It reduces glutathione (Rana 2008) and Hb and these reductions can lead to anaemia (Bertinato *et al*. 2010). Cu binds and oxidizes thiol groups to disulfides, especially in the cell membrane (Rana 2008). It also participates in one electron exchange reactions where the reactions can also generate free radicals which can have a negative effect (Rana 2008).

The liver and brain contain the highest Cu concentration (Nordberg *et al*. 2007). If cellular Cu levels are too high, resulting in toxicity, intricate cellular mechanisms regulate Cu uptake and elimination (Bertinato *et al*. 2010). Accumulation is also prevented by Cu chaperones which bind specifically to Cu and deliver the metal to specific enzymes or subcellular compartments (Bertinato *et al*. 2010).

It is clear that exposure to heavy metals can cause severe damage and that the risk of being exposed is high in SA as a result of prevalent mining activity and the dependence on fossil fuels for energy generation. The fact that heavy metals generally occur in combinations as has been indicated in Tables 2.1 – 2.8, underlines the importance of developing a rapid screening procedure indicating whether combinations have a greater effect than expected on the human body. The possibility of using cellular indicators as a metric of heavy metal toxicity is discussed in the following paragraphs.

2.4 *In vitro* models for cellular toxicity

The cellular toxicity of heavy metals have been evaluated in a wide range of cell types; these include the human trophoblast cell line, (Valbonesi *et al*. 2008); a rat proximal tubular cell line (Stacchiotti *et al*. 2009); mouse skin epidermal cell line (Son *et al*. 2010); human embryonic kidney cell line (Simmons *et al*. 2011), human hepatoma cell line (Korashy & El-Kadi 2008; Shea *et al*. 2008; Simmons *et al*. 2011); breast cancer cell line; adenocarcinomic human alveolar basal epithelial cell line; glioma cell line (Simmons *et al*. 2011); rat liver-derived cell line (Permenter *et al*. 2011); a Jurkat T cell line (Nemmiche *et al*. 2011), and a neuroblastoma cell line (Valbonesi *et al*. 2008).

These cell lines were used to measure signal transduction, stress-related pathways, teratogenicity (Valbonesi *et al*. 2008); biochemical and morphological markers to test for oxidative damage, activation of heat shock proteins, glucose-regulated proteins and metallothioneins (Stacchiotti *et al*. 2009; Shea *et al*. 2008). Induction of apoptosis (Son *et al*. 2010; Permenter *et al*. 2011); activation of transcription factor Nrf2 due to oxidative stress

(Simmons *et al*. 2011); gene response and activation of pathways responding to oxidative stress (Permenter *et al*. 2011) were also evaluated. The effect on intracellular trace element levels, antioxidant enzyme activities and DNA damage (Nemmiche *et al*. 2011); induction of cytochrome P450 1A1, a zenobiotic metabolising enzyme (Korashy & El-Kadi 2008) as well as cytotoxicity were measured.

Effects of Pb on erythrocytes *in vitro* have been investigated by Quintanar-Escorza *et al*. (2010) and Hunaiti & Soud (2000) who found that Pb increased the intracellular free Ca concentration, caused lipid peroxidation, and decreased the reduced glutathione / oxidised glutathione ratio in a time- and dose dependent manner. Comparable studies have been done on different heavy metals but only a few studies have been undertaken to determine the effect of metal combinations i.e. simultaneous exposure to more than one metal.

The effects of oxidative damage on cell morphology and membrane composition have been well described. As oxidative effects are one of the most common consequences of heavy metal toxicity the erythrocyte is ideal for the investigation of heavy metal combinations. Erythrocytes have a known ability to cope with reactive oxygen and nitrogen species in the body. Due to erythrocytes being cells without nuclei and mitochondria, the inference, of oxygen radicals and gene transcription as well as mitochondrial radical formation, with assays is excluded (Blasa *et al.,* 2011).

Furthermore the literature review presented, indicated that erythrocytes are a common target of heavy metal toxicity. Erythrocytes have thus been identified as a relevant cellular system to study the impact of metal combinations on a cellular level. Erythrocytes from different human donors also reflect the genetic heterogeneity of the population for this study. An added advantage is that a single blood sample can be used to measure several parameters.

2.5 Erythrocytes

Mature erythrocytes have a characteristic biconcave shape that contain a phospholipid membrane but have no nucleus, mitochondria or any other organelles (Van Papendorp & Claassen 2002). The membrane consists of 49% protein, 43% lipid and 8% carbohydrate. The main function of erythrocytes is to transport oxygen and carbon dioxide (Silverthorn 2007). This transport is mediated by Hb a major intracellular protein of erythrocytes present at a concentration of approximately 7.7 mM (Föller 2008).

2.6 Haemoglobin

Hb is a tetrameric protein which permits cooperative interactions e.g. 2,3-bisphosphoglycerate (BPG) as indicated with the darkest blue in Figure 2. BPG promotes the efficient release of O_2 through stabilisation of the quaternary structure of deoxyhaemoglobin (Kennely & Rodwell 2009). Hb consists of a porphyrin pigment to which iron is attached and a protein component (Van Papendorp & Claassen 2002).

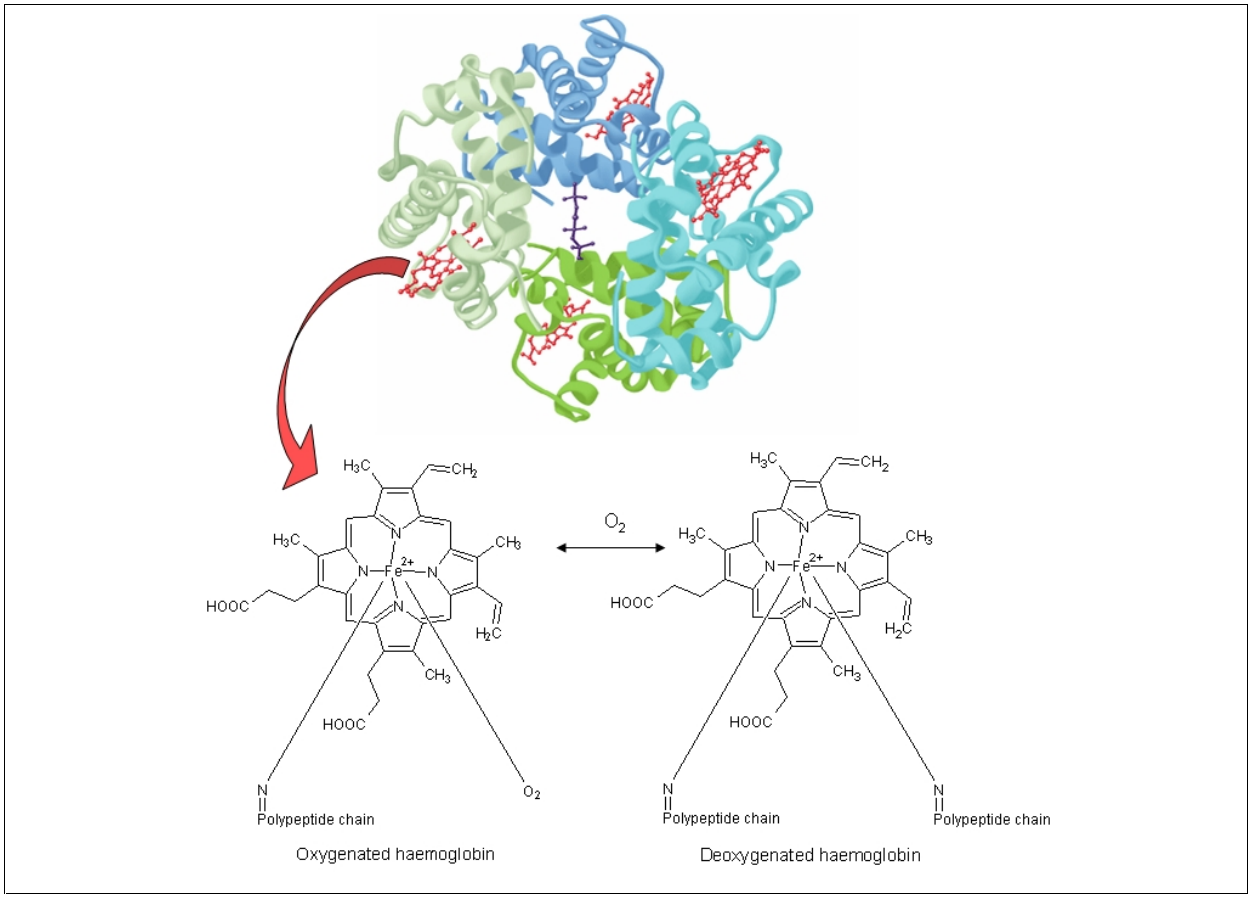

Figure 2.2: The three-dimensional structure of deoxyhaemoglobin attached to BPG (Kennely & Rodwell 2009). **Insert:** The chemical structure of haeme (Barrett *et al*. 2010).

Haeme is a cyclic tetrapyrrole, consisting of pyrrole linked by α-methylene bridges. One atom of ferrous iron (Fe^{2+}) is present at the center of the tetrapyrrole. Oxidation of the Fe^{2+} to Fe^{3+} destroys haemoglobin's biological activity (Kennely & Rodwell 2009). The protein component consists of two different polypeptide subunits, with human normal adult Hb having a $\alpha_2\beta_2$ subunit composition, as shown in Figure 2 with the α subunits coloured in the darker shades of green and blue and the two β subunits in the lighter shades of green and blue. The haeme prosthetic groups are indicated with red (Kennely & Rodwell 2009).

2.7 The erythrocyte membrane

Although the erythrocyte membrane only accounts for 1% of the total weight of the cell it plays an irreplaceable role in erythrocyte function and integrity. The composition of the membrane and the accompanying cytoskeleton provide the erythrocyte with the needed flexibility, durability and tensile strength. The membrane has a nonreactive exterior that prevents adherence to endothelial cells and it helps with the maintenance of the pH homeostasis through the exchange of chloride and bicarbonate. Erythrocytes are easily accessible and therefore the erythrocyte membrane has been thoroughly studied in cell biology. The erythrocyte membrane is a paradigm for studies of other cell types because its normal structure and function have been studied extensively. The erythrocyte membrane are composed of three major structural elements: a lipid bilayer primarily composed of phospholipids and cholesterol – lipids comprise 50 to 60% of the membrane mass; integral proteins embedded in the lipid bilayer; and a membrane skeleton, which provides structural integrity to the cell, on the internal side of the membrane (Gallagher 2010; Bull & Herrmann 2010). Damage to the erythrocyte membrane results in the leakage of protein such as Hb. Quantification of the amount of Hb, due to its inherent colour is widely used as an indicator of cellular damage (Quintanar-Escorza *et al*. 2010; Hunaiti & Soud 2000; Snyder *et al*. 1985).

2.8 Oxidative damage in membranes

Metal-induced oxidative stress in cells can be partially responsible for the toxic effects of heavy metals (Al-Attar 2011). An increased level of lipid peroxidation and decreased levels of enzymatic and non-enzymatic antioxidants were noticed in the presence of ROS in erythrocytes (Kalahasthi *et al*. 2006). ROS are classified according to longevity; short lived diffusible species include hydroxyl ($OH^{\bullet}$), alkoxyl ($RO^{\bullet}$) and peroxyl ($ROO^{\bullet}$) radicals. Medium lifetime species are nitroxyl ($NO^{\bullet}$) and superoxide ($O_2^{\bullet -}$) radicals. Some non-radicals are also ROS and these include hydrogen peroxide (H_2O_2), organic hydroperoxides (ROOH) and hypochlorous acid (HOCl) (Simon *et al*. 2000). ROS must be detoxified by antioxidants, but if the antioxidant systems are impaired or if there are excessive production of ROS, oxidative stress occurs in the cell (Schäfer & Werner 2008).

Unsaturated fatty acids as well as oxygen are two major components in lipid peroxidation (Benedet & Shibamoto 2008). The lipid peroxidation in polyunsaturated fatty acids is a free radical mediated chain oxidation reaction, providing a continuous supply of free radicals that initiate further peroxidation (Benedet & Shibamoto 2008; Singh *et al*. 2011). The lipid

peroxidation chain reaction occurs as follows (Botham & Mayes 2009, Kennely & Rodwell 2009):

2.8.1. Initiation:

$$ROOH + Metal^{(n)+} \rightarrow ROO^{\bullet} + Metal^{(n-1)+} + H^{+}$$

$$X^{\bullet} + RH \rightarrow R^{\bullet} + XH$$

Polyunsaturated fatty acids contain methylene-interrupted double bonds which play a role in the formation of radicals during lipid peroxidation. Lipid peroxidation can be initiated by an existing free radical ($X^{\bullet}$), by light or by metal ions. Organic hydroperoxides (ROOH) can for example react with a catalytic metal like Fe^{3+} ($Metal^{(n)+}$) which causes the formation of a peroxyl radical ($ROO^{\bullet}$). The peroxyl radical in turn substitutes hydrogen from the polyunsaturated fatty acid chain (RH) with a free radical ($R^{\bullet}$).

2.8.2. Propagation:

$$R^{\bullet} + O_2 \rightarrow ROO^{\bullet}$$

$$ROO^{\bullet} + RH \rightarrow ROOH + R^{\bullet}, \text{ etc}$$

This free radical attached to the polyunsaturated fatty acid chain can then react with oxygen (O_2) resulting in the formation of a peroxyl radical which in turn can react with another polyunsaturated fatty acid.

2.8.3. Termination:

$$ROO^{\bullet} + ROO^{\bullet} \rightarrow ROOR + O_2$$

$$ROO^{\bullet}\ R^{\bullet} \rightarrow ROOR$$

$$R^{\bullet} + R^{\bullet} \rightarrow RR \text{ (Kennely \& Rodwell 2009)}$$

The formed peroxyl radicals can bind to each other or bind to other radicals forming for example hydroperoxide or endoperoxide which are unstable and breaks down to stable secondary products, for example malondialdehyde (MDA).

Lipid peroxidation disrupts the structural and protective functions of cell membranes. MDA a well-known product of the lipid peroxidation of erythrocytes cross-links erythrocyte phospholipids and proteins. This leads to a reduction of membrane function and ultimately to erythrocyte death (Singh *et al*. 2011).

2.9 Eryptosis

Erythrocytes cannot undergo the same kind of programmed cellular death that cells with nuclei do. Erythrocytes, however, do undergo a form of programmed cell death similar to apoptosis – eryptosis (Föller 2008). The main difference between apoptosis and eryptosis being that no organelles are present in the erythrocyte and the focus of eryptosis is thus the erythrocyte membrane. The mechanisms of eryptosis are summarised in Figure 2.3.

Cholesterol of the erythrocyte membrane is mostly hydrophobic and present in a free, un-esterified form. Its main function is to control membrane fluidity even under stress conditions which can lead to phospholipid crystallisation and bilayer rigidification. Phospholipids are asymmetrically arranged in the membrane, with phosphatidylserine and phosphatidylethanolamine in the inner hemileaflet and sphingomeylin and phosphatidylcholine on the outside. The maintenance of this asymmetry is important for cell haemostasis. Phosphatidylserine exposure on the outside of the cell is an indication of eryptosis. This exposure has been correlated with complement activation and erythrocyte clearance by macrophages and liposomes. Two enzymes are responsible for the maintenance of the asymmetric haemostasis, namely flippases and floppases. Flippases actively translocate phosphatidylserine and phosphatidylethanolamine to the inside and floppases is responsible for the translocation to the outer leaflet. The haemostatic asymmetry is dependent on flipping occurring at a higher rate than flopping. An increase in intracellular calcium leads to the activation of scramblase which promotes randomisation and loss of membrane. Scramblase causes the redistribution of membrane phospholipids in activated, injured or apoptotic cells (Gallagher 2010).

Apoptosis is one of best known forms of programmed cellular death (Föller 2008). Apoptosis is triggered by stimulation of certain receptors or by cell exposure to stressors, such as oxidants, radiation or osmotic shock (Lang *et al*. 2005). It is characterised by cell shrinkage and associated with loss of intracellular potassium. Other known effects are nuclear condensation, DNA fragmentation, mitochondrial depolarisation, cell membrane blebbing, and breakdown of the phosphatidylserine asymmetry of the plasma membrane (Lang *et al*. 2005). This phosphatidylserine exposure on the surface leads to macrophage recognition and these cells are then engulfed and degraded. Apoptosis thus leads to the elimination of damaged cells

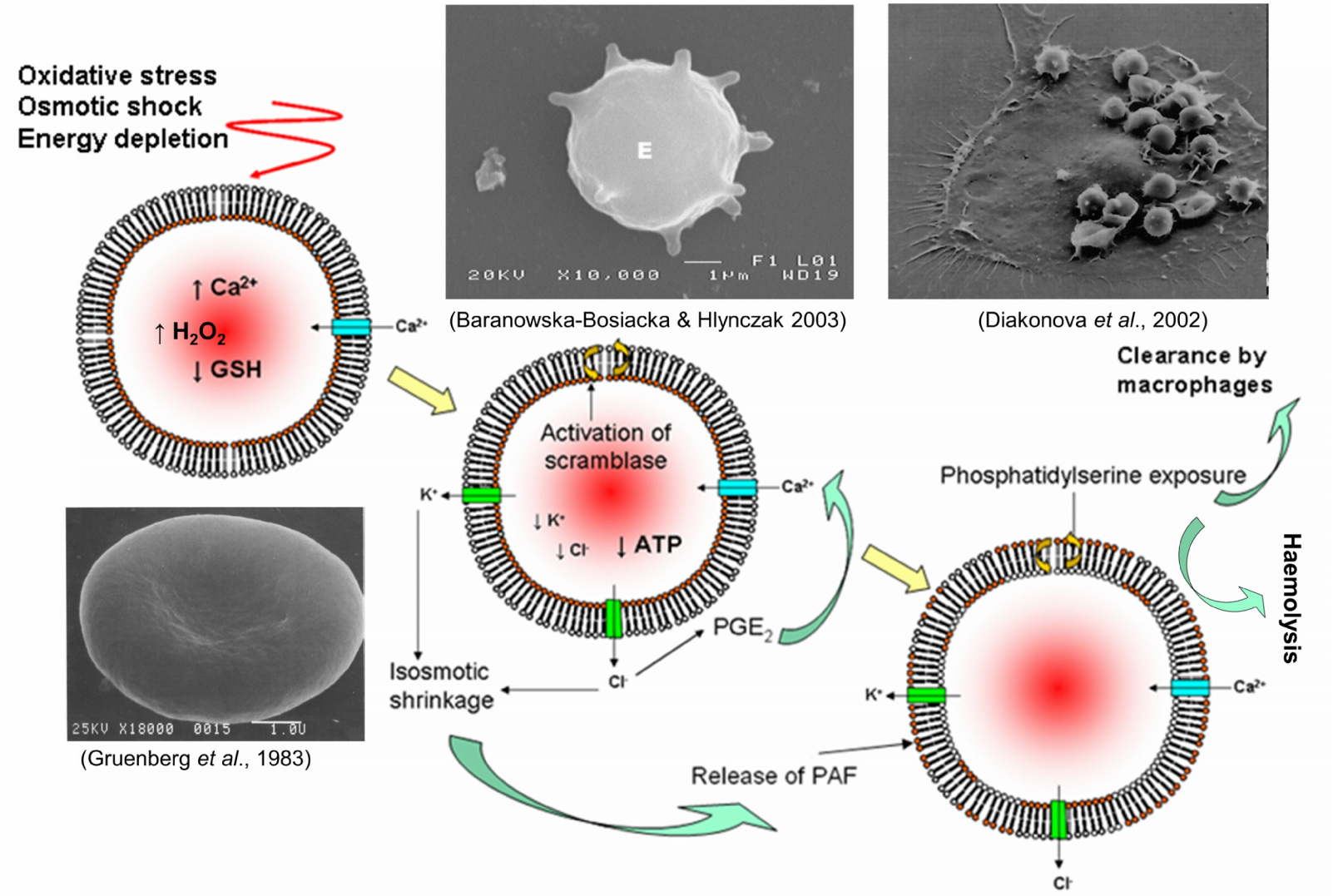

Figure 2.3: Mechanisms of eryptosis (Adapted from: Föller 2008; Lang *et al*. 2005; Cohen & Hochstein 1964; Baranowska-Bosiacka & Hlynczak 2003; Diakonova *et al.* 2002; Gurenberg *et al.* 1983).

without release of intracellular proteins which would lead to inflammation (Lang *et al*. 2005). Studies found that Co, Cr (Catelas *et al*. 2005), Cd (Bertin & Averbeck 2006), Mn (Hirata 2002), Pb (Yedjou *et al*. 2010), and Hg (Eisele *et al*. 2006) cause apoptosis.

Erythrocyte membranes usually have little channel activity and are predominantly permeable to the chloride ion (Cl^-). However, osmotic cell shrinkage as well as oxidative stress and energy depletion opens non-selective cation channels (Lang *et al*. 2005). This leads to the uptake of monovalent cations as well as Ca^{2+} (Lang *et al*. 2005) and a reduction in glutathione. The generation of H_2O_2 in intact erythrocytes is also associated with exposure to haemolytic agents (Cohen & Hochstein 1964).

The increase of intracellular Ca has various effects on erythrocytes. These effects include the stimulation of erythrocyte scramblase leading to the exposure of phosphatedylserine on the erythrocyte surface. Ca also activates the Ca^{2+}-dependent cysteine endopeptidase calpain. This activation of calpain leads to cell membrane blebbing (Föller 2008). The Gardos K^+ channel is also activated, leading to a decreased cytosolic K^+ concentration. This decreased concentration accelerates phosphatidylserine exposure and delays swelling and disruption of defective erythrocytes. The triggering of eryptosis is an important mechanism to clear erythrocytes before haemolysis can occur (Lang *et al*. 2005).

2.10 Antioxidant mechanisms in erythrocytes

Erythrocytes are continuously exposed to oxidative stress due to their high cellular oxygen concentrations, the fact that they have a high polyunsaturated fatty acid content in their membranes and have a high content of haemoglobin bound iron (Jadhav *et al*. 2007; Singh *et al*. 2011; Jiang *et al*. 2009). Polyunsaturated fatty acids with more than two double bonds are more susceptible to oxidative stress due to the weakened carbon-hydrogen bonds on the carbon atom adjacent to the double bonds (Patra *et al*. 2011). Erythrocytes can however be damaged by external factors, especially exposure to toxic chemicals and environmental pollutants. Oxidative stress can also lead to alterations in the structural conformation of erythrocytes, which in turn can compromise effective blood flow, oxygen uptake and release (Jiang *et al*. 2009).

This exposure to oxidative stress has resulted in the development of very effective antioxidant mechanisms by erythrocytes (Jadhav *et al*. 2007). These antioxidant mechanisms include enzymatic mechanisms (catalase, glutathione peroxidase, superoxide dismutase, glutathione-6-phosphate dehydrogenase) which scavenge free radicals and remove peroxides (Ścibior *et al*. 2010; Jadhav *et al*. 2007), and non-enzymatic mechanisms

(reduced glutathione, Vitamin C, Vitamin E, melatonin) which are involved in detoxification processes as well as antioxidant protection (Jadhav *et al*. 2007; Ścibior *et al*. 2010; Jiang *et al*. 2009).

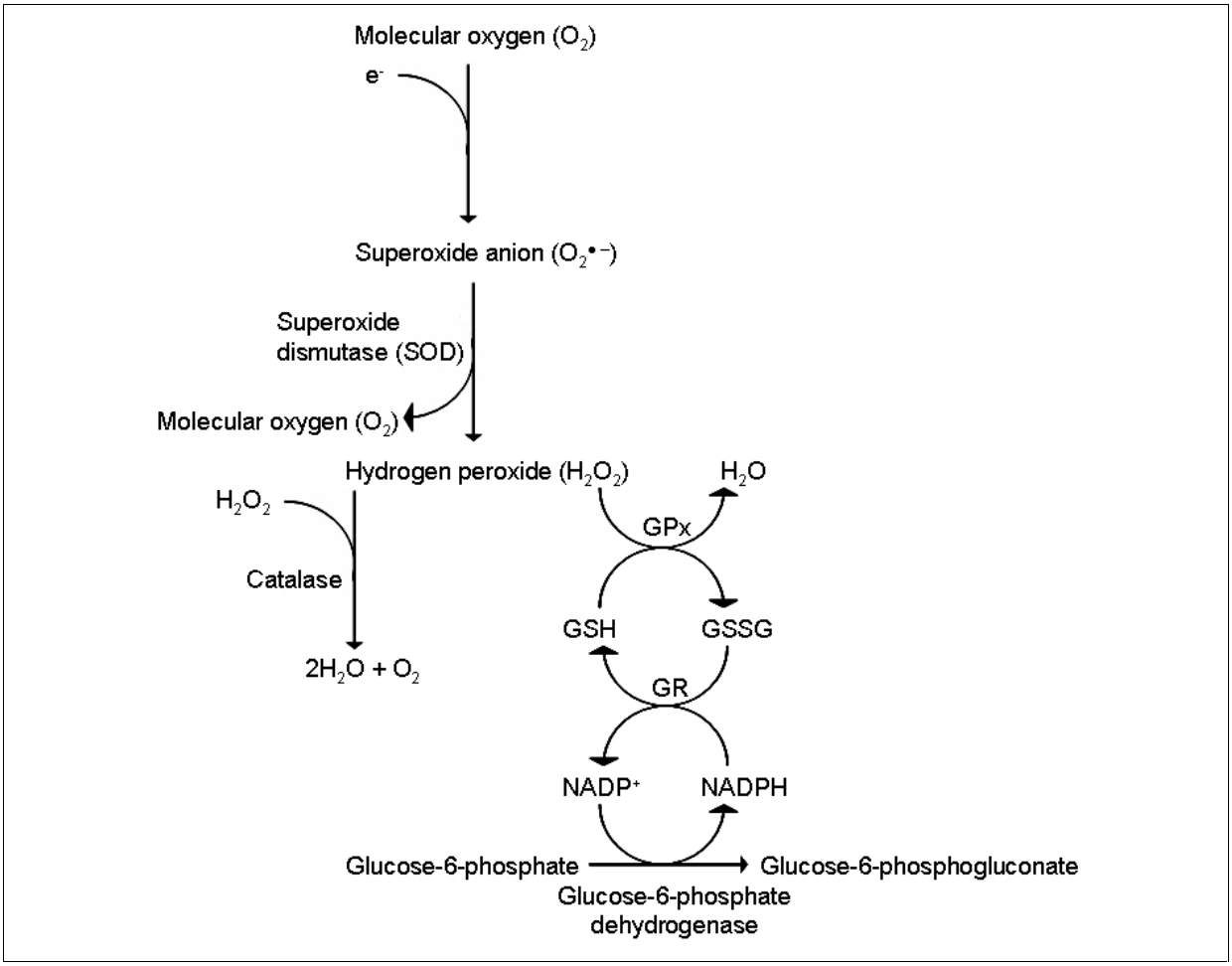

Figure 2.4: Summary of some antioxidant mechanisms present in erythrocytes (Adapted from: Salway 2006).

Figure 2.4 summarises the function of the erythrocyte antioxidant mechanisms. Superoxide dismutase catalyses the dismutation of the superoxide anion (O_2^-) into H_2O_2 and molecular oxygen. Glutathione peroxidase reduces H_2O_2 to H_2O thus deactivating it (Kalahasthi *et al*. 2006). Glutathione is a co-factor in the breakdown of H_2O_2 by glutathione peroxidase (Kalahasthi *et al*. 2006).

Erythrocytes are a common target of heavy metal toxicity and due to this a relevant cellular system to study the effects and pathways of metals and metal combinations. Cd, Co, Cr, Cu, Mn, Ni, Pb, and Hg were identified as metals prevalent in SA, mainly because of anthropogenic activity. These metals do not occur singularly in nature, but in mixtures. There is however a lack of primary data on the effects of metal mixtures. This study used simple screening methods to determine the effects of single- as well as mixtures of metals.

The possible mechanism of metal toxicity on erythrocytes has been indicated in the preceding paragraphs. The methodology used in this study to test for toxicity and oxidative effects on erythrocytes due to heavy metal exposure alone and in combination is summarised in Figure 2.5.

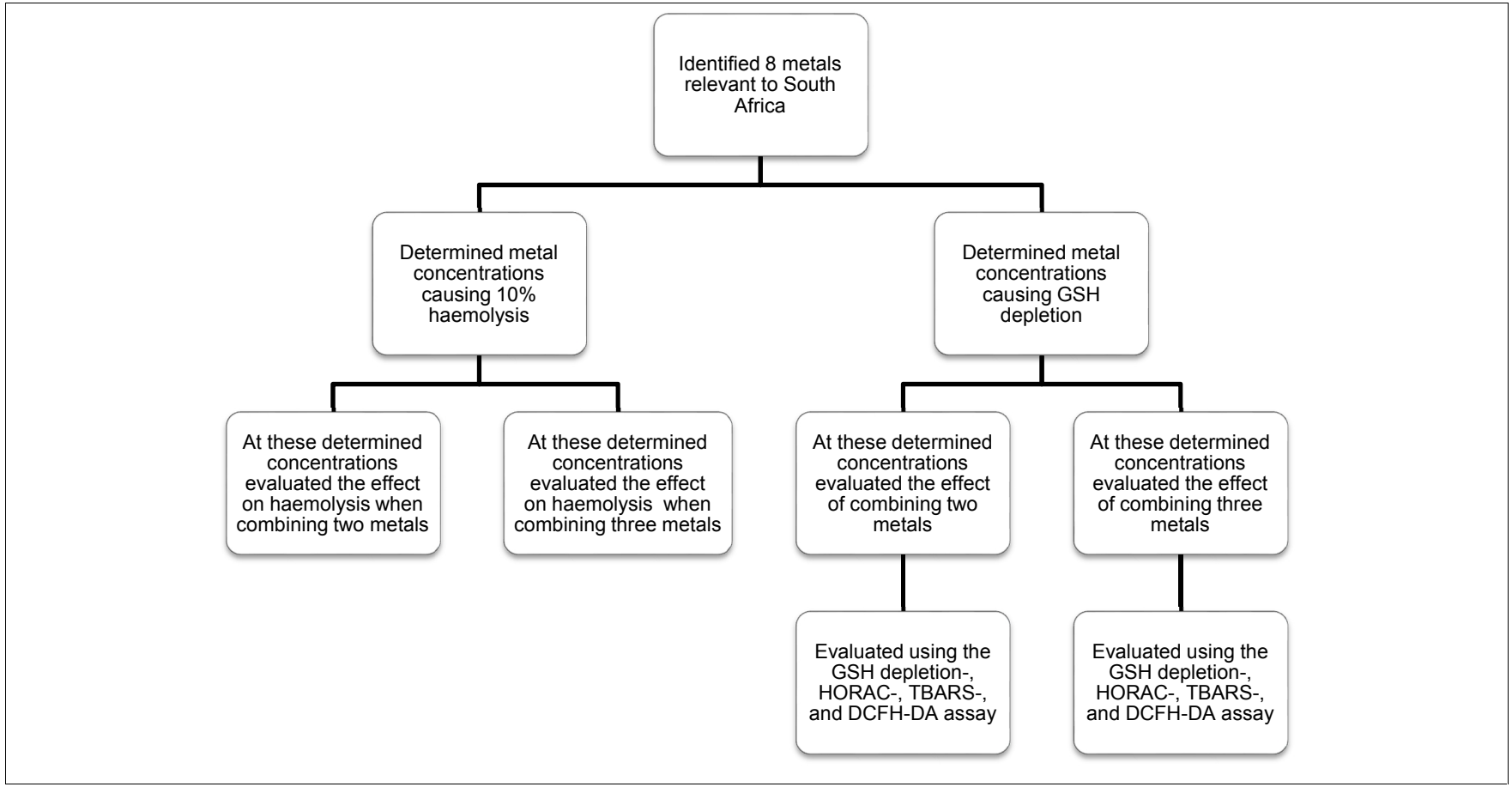

Figure 2.5: Flow diagram showing the methodology used in this study to test for toxicity and oxidative effects on erythrocytes due to single and combination heavy metal exposure.

2.11 Aims

South Africa is a highly industrialised country with anthropogenic activities influencing the quality of water. The increased concentrations of heavy metals in water due to these activities are of great concern. Heavy metals do not occur singularly, but in combination. However, the effects of exposure to combinations of metals are not well known.

The objectives of this study using the strategy as shown in Figure 2.5 were therefore to:

1. Identify metals of concern in South Africa.
2. Determine the concentrations of Cd, Co, Cr, Cu, Ni, Mn, Pb and Hg that cause 10% erythrocyte haemolysis.
3. Investigate at these determined concentrations whether double- and triple metal combinations cause an additive, synergistic or antagonistic haemolytic effect.
4. Identify which single metals bind GSH.

   The following experiments were done using the metal concentrations determined in objective 4.
5. Determine for double and triple metal combinations whether GSH binding effects are additive, synergistic or antagonistic.
6. Identify which metals act as catalysts in the Fenton reaction.
7. Determine which double and triple metal combinations alter hydroxyl radical formation in the Fenton reaction i.e. are these effects additive, synergistic or antagonistic.
8. In erythrocytes determine which metals cause oxidative damage due to increased MDA formation. .
9. In erythrocytes, determine if double and triple metal combinations have an additive, synergistic or antagonistic oxidative effect.
10. In erythrocytes, determine which metals cause an increase in oxidative stress using the 2',7'-dichlorofluorescein diacetate (DCFH-DA) assay.
11. In erythrocytes, determine if double and triple metal combinations have an additive, synergistic or antagonistic oxidative effect.

2.12 Hypotheses

Hypothesis 1: From most toxic to least toxic the metals are as follow: Hg > Cd > Pb > Ni > Co > Cr > Mn > Cu.

Hypothesis 2: Two metal combinations will present with additive effects when evaluated with chemical and cellular assays.

Hypothesis 3: Triple metal combinations will present with additive effects when evaluated with chemical and cellular assays.

Chapter 3: The haemolytic effect of metal pollutants

3.1 Introduction

"Lysis of RBCs is part of the daily physiological process of RBC turnover. However, the term 'haemolysis' is used when referring to the accelerated, pathological forms of haemolysis that result in anaemia and jaundice" (Hall 2007).

Haemolysis can also be defined as the release of haemoglobin into plasma due to the breakup of the erythrocyte cell membrane (Lee *et al.* 2004). Haemolysis occurs due to different stress factors, including mechanical-, shear, and osmotic stress. Oxidative stress can also cause haemolysis due to ROS destabilising the membranes of the erythrocytes (Číž *et al.* 2010). The amount of haemolysis that occurs depends on the magnitude of the stress as well as the time of exposure to the stress. Haemoglobin (Hb) leakage is the final step in haemolysis (Jay & Rowlands 1975) and also the step that makes the quantification of haemolysis possible. Haemolysis is the total sum of events such as oxidative stress, osmotic shock, and energy depletion that leads to the loss of membrane integrity and leakage of cellular content.

Haemolysis is seen as a multistage process, irrelevant of the stress that causes it. Different stages can be identified, namely swelling, popping and lastly reduction in volume which is associated with haemoglobin release (Jay & Rowlands 1975). The measurement of the amount of haemolysis is possible due to the fact that methaemoglobin's absorbance can be measured spectrophotometrically at 540 nm (Hematology 1998). The *ex vivo* haemolysis assay utilises this principle – the amount of Hb released, measured spectrophotometrically at 540 nm, is quantified to measure erythrocyte lysis (Evans *et al*. 2013). Drabkin's reagent is used to quantify Hb levels in solution – this reagent lends sensitivity to the *ex vivo* haemolysis assay.

Erythrocytes are widely used in the haemolysis assay and this assay has been used to evaluate the toxicity of various substances, including Pb (Quintanar-Escorza *et al*. 2010; Hunaiti & Soud 2000) and hydrogen peroxide (Snyder *et al*. 1985). In antioxidant studies (Singh & Rajini 2008) the ability of antioxidants to protect erythrocytes against oxidative damage is investigated. Alves *et al*. (2008) found that the haemolysis assay is a rapid test and useful as a screening method.

Numerous studies have found that metals cause haemolysis *in vivo.* Copper is known to be poisonous at high concentrations and can cause sudden haemolysis. In Wilson's disease, an inborn error of copper metabolism, life threatening haemolysis crises can develop in some patients (Aaseth *et al.* 1984). If erythrocytes are destroyed at a higher rate than at which they are replenished, it is known as haemolytic anaemia (Hall 2007). According to Sakai (2000) the haemolytic anaemia caused by Pb poisoning appears similar to that in hereditary pyrimidine 5'-nucleotidase deficiency. Horiguchi *et al.* (2011) found that Cd causes anaemia through haemolysis, body iron accumulation, and insufficient erythropoietin production in rats.

However, only a few studies have investigated the effect of metals using the *ex vivo* haemolysis assay. Brandão, *et al.,* (2005) found that mercuric chloride ($HgCl_2$) causes haemolysis *in vitro,* as expected. It was also found that Mn causes haemolysis *in vitro* at high concentrations and when incubated for extended periods of time (Lucaciu *et al.* 1997). Quintanar-Escorza *et al*. (2010) found higher than 10% haemolysis when erythrocytes were incubated for longer than 120 hours with Pb at concentrations higher than 40 µM. No literature could be found regarding the combinational effects of metals or erythrocytes using the *ex vivo* assay.

Human exposure to metals, however, normally does not occur in singularity, but rather to a mixture of heavy metals. When exposed to mixtures of substances, e.g. metals, a cocktail effect can be seen (Cedergreen 2014). The assumption is made that exposure to more than one toxin/metal will lead to an additive effect, meaning the sum of the parts, thus the interaction of two or more toxins/metals to produce an effect equal to the sum of the individual effects of the toxins in the whole mixture. However, the effect of toxins can also be synergistic or antagonistic, depending on the influence of the toxins on each other, as well as the exposed cell or organism. Derived from the Greek word *synergos* meaning working together; a synergistic effect can be defined as an interaction of two or more chemicals to produce an effect greater than the additive effect. According to the Oxford dictionary, an antagonist can be defined as a substance which interferes with or inhibits the physiological action of another. An antagonistic interaction is thus an interaction where the produced effect is lower than the additive effect (Parvez *et al*. 2009).

Therefore the aim of the research presented in this chapter was to screen a selection of metals alone and in combination for toxicity, synergistic, and antagonistic effects using an *ex vivo* erythrocyte model.

The specific objectives of this chapter were to:

1. Identify based on a literature review metals that have an adverse impact on the health of the South African population.
2. Establish methodologies for the determination of the effects of metals on erythrocytes.
3. Determine the concentrations of Cd, Co, Cr, Cu, Ni, Mn, Pb and Hg that cause 10% erythrocyte haemolysis.
4. Investigate at these determined concentrations whether double- and triple metal combinations cause an additive, synergistic, or antagonistic haemolytic effect.

3.2 Materials

3.2.1 Reagents, equipment and disposable plasticware

Sodium chloride (NaCl), potassium chloride (KCl), sodium phosphate (NaH_2PO_4), sodium phosphate dibasic dehydrate ($Na_2HPO_4 \bullet 2H_2O$), potassium cyanide (KCN), potassium ferricyanide ($K_3Fe^{3+}(CN)_6$) sodium bicarbonate ($NaHCO_3$), cadmium chloride ($CdCl_2$), nickel(II) chloride ($NiCl_2$), cobalt(II) chloride ($CoCl_2$), chromium potassium sulfate ($KCr(SO_4)_2$), lead acetate ($(CH_3COO)_2Pb$), copper(II) sulfate ($CuSO_4$), manganese(II) chloride ($MnCl_2$), and mercuric chloride ($HgCl_2$) were of analytical quality and were obtained from Merck Chemicals, Modderfontein, South Africa (SA). Triton X-100 was obtained from the Sigma-Aldrich Company, Atlasville, SA.

Equipment used included: a FLUOstar OPTIMA plate reader from BMG labtechnologies, Offenburg, Germany. A Hermle Z300 centrifuge, a Crison GLP 21 pH Meter and Eppendorf pipettes from Eppendorf AG, Hamburg, Germany, supplied by the Scientific Laboratory Equipment Company (LASEC), Cape Town, SA.

Disposable plasticware included: 0.5ml and 2ml Eppendorf tubes, 96 well plates, 50ml and 15ml tubes and pipette tips (10, 25, 100, 200, and 1000 µl) which were obtained from Greiner Bio-one, supplied by LASEC.

3.2.2 Laboratory facilities

All research was conducted in the research facilities of the Department of Anatomy of the Faculty of Health Sciences, University of Pretoria.

3.3 Methods

3.3.1 Erythrocyte collection

Blood was collected from 15 healthy, consenting volunteers as stipulated by the Main Ethics Committee regulations (SA2011) with Ethics Reference number 90/2015. Using a sterile needle connected to a 5 ml EDTA vacuum extraction blood tube, 5 ml blood was collected. The erythrocytes were collected by centrifugation at 2540 x g, the plasma and buffy coat was removed after which the erythrocytes were washed 2 times with equivalent volumes of isotonic phosphate buffered saline (isoPBS: 0.137 M NaCl, 3 mM KCl, 1.9 mM NaH_2PO_4, 8.1 mM Na_2HPO_4, pH 7.4). The pooled erythrocytes were stored as a 20% (v/v) dilution, made up in isoPBS, at 4ºC. The erythrocytes were stored for up to 3 days since no significant haemolysis in the stored sample was observed in this time period.

3.3.2 Preparation of metals

For exposure of erythrocytes to a single metal, a concentration series of $CdCl_2$, $NiCl_2$, $CoCl_2$, $KCr(SO_4)_2$, $(CH_3COO)_2Pb$, $CuSO_4$, $MnCl_2$, and $HgCl_2$ was prepared, ranging from 0 – 100 mM, using isoPBS.

3.3.3 *Ex vivo* haemolysis assay

For each experiment, the erythrocyte solution was removed from the fridge and left to warm to room temperature. A volume of 140 µl of the erythrocyte solution was pipetted into separate Eppendorf tubes and exposed to 60 µl of each of the metals at a range from 0 – 100 mM. After exposure the samples were incubated for 16 hours. The samples were then removed from the incubator, vortexed, and centrifuged at 1201 x g for 2 minutes. Of the supernatant 50 µl were placed into a well of a 96 well plate and the absorbance was read spectrophotometrically at 570 nm. The control solutions were prepared as follows:

1. 0% haemolysis (Blank): 60 µl isoPBS added to 140 µl erythrocyte solution
2. 100% haemolysis: 60 µl Triton X-100 added to 140 µl erythrocyte solution.

Percentage haemolysis was calculated using the following formula:

% Haemolysis = (Sample – Blank) / (100% Haemolysis – Blank) x 100

After determination of metal concentrations causing 10% haemolysis, the experiment was repeated with exposure of erythrocytes to single as well as double- and triple metal combinations.

In a separate experiment, 60 µl of each of the metals/metal combinations were added to 140 µl isoPBS in separate Eppendorf tubes. It was incubated overnight, vortexed and 50 µl of the supernatant, after centrifuging at 1201 x g for 2 min, were pipetted into a 96 well plate and read at 570 nm.

3.3.4 Measuring Hb using Drabkin's reagent

To the 50 µl supernatant from the previous experiment, 100 µl Drabkin's reagent was added to each well and the absorbance was read spectrophotometrically at 570 nm.

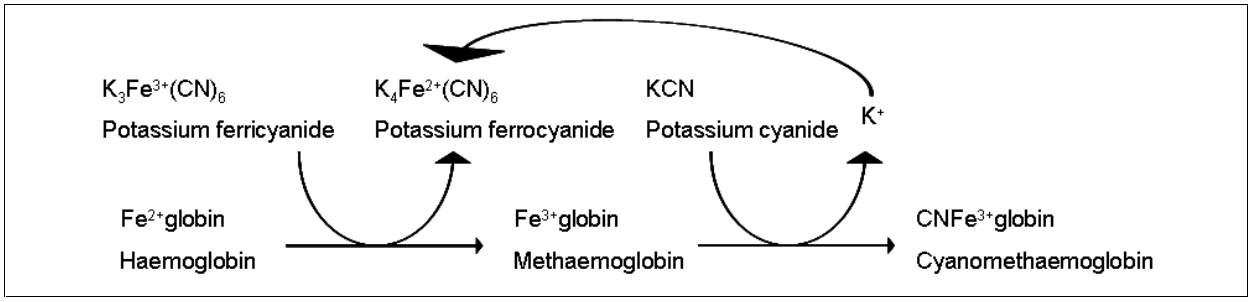

Figure 3.1: The reaction of Drabkin's reagent with Hb.

3.3.5 Determination of combination effect

For the double combinational effects the following metal concentrations were used:

$$\mathbf{A}_{10\%\ H} + \mathbf{B}_{10\%\ H}$$

For the triple combinational effects the following metal concentrations were used:

$$\mathbf{A}_{10\%\ H} + \mathbf{B}_{10\%\ H} + \mathbf{C}_{10\%\ H}$$

Where for metal A the concentration that causes 10% hemolysis.
Where for metal B the concentration that causes 10% hemolysis.
Where for metal C the concentration that causes 10% hemolysis.

The double and triple combinations that were evaluated are presented in Tables 3.1 and 3.2.

Table 3.1: Double combinations used at concentrations that caused 10% haemolysis to determine interaction effects.

	Cd	Co	Cr	Cu	Ni	Mn	Pb	Hg
Cd	-	√	√	√	√	√	√	√
Co	-	-	√	√	√	√	√	√
Cr	-	-	-	√	√	√	√	√
Cu	-	-		-	√	√	√	√
Ni	-	-	-	-	-	√	√	√
Mn	-	-	-	-	-	-	√	√
Pb	-	-	-	-	-	-	-	√
Hg	-	-	-	-	-	-	-	-

n=28

Table 3.2: Triple combinations used at concentrations that caused 10% haemolysis to determine interaction effects.

	Cr	Cu	Ni	Mn	Pb	Hg
Cd:Co	√	√	√	√	√	√
Cd:Cr	-	√	√	√	√	√
Cd:Cu	-	-	√	√	√	√
Cd:Ni	-	-	-	√	√	√
Cd:Mn	-	-	-	-	√	√
Cd:Pb	-	-	-	-	-	√
Co:Cr	-	√	√	√	√	√
Co:Cu	-	-	√	√	√	√
Co:Ni	-	-	-	√	√	√
Co:Mn	-	-	-	-	√	√
Co:Pb	-	-	-	-	-	√
Cr:Cu	-	-	√	√	√	√
Cr:Ni	-	-	-	√	√	√
Cr:Mn	-	-	-	-	√	√
Cr:Pb	-	-	-	-	-	√
Cu:Ni	-	-	-	√	√	√
Cu:Mn	-	-	-	-	√	√
Cu:Pb	-	-	-	-	-	√
Ni:Mn	-	-	-	-	√	√
Ni:Pb	-	-	-	-	-	√
Mn:Pb	-	-	-	-		√

n=56

To determine if metal interactions were antagonistic, additive, or synergistic an effect addition model was used with a model deviation ratio (MDR) based on the studies done by Cedergreen (2014) and Belden *et al.* (2007). The effect of the single metals compared to their relevant mixtures was used. The MDR was calculated as follows:

$$\mathbf{MDR = O_v/E_v}$$

$\mathbf{O_v}$ is the observed effect value (% Haemolysis) and $\mathbf{E_v}$ the expected additive effect value. An additive effect was indicated where 0. 5≤ MDR ≤ 2, antagonism where MDR < 0.5, and

synergism where MDR > 2. These limits were set according to Cedergreen (2014) to exclude false positives and to focus on combinations where the size of the interactions might be of quantitative importance, especially regarding synergistic interactions.

3.3.6 Data management and statistical analysis

Data for single metal exposure is an average of three independent experiments with each experiment done in triplicate, generating nine data points. Due to the large sample size when testing the metal combinations (79 samples) triple independent experiments with a single data point were undertaken, generating three data points. The results are expressed as mean ± standard error of mean (SEM), where each point is the average of the mean of the three experiments. Data was statistically evaluated using the Dunn's multiple comparisons test (one way ANOVA), with a p-value < 0.05 indicating a significant difference between data sets. This was done using GraphPad version 6.01 for Windows, GraphPad Software, San Diego California, USA.

3.4 Results and Discussion

Based on an extensive review of the literature the following metals were identified to have an impact on the health of the South African population. These metals were Cd, Co, Cr, Cu, Mn, Ni, Pb, and Hg.

3.4.1 Methodology optimisation.

Many transition metals are naturally coloured. In order to determine if these metals cause interference in the assay each metal as used in each experiment was incubated with only buffer (no erythrocytes) and the absorbance was measured at 570 nm. Only Cr^{3+} showed an increase in absorbance at 570 nm (Figure 3.3) (no Drabkin's).

Drabkin's reagent is widely used to quantify Hb levels in solution. This reagent contains potassium cyanide, potassium ferricyanide and sodium bicarbonate. It measures oxyhaemoglobin as well as carboxyhaemoglobin and methaemoglobin. The mechanism by which it measures Hb can be seen in Figure 3.1. It includes the conversion of the ferrous Hb iron into the ferric state, forming methaemoglobin. The stable pigment cyanomethaemoglobin is then formed due to the combination of cyanide with methaemoglobin. The two reactions are rapid as well as stoichiometric. The absorbance of the solution can then be spectrophotometrically measured at 540 nm and the Hb concentration thus determined (Hematology 1998).

Drabkin's reagent was added to metals incubated with only buffer, to ensure the metals did not react with Drabkin's reagent. An increase in absorbance was observed for Cd, Pb, Mn, and Co and to a lesser degree for Ni and Cu (Figure 3.3). Drabkin's reagent converts Fe^{2+} ion into Fe^{3+} ion, however all metals that show interference do not occur in the ionic 3+ form. Therefore a possible explanation is that metals such as Co form a chelate with cyanide to form yellow $K_3Co(CN)_6$.

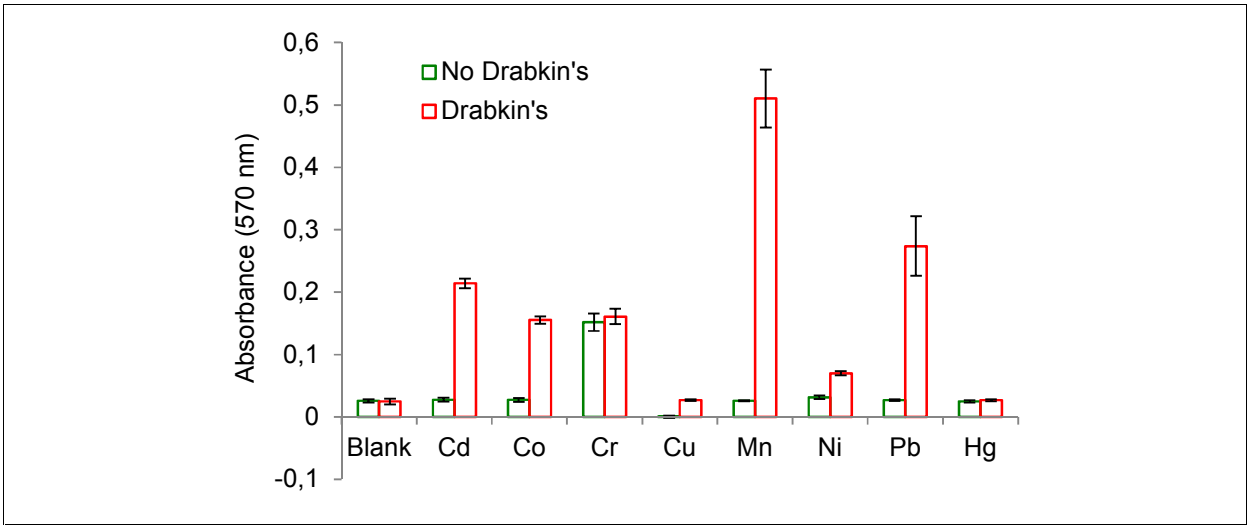

Figure 3.2: Comparison of absorbance readings at 570 nm, *of ex vivo* haemolysis assay without and with Drabkin's reagent, of supernatant of metals incubated with buffer only.

3.4.2 Induction of haemolysis by single metals

To determine the concentration of each metal where 10% haemolysis occurs, erythrocytes were exposed to increasing concentrations of each metal After 16 hrs incubation the extent of haemolysis was measured. With increasing concentrations of each metal there was a linear or exponential increase in haemolysis with a $R^2 > 0.97$ for all metals, as seen in Figure 3.3.

$CuSO_4$, as shown in Figure 3.3, did not cause much haemolysis, but erythrocytes exposed to Cu changed colour from red to brown and this was used as an indication of toxicity rather than haemolysis. The concentration range and the concentrations of each metal, determined from each experiment separately, that caused 10% haemolysis are presented in Table 3.3.

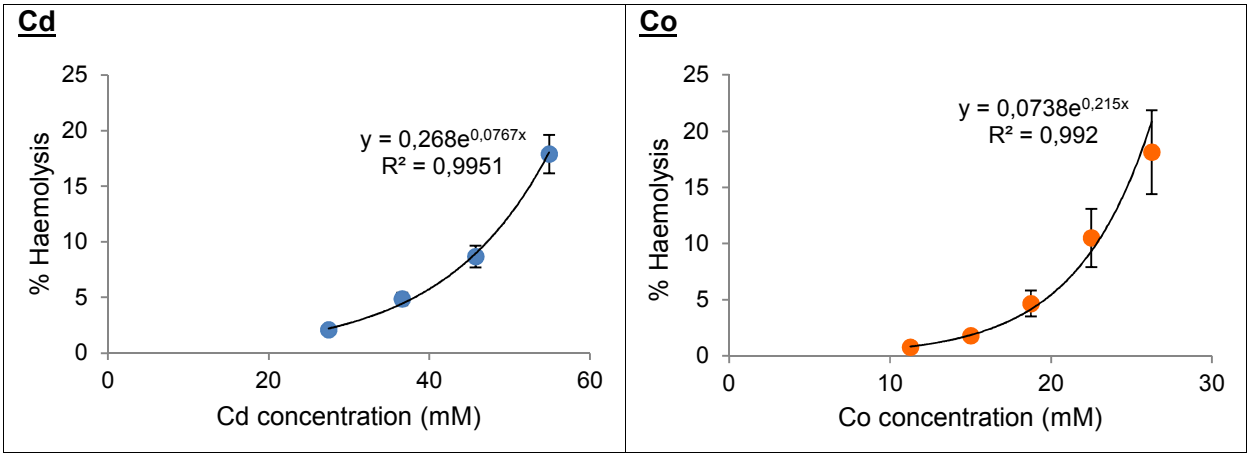

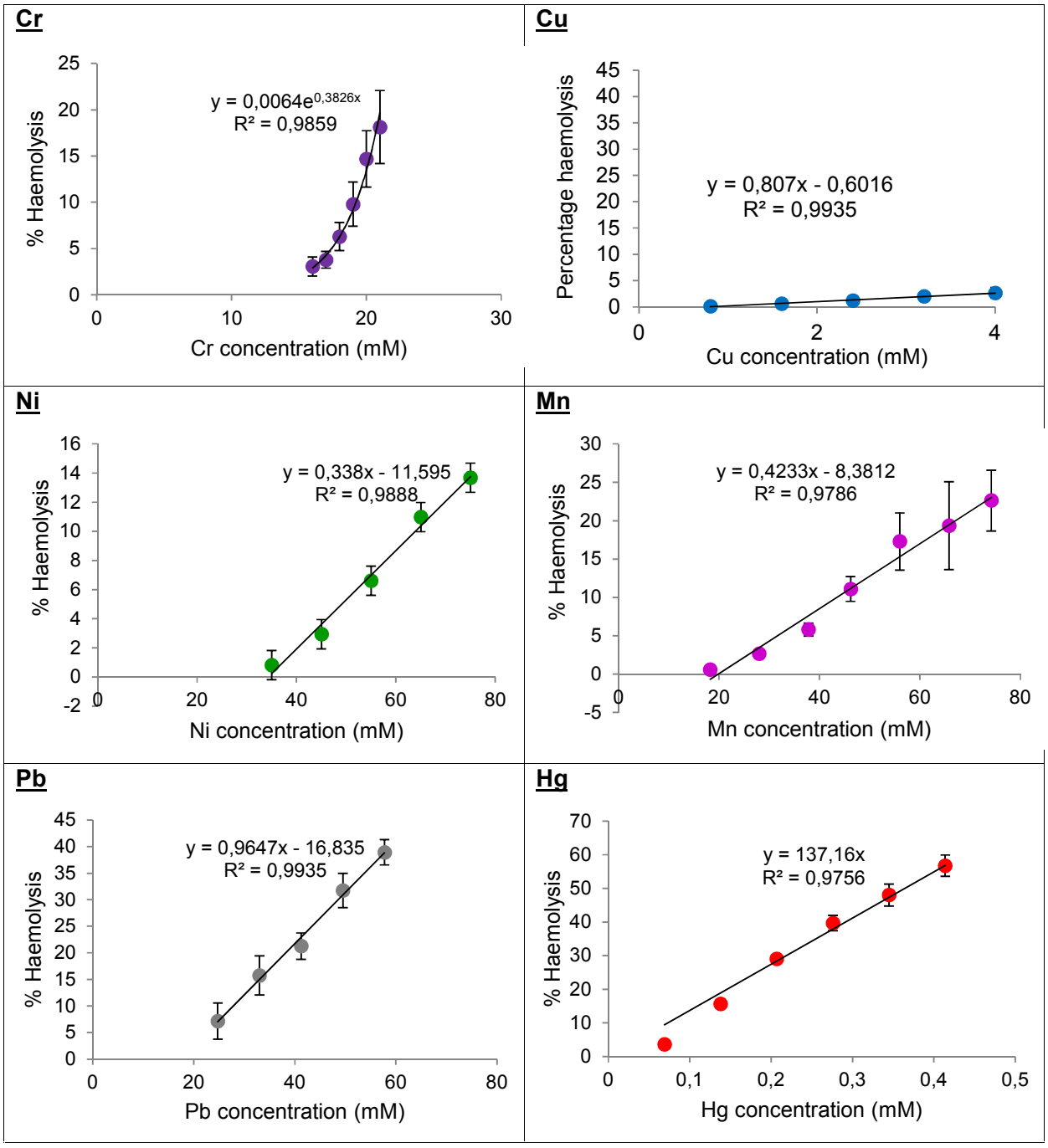

Figure 3.3: Ability of increasing concentrations of Cd, Co, Cr, Cu, Ni, Mn, Pb, and Hg to induce heamolysis in human erythrocyes. Data is an average of 3 independent experiments expressed as the mean ± standard error of the mean (SEM).

Table 3.3: Range, mean concentrations of metals that induce 10% haemolysis.

Metal	Cd	Co	Mn	Ni	Pb	Hg
Range (mM)	43-51	23-26	45-47	51-77	22-34	0.09-0.12
Mean ± SEM (mM)	48.3±1.43	24.9±0.58	46.4±0.43	65.8±6.61	25.7±3.1	0.1±0.006

* Cu caused significant colour change in cells at 4 mM

Using the equations of the respective functions generated for each metal the percentage haemolysis caused by 1 mM metal was calculated as follows: Hg (100%) >> Co (0.43%) > Cu (0.43%) > Pb (0.39%) > Mn (0.22%) > Cd (0.21%) > Ni (0.15%). Of these metals Co, Cu, Pb, Mn, Cd, and Ni showed similar toxicity while Hg was the most toxic.

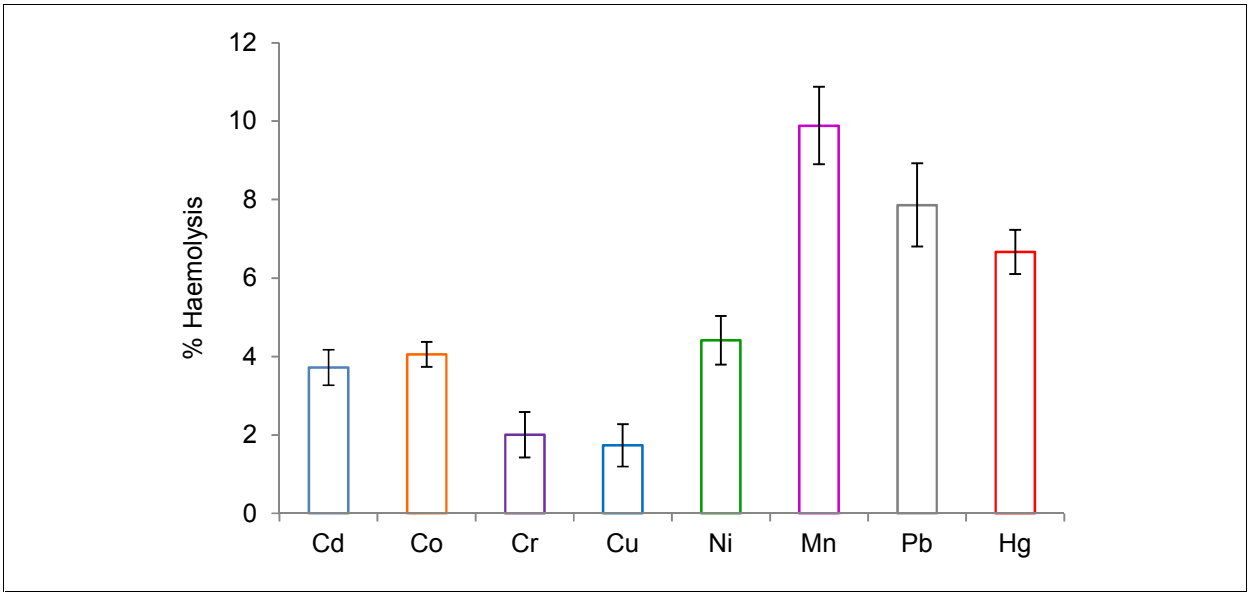

Figure 3.4: Percentage haemolysis caused by each metal at concentrations calculated to cause 10% haemolysis. Data is an average of 3 independent experiments expressed as the mean ± SEM.

Using the equations of the respective functions for each metal, in Figure 3.2, the concentration that caused 10% haemolysis was calculated and these were: Cd - 47 mM, Co - 23 mM, Ni - 69 mM, Mn - 43 mM, Pb - 31 mM, and Hg - 0.1 mM. For Cu a concentration of 4 mM was used as this was the concentration where a colour change was observed. These concentrations fell into the range determined from each experiment separately (Table 3.3) and were used in the mixture experiments. Erythrocytes were exposed to these determined concentrations. The results can be seen in Figure 3.4.

Table 3.4: HAEMOLYSIS ASSAY: Dunn's multiple comparisons test between single metals.

		P Value			P Value
Cd vs	**Co**	> 0.9999	**Co vs**	**Hg**	0.9267
	Mn	> 0.9999	**Mn vs**	**Ni**	> 0.9999
	Ni	> 0.9999		**Pb**	> 0.9999
	Pb	> 0.9999		**Hg**	0.1319
	Hg	*0.0067*	**Ni vs**	**Pb**	0.2679
Co vs	**Mn**	> 0.9999		**Hg**	*0.0004*
	Ni	0.6486	**Pb vs**	**Hg**	> 0.9999
	Pb	> 0.9999			

P-Value < 0.05 indicates significant difference; Italic: P-value < 0.01.

Statistically comparing the haemolysis caused by the metals at these determined concentrations showed only two statistically significant differences. These differences are between Cd and Hg and Ni and Hg as can be seen in Table 3.4. No statistically significant difference was expected as all concentrations were determined to cause 10% haemolysis. Due to the haemolysis assay being a biological assay the biological differences between blood samples could have had an effect on the results obtained. The use of 0.5 ml Eppendorf tubes instead of 2 ml Eppendorf tubes, due to limitations on stock, could also have had an effect since the reaction area would have been smaller. The expected 10% haemolysis according to the serial exposure (as seen in Figure 3.1) was thus not obtained as shown by the statistically significant differences between these metals.

3.4.3 Metal combinations causing more than 15% haemolysis

A total of 71 combinations were analysed. For the purpose of this dissertation a cut-off of > 15% haemolysis was selected, which is half of the expected additive values of the triple metal combinations. This was done to reduce the volume of data reported in this dissertation, reducing the number of combinations to 20 samples (Figure 3.5). For the double combinations these were Pb:Hg, Cd:Mn, Cd:Ni, Mn:Pb, Mn:Ni, and Co:Mn (Figure 3.5). For the triple combinations these were Cd:Ni:Pb, Cd:Mn:Pb, Cd:Co:Ni, Cd:Cu:Hg, Cd:Ni:Hg, Cu:Mn:Pb, Co:Cu:Hg, Cu:Mn:Hg, Cu:Pb:Hg, Co:Mn:Pb, Mn:Ni:Hg, Mn:Pb:Hg, Co:Mn:Hg, Mn:Ni:Hg, Mn:Pb:Hg, Co:Mn:Hg, and Cd:Co:Hg (Figure 3.5).

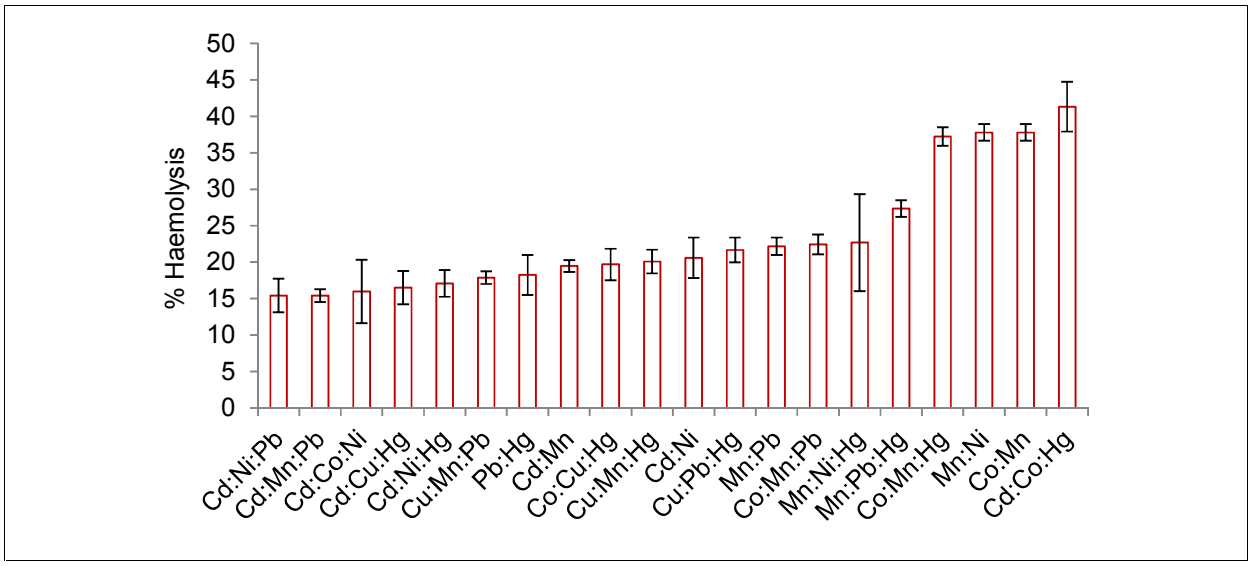

Figure 3.5: Metal combinations that caused more than 15% haemolysis from lowest to highest % haemolysis caused, at 47 mM, 23 mM, 20 mM, 10 mM, 69 mM, 43 mM, 31 mM, and 0.1 mM for Cd^{2+}, Co^{2+}, Cr^{3+}, Cu^{2+}, Ni^{2+}, Mn^{2+}, Pb^{2+}, and Hg^{2+} respectively. Data is an average of 3 independent experiments expressed as the mean ± SEM.

When comparing these combinations statistically with the single metals comprising the mixture (refer to Table 3.5), significant differences were seen. The percentage haemolysis caused by Pb:Hg, Cd:Mn:Pb, Cd:Co:Ni, and Mn:Ni:Hg doesn't differ significantly from the haemolysis caused by the separate metals they are made up of, meaning the addition of the other metals didn't have significant effects, even though these mixtures do cause more than 15% haemolysis. Cd:Mn and Mn:Ni differ significantly from Cd and Ni respectively, but not Mn, meaning the addition of Cd and Ni to Mn did not cause a significant increase in the haemolysis caused by Mn. Cd:Ni, Mn:Pb, and Co:Mn does however differ significantly from both metals they are made up of, meaning the combinations of these mixtures does cause a significant increase in the haemolysis caused compared to the metals on their own. Of the triple metal combinations, only Co:Cu:Hg, Cu:Pb:Hg, Mn:Pb:Hg, Co:Mn:Hg, and Cd:Co:Hg differed significantly from the haemolysis caused by the three separate metals they are made up of.

Table 3.5: HAEMOLYSIS ASSAY: Metal combinations for which significant differences were observed between single metals vs. double- and triple metal combinations causing > 15% haemolysis (Figure 3.5) (non-significant differences not included).

		P Value			P Value
Cd vs.	**Cd:Ni‡**	*0.0008*	**Mn vs.**	**Co:Mn:Hg**	*0.0009*
	Cd:Mn	*0.0003*		**Mn:Pb:Hg**	0.0259
.	**Cd:Co:Hg‡**	*< 0.0001*	**Ni vs.**	**Cd:Ni‡**	*0.0014*

	Cd:Ni:Hg	0.0102		**Mn:Ni**	0.0104
Co vs.	**Co:Mn‡**	*< 0.0001*		**Cd:Ni:Pb**	0.0373
	Cd:Co:Hg‡	*< 0.0001*		**Cd:Ni:Hg**	0.0142
	Co:Cu:Hg	0.0122	**Pb vs.**	**Mn:Pb**	0.0132
	Co:Mn:Pb	*0.0040*		**Co:Mn:Pb**	0.0243
	Co:Mn:Hg	*< 0.0001*		**Cu:Pb:Hg**	0.0365
Cu vs.	**Cd:Cu:Hg**	0.0110		**Mn:Pb:Hg**	0.0105
	Co:Cu:Hg	*0.0004*	**Hg vs.**	**Cd:Co:Hg‡**	*< 0.0001*
	Cu:Mn:Pb	*0.0010*		**Co:Cu:Hg**	0.0447
	Cu:Mn:Hg	*0.0002*		**Co:Mn:Hg**	*0.0001*
	Cu:Pb:Hg	*< 0.0001*		**Cu:Mn:Hg**	0.0318
Mn vs.	**Co:Mn‡**	*0.0002*		**Cu:Pb:Hg**	0.0129
	Mn:Pb	0.0366		**Mn:Pb:Hg**	*0.0049*

P-Value < 0.05 indicates significant difference; Italic: P-value < 0.01.
Key: ‡ – synergistic interaction

Table 3.6: HAEMOLYSIS ASSAY: Metal combinations for which significant differences were observed between double- vs. triple metal combinations causing > 15% haemolysis (Figure 3.5) (non-significant differences not included).

		P Value			**P Value**
Cd:Co vs.	**Cd:Co:Hg‡ ***	*0.0077*	**Co:Hg vs.**	**Co:Mn:Hg ***	0.0245
Cd:Cu vs.	**Cd:Cu:Hg ***	0.0326	**Cu:Hg vs.**	**Cu:Pb:Hg ***	0.0354
Co:Mn vs.	**Co:Cu:Mn**	0.0277	**Ni:Pb vs.**	**Cd:Ni:Pb ***	*0.0015*
Co:Pb vs.	**Co:Mn:Pb ***	*0.0040*	**Mn:Hg vs.**	**Co:Mn:Hg ***	0.0165
Co:Hg vs.	**Cd:Co:Hg‡ ***	*0.0062*			

P-Value < 0.05 indicates significant difference; Italic: P-value < 0.01.
Key: ‡ – synergistic interaction; * - differs significantly from one of the double metal mixtures it contains

Most of the significant differences seen are between the combinations and the single metals they were made up of. In Table 3.6 the significant differences between the haemolysis caused by the double metal combinations compared to the triple metal combinations are shown. Although Cd:Co:Hg differs significantly from Cd:Co and Co:Hg, it does not differ significantly from Cd:Hg (non-significant differences not included in Table 3.6), meaning the addition of Co to Cd:Hg does not cause a statistically significant increase in haemolysis. The same was seen when looking at Co:Mn:Hg where it differs significantly from Mn:Hg and Co:Hg, but not from Co:Mn (non-significant differences not included in Table 3.6), meaning the addition of Hg does not cause a statistically significant increase in the haemolysis caused by Co:Mn. Some of the other triple metal combinations also differ statistically from one of the double metal combinations

it contains (indicated by * in table 3.6), meaning that the addition of a third metal does not increase the haemolysis caused significantly.

3.4.4 Synergistic, antagonistic, and additive haemolytic effects of metals

Although there are statistical differences between single and double / triple metal combinations as well as between double and triple metal combinations this may not necessary translate into biological relevance. Also, statistical analysis does not identify whether differences are due to synergistic or antagonistic effects. For this reason MDR analysis was developed in order to identify drug, insecticide and in this study metal combinations that have a biologically relevant effect. To determine whether a combination of metals caused a synergistic, antagonistic, or additive effect, the MDR was calculated as shown in Table 3.7:

Table 3.7: HAEMOLYSIS ASSAY: Calculation of MDR.

Metal/s	Cd	Co	Hg	Cd:Co:Hg
Average % haemolysis	3.71856	4.05262	6.66621	41.3484
SEM	0.45346	0.29854	0.52665	3.42163

Add % haemolysis of single metals: Cd + Co + Hg = 0.45346 + 0.29854 + 0.52665 = **14.4374**

Divide observed value of triple metal combination by expected additive value: 14.44 / 41.35 = **2.86**

Calculated value > 2: synergistic interaction (if calculated value < 0.5 then antagonistic interaction)

According to Cedergreen (2014) synergistic effects are seen rarely and are found in approximately 5% of tested mixture combinations. It was found that of the double- and triple metal combinations tested in this study only four showed a synergistic effect; that is 7% of all combinations (Table 3.8).

In Figure 3.6 and Figure 3.7 the metal mixtures that caused synergistic- and antagonistic effects are shown. The observed interaction between the mixtures shown in Figure 3.6 is at least two fold greater than the expected, additive effects, thus synergistic. Metal combinations can also have an antagonistic effect i.e. the observed effect is less than the sum of the individual effects. The metal mixtures that had antagonistic interactions are shown in Figure 3.7.

The MDR, calculated using the observed- and expected effects, for all metal combinations is summarised in Table 3.8. For the double metal combinations interactions were synergistic for Cd:Ni, Co:Cu, Co:Mn, and antagonistic for Ni:Pb. The metal combination with the highest synergistic ratio, of 2.712, was Mn:Co. Only one triple metal combination had a synergistic toxic effect and this was Cd:Co:Hg with a ratio of 2.864. The MDR > 2 correlates with mixtures that

differ significantly (Table 3.6 and Figure 3.6) from the haemolysis caused by the single metals they are made up of, except the combination of Co and Cu. However, this mixture when compared to Cu has an adjusted p-value, when using Dunn's multiple comparisons test, of 0.0522, which is on the border of being significantly different.

An antagonistic effect was found for seven of the fifty-six evaluated triple combinations (12.5%). For double metal combinations, only Ni:Pb showed an antagonistic interaction, while for the triple metal combinations antagonistic effects were observed for Cd:Cu:Ni, Cd:Cu:Mn, Cd:Ni:Mn, Cd:Cu:Ni, Cd:Ni:Mn, and Ni:Mn:Pb (Figure 3.7). All MDR ratios were similar. Each antagonistic combination contained either Ni or Mn or both as seen in the combinations of Cd:Ni:Mn and Ni:Mn:Pb. Five of these metal mixtures which had an antagonistic effect contained Ni, two Mn and three Cu.

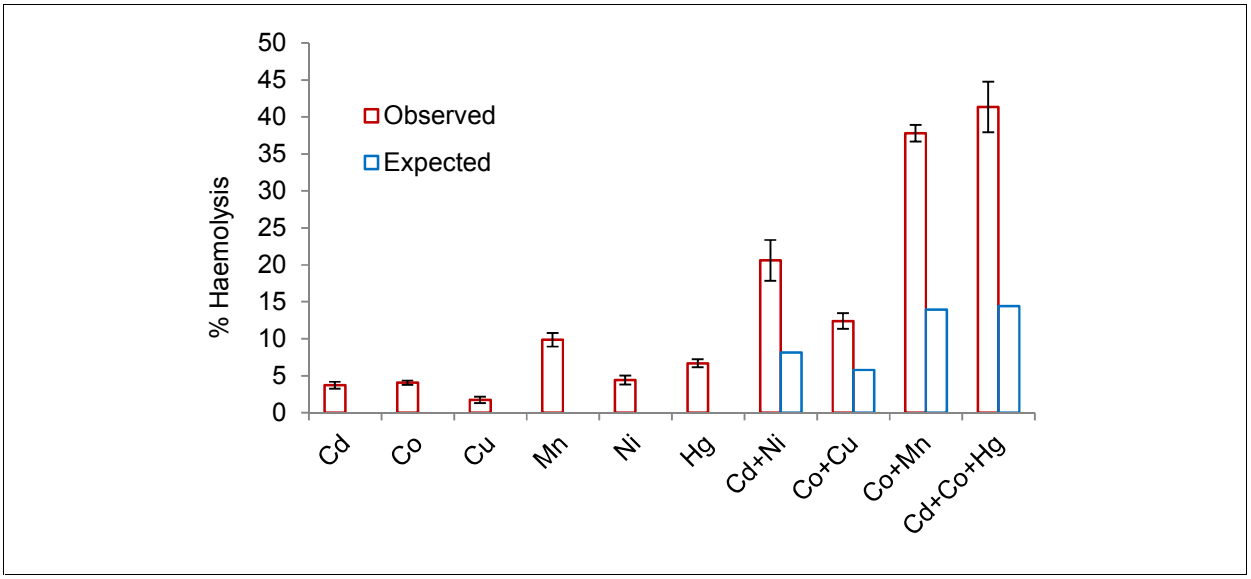

Figure 3.6: Synergistic effects (MDR > 2) found between double and triple metal combinations composed of Cd, Co, Cu, Mn, Ni, and Hg. Data is an average of 3 independent experiments expressed as the mean ± SEM.

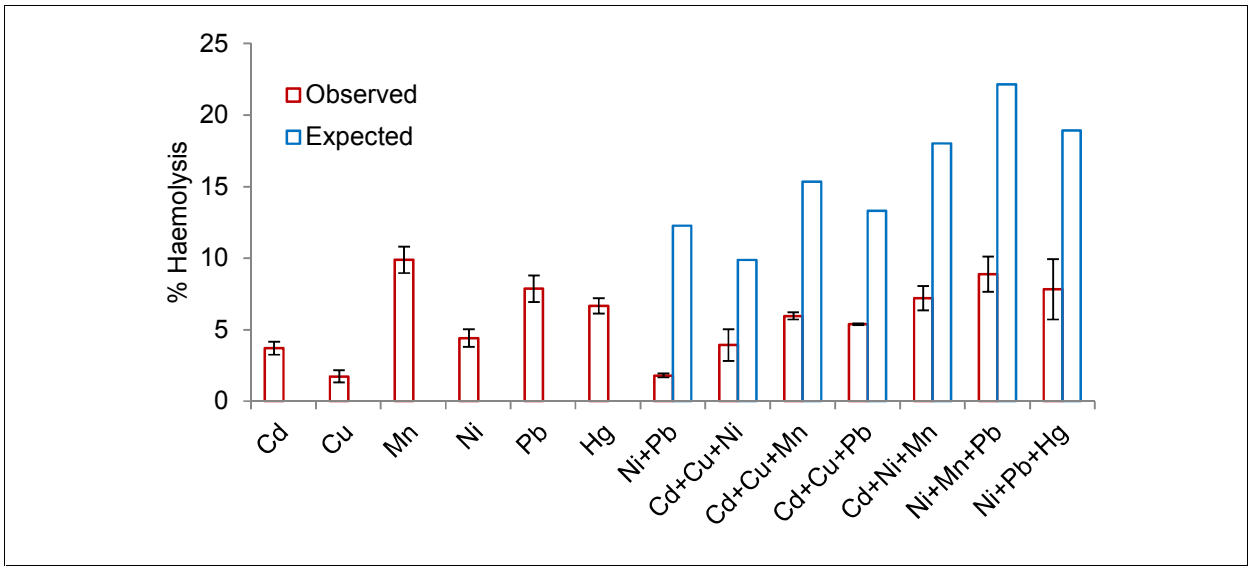

Figure 3.7: Antagonistic effects (MDR < 0.5) between double and triple combinations composed of Cd, Cu, Mn, Ni, Pb,and Hg. Data is an average of 3 independent experiments expressed as the mean ± SEM.

Mn and Cu play an essential role in the human body and thus could play a protective role in the metal mixtures. Although numerous studies found that Ni does cause haemolysis as well as oxidative effects (Das *et al.* 2007; Das *et al.* 2008), other studies have also found that Ni plays a protective role. Yuan *et al.* (2014) also found that Cd and Pb have an additive effect when rats were exposed to these metals simultaneously. This finding correlates with the finding in this study.

The toxicity of individual metals has been well described. Of the metals that contribute to synergism, Cd, Ni, and Hg are known to cause lipid peroxidation (Valko *et al*. 2005). Lipid peroxidation causes cellular damage leading to apoptosis as has been reported for Cd and Hg (Bertin & Averbeck 2006; Eisele *et al*. 2006). Kanter *et al.* (2009) determined that Cd changes rat erythrocyte membranes and cause haemolysis. Cd also has an effect on the antioxidant enzymes (Valko *et al*. 2005; Bertin & Averbeck 2006). Ni utilizes the Fenton reaction to produce hydroxyl radicals (Valko *et al*. 2005) while Ni and Hg both cause a decrease in the antioxidant enzymes (Valko *et al*. 2005; Pari & Amudha 2011).

Co, Cu and Mn are however essential metals and the assumption could be made that rather than instigating synergistic effects it should protect the cells. This study however found that Co and Mn in combination caused a 2.7 times increase in expected haemolysis. Indications are that although several metals are essential, at high concentrations these metals are toxic.

Horiguchi *et al.* (2004) found that rats exposed to Co present with methemoglobinuria due to the lysis of red blood cells and oxidation of iron in hemoglobin. Co as well as Mn causes lipid peroxidation and has an effect on antioxidant enzyme activity (Garoui *et al*. 2011; Chtourou *et al*. 2010). Co also utilizes the Fenton reaction (Valko *et al*. 2005). Cu is a catalyst in the Fenton reaction which generates hydroxyl radicals it also caused lipid peroxidation and decreased reduced glutathione (Rana 2008; Valko *et al*. 2005) but did not have an effect on the antioxidant enzymes.

Metals target several different antioxidant pathways and can cause radical formation, inhibit antioxidant molecules such as glutathione and/or enzymes. These effects alter cellular homeostasis, protein-, and membrane structure as well as -function which can lead to cell death. This effect is a function of metal concentration, exposure time, and the end point measured, and these are contributing factors to differences found between studies.

Chemotherapeutic drugs are effective at lower dosages especially when drug combinations are used. The most effective drug therapies are those that target different biochemical pathways or cellular processes. Likewise in this study metals may target different antioxidant molecules (Ahamed & Siddiqui 2007; Al-Fartosy *et al.* 2014) causing synergistic toxic effects. These effects were further evaluated in the following chapters.

Table 3.8: HAEMOLYSIS ASSAY: Synergistic, antagonistic and additive effect of mixtures of metals, calculated using the MDR.

	Co	Cu	Ni	Mn	Pb	Hg	Co	Cu	Ni	Mn	Pb	Hg
Cd	1.431	0.935	2.533	1.434	1.185	1.437	Add	Add	Syn	Add	Add	Add
Co	-	2.141	0.643	2.712	0.571	0.708	-	Syn	Add	Syn	Add	Add
Cu	-	-	1.849	1.175	1.036	1.583	-	-	Add	Add	Add	Add
Ni	-	-	-	1.064	0.147	0.656	-	-	-	Add	Ant	Add
Mn	-	-	-	-	1.250	0.897	-	-	-	-	Add	Add
Pb	-	-	-	-	-	1.542	-	-	-	-	-	Add
Cd:Co	-	0.880	1.314	0.834	0.895	2.864	-	Add	Add	Add	Add	Syn
Cd:Cu	-	-	0.399	0.389	0.404	1.363	-	-	Ant	Ant	Ant	Add
Cd:Ni	-	-	-	0.400	0.965	1.157	-	-	-	Ant	Add	Add
Cd:Mn	-	-	-	-	0.719	0.536	-	-	-	-	Add	Add
Cd:Pb	-	-	-	-	-	0.713	-	-	-	-	-	Add
Co:Cu	-	-	0.617	0.926	0.508	1.582	-	-	Add	Add	Add	Add
Co:Ni	-	-	-	0.652	0.885	0.986	-	-	-	Add	Add	Add
Co:Mn	-	-	-	-	1.030	1.806	-	-	-	-	Add	Add
Co:Pb	-	-	-	-	-	0.721	-	-	-	-	-	Add
Cu:Ni	-	-	-	0.776	0.503	1.0369	-	-	-	Add	Add	Add
Cu:Mn	-	-	-	-	0.918	1.099	-	-	-	-	Add	Add
Cu:Pb	-	-	-	-	-	1.333	-	-	-	-	-	Add
Ni:Mn	-	-	-	-	0.401	1.082	-	-	-	-	Ant	Add
Ni:Pb	-	-	-	-	-	0.413	-	-	-	-	-	Ant
Mn:Pb	-	-	-	-	-	1.122	-	-	-	-	-	Add

Key: ■ – antagonistic interaction; ■ – synergistic interaction

3.5 Conclusion

In this, *ex vivo* erythrocyte study, Hg was the most toxic of the single metals evaluated. Of the seventy-one combinations evaluated synergism was found for the mixtures Cd:Ni, Co:Cu, Co:Mn and Cd:Co:Hg. All combinations causing synergism contained either Cd or Co or both. An antagonistic effect was found for seven combinations and these were for Ni:Pb, Cd:Cu:Ni, Cd:Cu:Mn, Cd:Ni, Mn, Cd:Cu:Ni, Cd:Ni:Mn and Ni:Mn:Pb (Figure 3.6). Ni and Mn alone and in combination were major constituents of combinations that were found to be antagonistic. Cd:Co:Hg and Co:Mn caused the most haemolysis of all combinations evaluated.

Chapter 4: Heavy metal effects: Reduced glutathione depletion and catalysts of the Fenton reaction

4.1 Introduction

A possible explanation, for the synergistic- as well as other haemolysis seen in the previous chapter, is oxidative stress. Dubost *et al.* (2007) defined oxidative stress as the state in which the balance between pro-oxidants and antioxidants is disturbed resulting in an increased rate of oxidation. Oxidative stress can thus be induced by the depletion of antioxidant elements such as glutathione and/or via the formation of ROS.

Glutathione plays a major role as a reductant in oxidation-reduction processes. In the erythrocyte it exists principally in the reduced form (GSH) and is believed to act to protect the cell from the toxic effects of ROS. Normally, the concentration of GSH in human erythrocytes is ≈2 mM and that of the oxidised form (GSSG) is ≈4 μM (Kondo *et al.* 1980). Glutathione is present in two forms: oxidised as well as reduced, the ratio of these forms plays a fundamental role in cell homeostasis and qualitative or quantitative disturbances in this ratio are used to characterise oxidative stress in cells (Kand'ár *et al*. 2007; Hemmateenejad *et al*. 2009; Monostori *et al*. 2009). GSH is the reduced form as well as the predominant form; the best known oxidised form is GSSG (glutathione disulfide). GSSG is both enzymatically and non-enzymatically formed by GSH (Hemmateenejad *et al*. 2009).

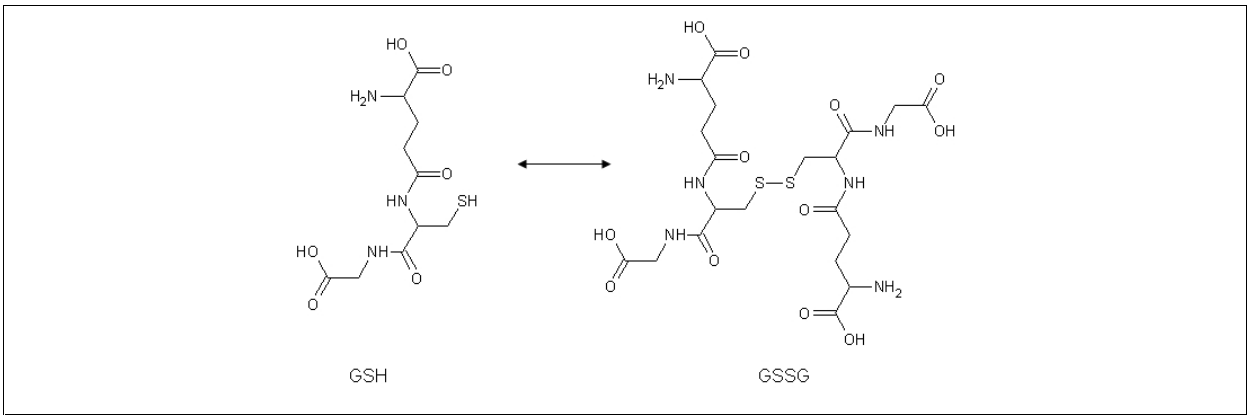

Figure 4.1: Reduced and oxidised glutathione (Adapted from: Sakhi *et al*. 2006).

The GSH-GSSG system is the most abundant redox system in eukaryotic cells (Monostori *et al*. 2009), it can thus be considered as a redox buffer (Hemmateenejad *et al*. 2009) and due to this

plays important roles in biological systems. It scavenges free radicals and is a strong defence against oxidative as well as nitrosative stresses. Adding to this, glutathione plays a role in the regeneration of other antioxidants including ascorbic acid and is a co-factor for multiple enzymes e.g. glutathione peroxidase (Kand'ár *et al*. 2007). In doing so, GSH is oxidised to GSSG which is either reduced enzymatically by glutathione reductase or excreted from cells into extracellular fluids (Sakhi *et al*. 2006). Because of the reducing action of the NADPH-dependant enzyme glutathione reductase, the cellular content of glutathione is predominantly in favour of GSH under normal physiological conditions. However, conditions causing oxidative stress would result in an increase in GSSG (Shaik & Mehvar 2006). Glutathione also plays a role in regulating cell proliferation and is involved in the signalling processes associated with apoptosis (Hemmateenejad *et al*. 2009; Monostori *et al*. 2009; Neumann *et al*. 2003) (refer to Figure 2.3). Glutathione loss has been linked with apoptosis and caspase activation in a number of cell types including macrophages (Boggs *et al*. 1998) and Jurkat T lymphocytes (Van den Dobbelsteen *et al*. 1996). Several pathological conditions are characterised by GSH deficiency or an imbalance in the GSH/GSSG ratio (Cai *et al*. 2003; Jones *et al*. 2002). These include viral infections (Cai *et al*. 2003) and age related degenerative diseases (Jones *et al*. 2002)

Glutathione is a tripeptide consisting of the three amino acids: glutamate, cysteine, and glycine (Kand'ár *et al*. 2007; Hemmateenejad *et al*. 2009). The biologically active site of glutathione is represented by the thiol group of the Cys residue (Monostori *et al*. 2009). It is also the most prevalent intracellular source of nonprotein thiols (Neumann *et al*. 2003). This is also the preferred derivatisation site for labelling of glutathione due to its specificity and for its function as protective group (Monostori *et al*. 2009). Glutathione can be obtained from the diet or can be synthesised by the liver (Kand'ár *et al*. 2007). It is well known for its antioxidant activity against both endogenous and exogenous reactive species. It is able to bind, transport and store several metals and these metals are more easily eliminated from the cell.

Not only can metals catalyse the formation of radicals but metals can also bind antioxidant elements such as GSH. Hg as well as Cd cause oxidative stress by indirectly causing the formation of ROS or by depleting the natural antioxidant mechanisms, including the depletion of GSH (Valko *et al*. 2005). Metals that can bind to glutathione include Cu, Zn, Cr, Hg, Cd, and Pb. This binding can lead to the detoxification of these metals (Nordberg *et al*. 2007); however excessive binding can cause the depletion of this essential antioxidant molecule.

Numerous studies have found that metals have an antioxidant effect by depleting GSH. In the review article done by Valko *et al*. (2005) it was found that Cd, Cu, Cr, Ni, and Hg cause GSH depletion. Ahamed & Siddiqui (2007) determined that Pb depletes GSH and Chtourou *et al*. (2010) also found depletion of GSH in adult rats when exposed to Mn.

In addition, ROS formation can lead to cellular oxidative damage. In the Fenton reaction Fe^{2+} is known to cause the decomposition of hydrogen peroxide (H_2O_2) which yields the hydroxyl radical - this is known as the Fenton reaction. Two components are necessary for hydroxyl radical formation and these are H_2O_2 which is present in intact erythrocytes when exposed to haemolytic agents (Cohen & Hochstein 1964) and oxidisable metal ions (Ou *et al*. 2002). Cu, Cr, Co, and Ni are metals known to form hydroxyl radicals through the interaction with H_2O_2 (Benedet & Shibamoto 2008). Living cells have an innate antioxidant system to defend them against the toxic effects of the interaction between H_2O_2 and metal ions (Ou *et al*. 2002). However in the presence of excessive amounts of H_2O_2 and/or metals this system becomes overburdened and this oxidative stress results in cellular death.

Although several studies have identified the mechanism whereby metals cause oxidative damage, few studies have compared the effects of metals or have investigated the effect of several metal combinations. Therefore the aim of this chapter was to determine which metals and metal mixtures binds GSH thereby depleting the cellular levels and/or catalyse the formation of hydroxyl radicals.

The specific objectives of this chapter were to:

1. Determine the metal concentrations where significant GSH depletion occurs.
2. Identify metals and metal combinations that cause increased depletion of GSH.
3. Identify metals and metal combinations that cause increased hydroxyl radical formation.
4. Identify metals and metal combinations that both deplete GSH and catalyse the formation of ROS.

4.2 Materials

4.2.1 Reagents, equipment and disposable plasticware

The same reagents stated in Chapter 3 were used in this Chapter. Other reagents include: GSH (98-100%), 5.5-Dithiobis(2-nitrobenzoic acid) (DTNB) (≥98%), H_2O_2 (30%) and flourescein sodium salt which were obtained from Sigma-Aldrich Company, Atlasville, SA.

Equipment used was: a FLUOstar Omega Fluorometer from BMG LABTECH, Germany. All other equipment, disposable laboratory ware and laboratory facilities were the same as in Chapter 3.

4.3 Methods

4.3.1 Preparation of metals

For exposure to a single metal, a concentration series of $CdCl_2$, $NiCl_2$, $CoCl_2$, $KCr(SO_4)_2$, $(CH_3COO)_2Pb$, $CuSO_4$, $MnCl_2$, and $HgCl_2$ was prepared, ranging from 0 – 10 mM, using distilled water. For exposure to double- and triple metal combinations, solutions were prepared at a final concentration of 1 mM for $NiCl_2$, $CoCl_2$, $KCr(SO_4)_2$, $(CH_3COO)_2Pb$, $MnCl_2$ and at 0.05 mM for $CuSO_4$ and $HgCl_2$.

4.3.4 Reduced glutathione depletion

The Ellman's method for quantifying thiol groups is based on the reaction of a thiol (RSH) such as GSH with DTNB to form a yellow dianion of 5-thio-2-nitrobenzoate (Figure 4.2).

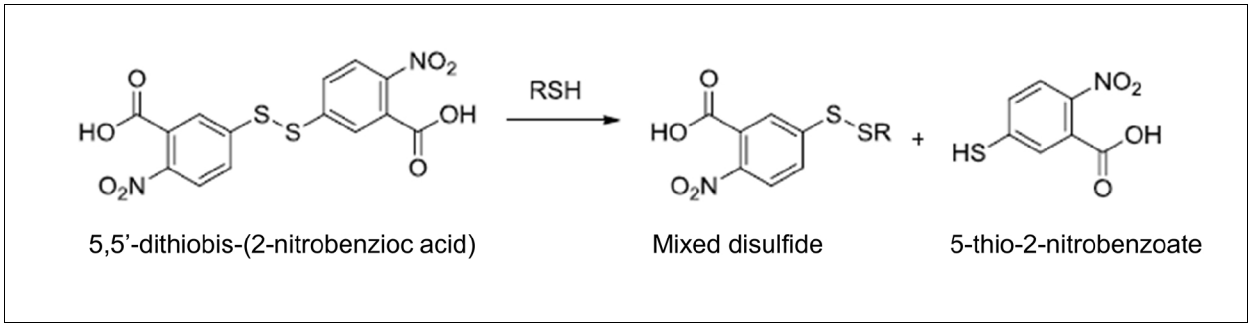

Figure 4.2: The reaction of a thiol group with DTNB (Adapted from: Peng *et al*. 2012).

For a standard curve a GSH concentration range of 0 – 0.25 mM was prepared. To the GSH in a volume of 50µl, 50 µl DTNB was added. The samples were mixed well and the absorbance was measured at 405nm.

To determine if individual metals or metal combinations bind GSH, a volume of 50 µl of the 0.45 mM GSH solution, giving a final concentration of 0.15 mM, were pipetted into each well of a 96 well plate. A volume of 50 µl of each metal and metal combination was added to their respective wells. The solutions were mixed well, after which 50 µl DTNB was added to each well. The spectrophotometric absorbance of each well was read immediately at 405 nm. The control solutions were prepared as follows:

1. 0% depletion (Blank): 100 µl buffer added to 50 µl DTNB.
2. 100% GSH: 50 µl buffer added to 50 µl GSH and 50 µl DTNB.

Depletion was calculated as % depletion, using the following formula:

% Depletion = (Sample – Blank) / (100% GSH – Blank) x 100

4.3.5 Fenton reaction (hydroxyl radical averting capacity assay)

The Hydroxyl Radical Averting Capacity (HORAC) assay was developed by Ou *et al.* (2002) to determine the metal-chelating capacity of polyphenolic compounds. In this method Ou *et al.* (2002) used Co(II) and H_2O_2 to generate hydroxyl radicals, these radicals then react with the added fluorescein. The fluorescence decay curve of fluorescein is then used to determine the scavenging ability of the evaluated antioxidants (MacDonald-Wicks *et al*. 2006). In this study this assay was used to determine which metals and metal mixtures can catalyse the Fenton reaction, resulting in radical formation.

Fluorescein sodium salt (0.0225 g) was dissolved in 50 ml phosphate buffered saline and stored in a freezer at -20ºC. A volume of 10 µl of the stock solution was added to 10 ml isoPBS and a 10% dilution was made from the latter solution which was used as the working solution. A volume of 10 µl of each metal / metal mixture was added to separate wells in a 96 well plate. To each well 180 µl fluorescein (working solution) was added. After 2 minutes incubation at 37ºC, 20 µl H_2O_2 was added to each well. The change in fluorescence was read at an excitation wavelength of 485 nm and emission at 520, twice every minute for 30 cycles. The control solution was prepared as follows:

1. 0% ROS production (Blank): 10 µl buffer added to 180 µl fluorescein and 20 µl H_2O_2.

Formation of ROS was indicated by a decrease in the relevant fluorescent unit reading and all data was reported as the positive gradient.

4.3.6 Determination of combination effect

Metal interactions were determined using the same MDR as in the previous chapter, using the following equation:

$$\mathbf{MDR = O_v/E_v}$$

$\mathbf{O_v}$ is the observed effect value (for this Chapter either % GSH depletion or calculated gradient) and $\mathbf{E_v}$ the expected additive effect value. An additive effect was indicated where $0.5 \leq MDR \leq 2$; antagonism where $MDR < 0.5$, and synergism where $MDR > 2$.

4.3.7 Data management and statistical analysis

Data for single metal exposure is an average of three experiments with each experiment done in triplicate, generating nine data points. For double and triple metal exposure data is an average of at least three single point experiments; 92 samples had to be tested making a three point experiment for all samples unattainable. The results are expressed as mean ± SEM, where each point is the average of the mean of three independent experiments. Data was statistically evaluated using the Dunn's multiple comparisons test (one way ANOVA), with a p-value < 0.05 and 0.01 indicating a significant difference between data sets. This was done using GraphPad version 6.01 for Windows, GraphPad Software, San Diego California, USA.

4.4 Results and Discussion

4.4.1 Metal binding to reduced glutathione

4.4.1.1 Methodology optimisation

Metals can bind the thiol group of GSH, thereby reducing intracellular levels of the antioxidant GSH. To investigate the ability of metals alone or in combination to bind GSH, the amount of GSH levels were quantified using DTNB. For the standard curve with increasing GSH concentrations a linear increase in absorbance was observed (R^2 = 0.9995) (Figure 4.3). To measure the ability to bind GSH and reduce the ability of GSH to bind DTNB a final GSH concentration of 0.15 mM was used. At this concentration the absorbance of GSH reacted with DTNB was 1.00.

The addition of DTNB to the metals on their own (without any GSH) did mostly not cause an increase in spectrophotometric readability. It was however found that Pb had a statistically significant spectrophotometric reaction with DTNB on its own. To calculate the correct decrease of GSH caused by Pb, the reading of the reaction of Pb with DTNB on its own is subtracted, as shown in Figure 4.4. This correction indicated that Pb did cause GSH depletion at concentrations of 1 mM and higher even though initially this was not observed.

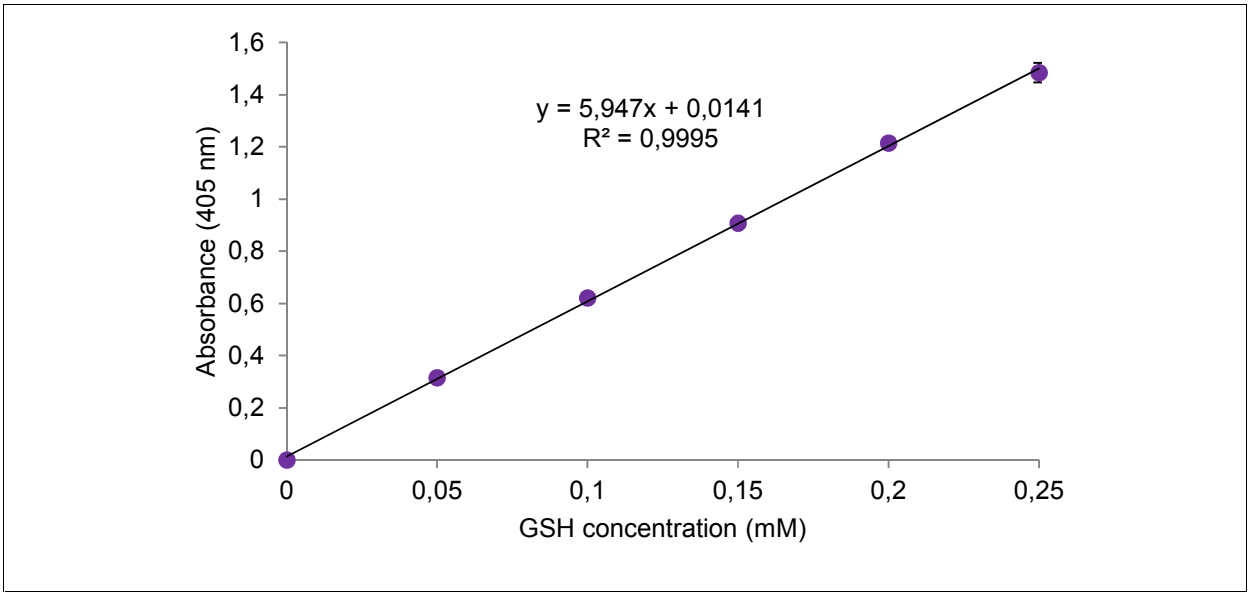

Figure 4.3: Standard curve of GSH measured with DTNB. Data is an average of 3 independent experiments expressed as the mean ± standard error of the mean (SEM).

Most metals and metal combinations did not interfere with the measurement of absorbance at 405nm. However, Pb does bind DTNB (Figure 4.4) and therefore the reading of the reaction of Pb with DTNB on its own is subtracted, as shown in Figure 4.4. This correction indicated that Pb did cause GSH depletion at concentrations of 1 mM and higher even though initially this was not observed.

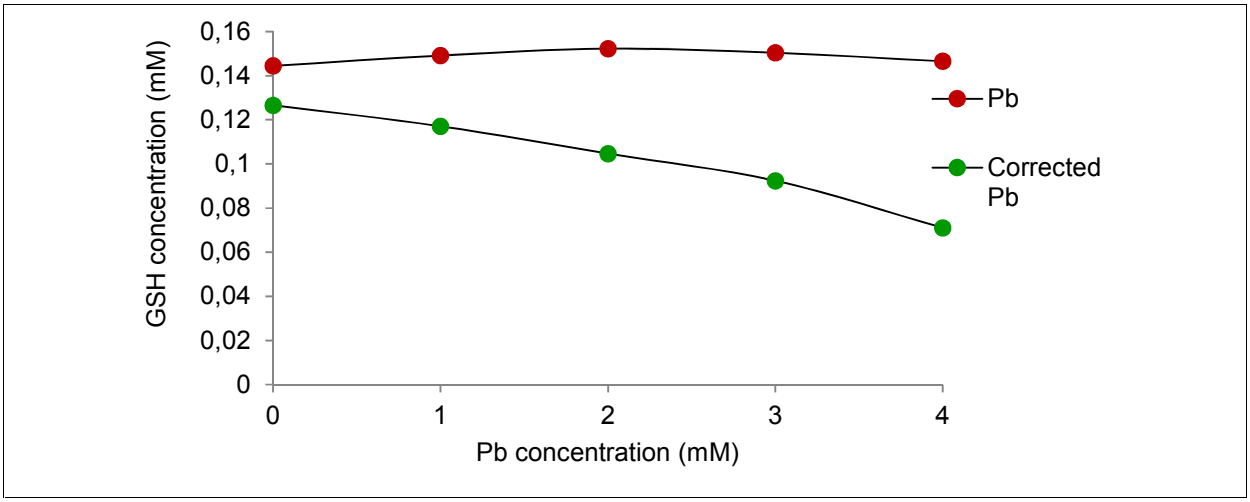

Figure 4.4: The correct decrease in GSH concentration caused by Pb as can be seen when the reaction of Pb with DTNB on its own is subtracted. Data is an average of 3 independent experiments expressed as the mean ± SEM.

4.4.1.2 Reduced glutathione depletion when exposed to single metals

As shown in Figure 4.5, 0 – 0.4 mM Cd, Cr and Pb while 0 – 0.08 mM Cu and Hg bound GSH and this would result in GSH depletion. This finding correlates with the findings by Valko *et al*. (2005) and Ahamed & Siddiqui (2007) who stated that Cd, Cu, Cr, Hg, and Pb causes GSH depletion. Chtourou *et al*. (2010) exposed rats to manganese chloride in their drinking water and tested the GSH levels in the cerebral cortex of the rats. A significant decrease in the GSH levels in the cerebral cortex of the rats was observed. In a literature review done by Valko *et al*. (2005) the authors also found that Ni depletes GSH. The depletion of GSH by Ni and Mn were not confirmed using this chemical assay.

In order to test the effect of mixtures of metals on GSH depletion one concentration was chosen for each metal. Cd, Co, Cr, Mn, Ni, and Pb were prepared at a final reaction concentration of 1 mM and Cu and Hg at a final concentration of 0.05 mM. The difference in concentration was necessitated due to Cu and Hg causing significant depletion at this low concentration. When comparing these concentrations to the concentrations that caused haemolysis in Chapter 3, it is clear that GSH depletion occurs before haemolysis. This is also illustrated in Figure 2.3.

Korashy & El-Kadi (2008) also found that Hg^{2+} and Cu^{2+} did cause intracellular depletion at concentrations of higher than 5 µM, but that Pb^{2+} only caused depletion at a concentration of 100 µM. Flora *et al*. (2013) did however find blood GSH depletion in mice exposed to Pb in their drinking water. After exposing rats to Cu, Roy *et al.* (2009) also found a significant decrease of the GSH/GSSG ratio indicating the oxidation of GSH to GSSG. Wang *et al.* (2012) found significantly decreased levels of GSH in the placenta of pregnant mice injected with $CdCl_2$. A significant decrease in GSH levels were seen after exposure to Mn in a study done by Huang *et al.* (2011).

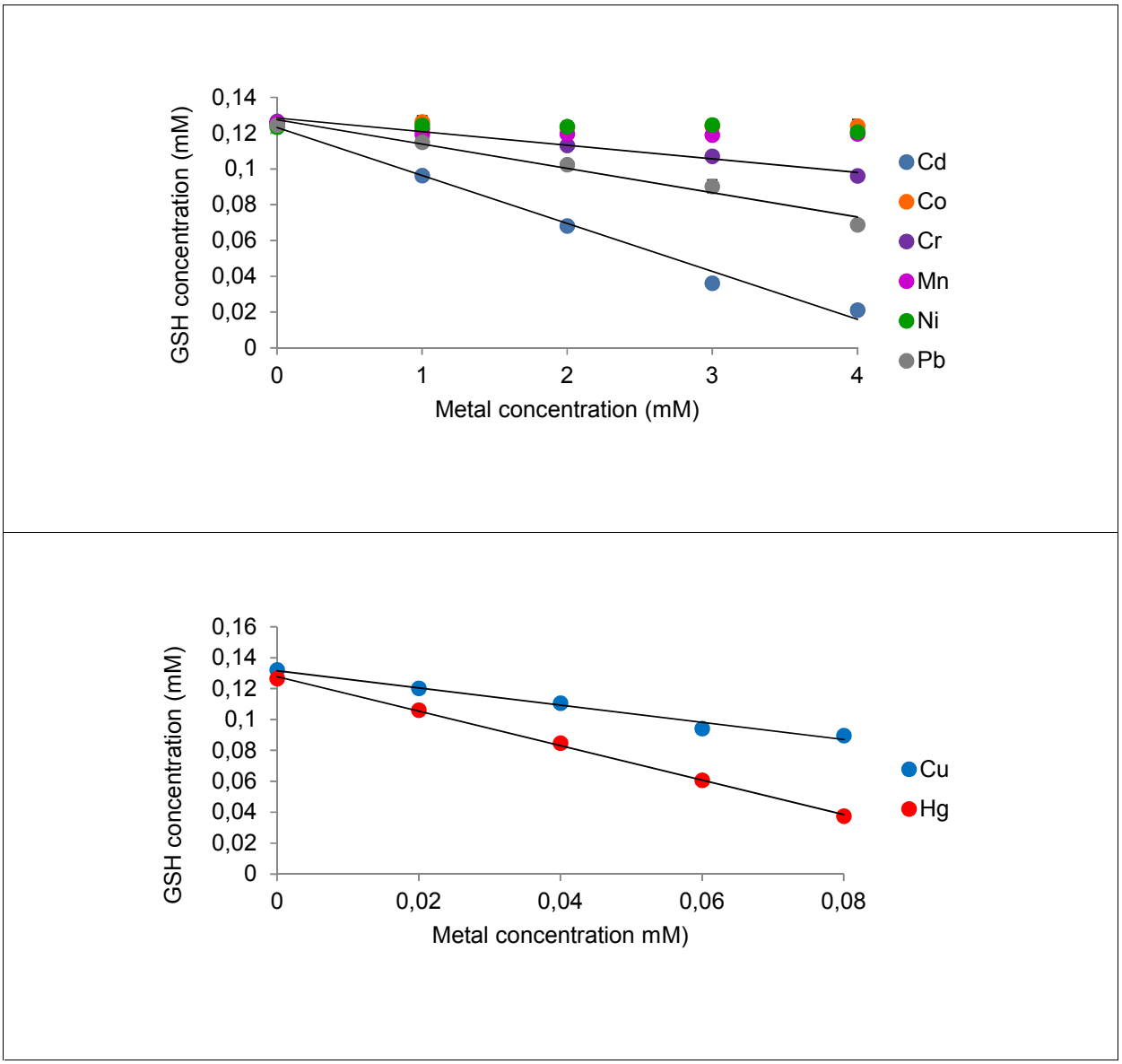

Figure 4.5: Ability of increasing concentrations of Cd, Co, Cr, Cu, Ni, Mn, Pb, and Hg to bind to GSH. With Cu and Hg at a concentration range of 0 – 0,08 mM and the rest at a concentration range of 0 – 4 mM. Data is an average of 3 independent experiments expressed as the mean ± SEM.

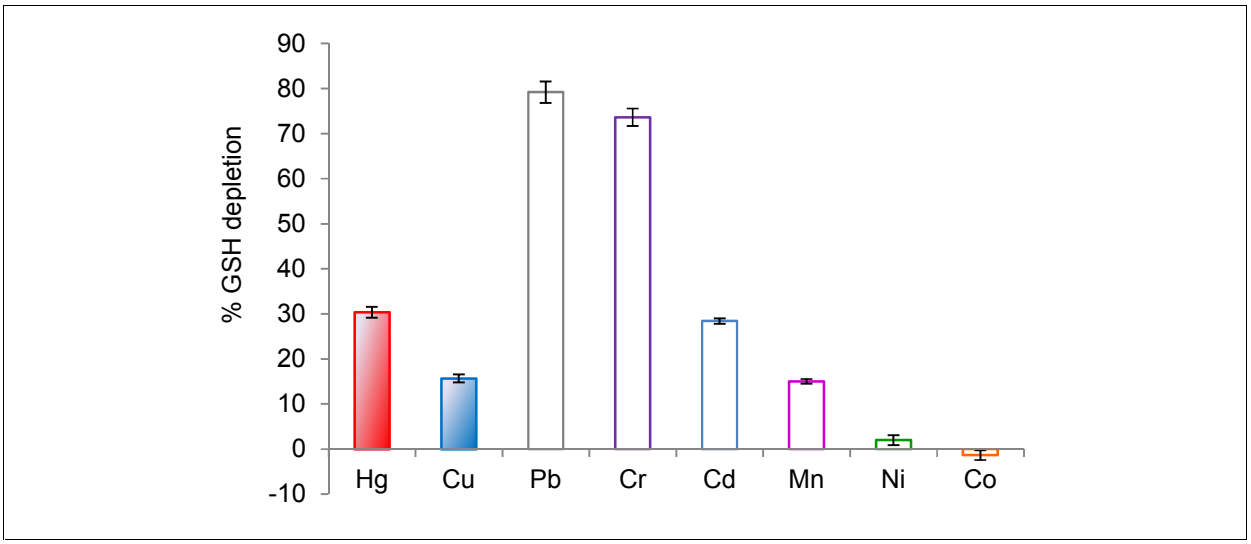

Figure 4.6: Ranking of increasing metal induced GSH depletion. Data is expressed as % GSH depletion for each metal at a concentration of 0.05 mM for Cu and Hg and 1 mM for Cd, Co, Cr, Mn, Ni, and Pb. . Data is an average of 3 independent experiments expressed as the mean ± SEM.

The % GSH depletion (with a higher percentage indicating more depletion) at these concentrations is indicated in Figure 4.6. Hg and Cu were evaluated at a concentration of 0.05 mM and all other metals at 1mM. When the % GSH depletion for each metal was evaluated at 0.05mM the order of GSH depletion was as follow: Hg: 30.38% > Cu: 15.69% > Pb: 4% > Cr: 3.7% > Cd: 1.4% > Mn: 0.75% > Ni: 0.1% > Co: 0%. At these concentrations there were a few statistically significant differences between the metals as can be seen in Table 4.1. Dunn's multiple comparison test revealed differences were significant between Hg and Co, Mn, and Ni respectively, also between Co and Cr, Cu, and Pb respectively; and between Cu and Ni. The significant difference between Co and Cr, Cu, Pb and Hg can also be visualised using Figure 4.5, as it is clear that Co did not cause any GSH depletion.

Table 4.1: GSH DEPLETION: Dunn's multiple comparisons test between single metals at 1 mM.

		P Value			P Value
Cd vs.	**Co**	0.4523	**Cu vs.**	**Mn**	0.2962
	Cr	> 0.9999		**Ni**	*0.0345
	Cu	> 0.9999		**Pb**	> 0.9999
	Mn	> 0.9999		**Hg**	> 0.9999
	Ni	> 0.9999	**Mn vs.**	**Ni**	> 0.9999
	Pb	> 0.9999		**Pb**	> 0.9999
	Hg	0.2962		**Hg**	*0.0345
Co vs.	**Cr**	*0.0447	**Ni vs.**	**Pb**	0.3669

	Cu	**0.0003*		**Hg**	**0.0027*
	Mn	> 0.9999	**Pb vs.**	**Hg**	> 0.9999
	Ni	> 0.9999			
	Pb	**0.0066*			
	Hg	**< 0.0001*			
Cr vs.	**Cu**	> 0.9999			
	Mn	> 0.9999			
	Ni	> 0.9999			
	Pb	> 0.9999			
	Hg	> 0.9999			

P-Value < 0.05 indicates significant difference, Italic: P < 0.01.
Key: * significant difference

4.4.1.2 Metal combinations causing more than 80% GSH depletion

Using the concentrations in Figure 4.6, the double and single combinational effects were evaluated. Again the effect of combinations that showed GSH binding greater than measured for Pb alone were evaluated. The metal combinations that caused more than 80% GSH depletion are ranked from least to most GSH depletion in Figure 4.7.

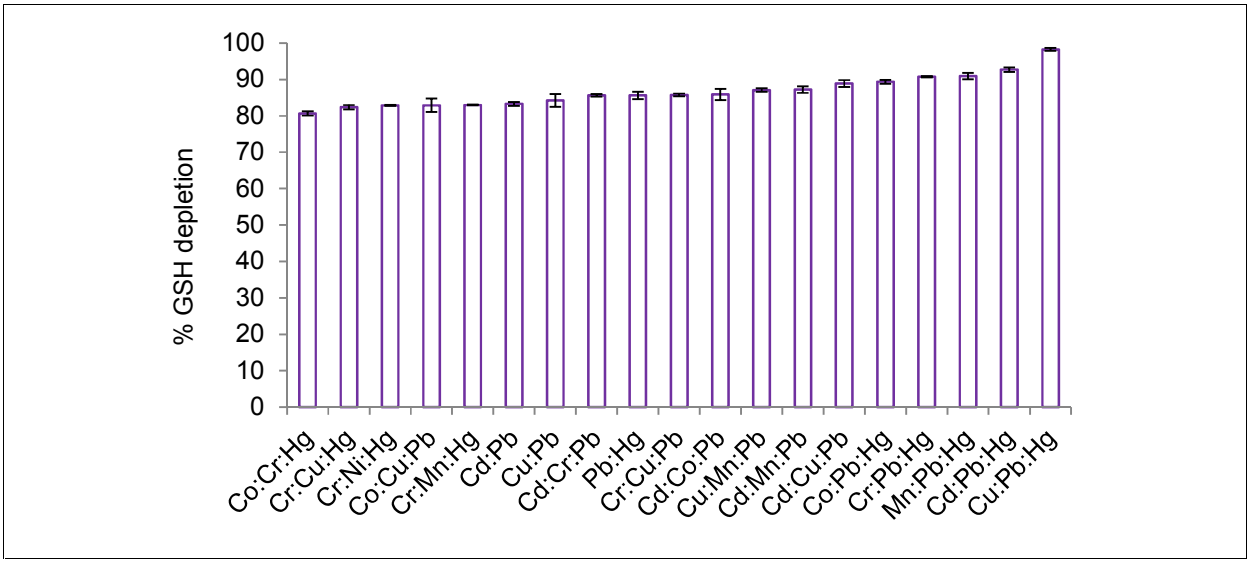

Figure 4.7: Ranking of metal combinations that caused more than 80% GSH depletion with a final concentration of 1 mM for Cd, Co, Cr, Mn, Ni, and Pb; Cu and Hg at 0.05 mM. Data is an average of 3 independent experiments expressed as the mean ± SEM.

All the combinations causing more than 80% depletion (Figure 4.7) either contains Pb or Hg or both Pb and Hg, indicating that GSH depletion is an important mechanism of oxidative damage

utilised by these two metals. It is also interesting to note that the 5 combinations causing the most GSH depletion contain Pb as well as Hg.

Table 4.2: GSH DEPLETION: Metal combinations for which significant differences were observed between single metals vs. double- and triple metal combinations causing > 80% GSH depletion (Figure 4.7) (non-significant differences not included).

		P Value			P Value
Cd vs.[1]	**Cd:Pb**	0.0432	**Cu vs.[2]**	**Co:Cu:Pb**	0.0496
	Cd:Co:Pb	0.0183		**Cr:Cu:Pb**	0.0252
	Cd:Cr:Pb	0.0218		**Cu:Mn:Pb**	*0.0097*
	Cd:Cu:Pb	*0.0069*		**Cu:Pb:Hg**	*0.0033*
	Cd:Mn:Pb	0.0120	**Mn vs.**	**Cd:Mn:Pb**	0.0173
	Cd:Pb:Hg	*0.0032*		**Cr:Mn:Hg**	0.0387
Co vs.	**Cd:Co:Pb**	*0.0034*		**Cu:Mn:Pb**	0.0183
	Co:Cr:Hg	*0.0088*		**Mn:Pb:Hg**	*0.0078*
	Co:Cu:Pb	*0.0061*	**Ni vs.**	**Cr:Ni:Hg**	*0.0024*
	Co:Pb:Hg	*0.0017*	**Pb vs.[1,2]**	**Cd:Pb:Hg**	0.0366
Cr vs.	**Cd:Cr:Pb**	*0.0088*		**Cu:Pb:Hg**	0.0194
	Cr:Cu:Pb	*0.0073*	**Hg vs.[1,2]**	**Pb:Hg**	0.0346
	Cr:Cu:Hg	0.0355		**Cd:Pb:Hg**	*0.0044*
	Cr:Mn:Hg	0.0275		**Co:Pb:Hg**	0.0194
	Cr:Ni:Hg	0.0317		**Cr:Pb:Hg**	0.0100
	Cr:Pb:Hg	*0.0034*		**Cu:Pb:Hg**	*0.0021*
Cu vs.[2]	**Cu:Pb**	0.0318ty		**Mn:Pb:Hg**	*0.0078*
	Cd:Cu:Pb	*0.0067*			

P-Value < 0.05 indicates significant difference, Italic: P < 0.01.
Key: 1 - differs significantly from Cd:Pb:Hg; 2 - differs significantly from Cu:Pb:Hg

Some statistically significant differences can be seen in Table 4.2 between the combinations of metals causing 80% depletion and the single metals they are made up of. However, only two of the combinations differ statistically from all three metals that were combined in the mixture. These combinations are Cu:Pb:Hg and Cd:Pg:Hg – the two combinations causing the most GSH depletion at 92.68% and 98.2% respectively.

Table 4.3: GSH DEPLETION: Metal combinations for which significant differences were observed between double- vs. triple metal combinations causing > 80% GSH depletion (Figure 4.7) (non-significant differences not included).

		P Value			P Value
Cd:Co vs.			**Cr:Ni vs.**	**Cr:Ni:Hg**	0.0204
	Cd:Co:Pb	*0.0038*	**Cr:Pb vs.**	**Cr:Cu:Pb**	0.0420
Cd:Cr vs.	**Cd:Cr:Pb**	0.0253		**Cr:Pb:Hg**	*0.0030*
Cd:Cu vs.	**Cd:Cu:Pb**	0.0106	**Cr:Hg vs.**	**Cr:Pb:Hg**	*0.0037*
Cd:Mn vs.	**Cd:Mn:Pb**	0.0419	**Cu:Mn vs.**	**Cu:Mn:Pb**	*0.0048*
Cd:Pb vs.[1]	**Cd:Pb:Hg**	0.0281	**Cu:Hg vs.**[2]	**Cr:Cu:Hg**	0.0253
Cd:Hg vs.[1]	**Cd:Pb:Hg**	0.0280		**Cu:Pb:Hg**	*0.0033*
Co:Cr vs.	**Co:Cr:Hg**	*0.0095*	**Mn:Pb vs.**	**Mn:Pb:Hg**	0.0280
Co:Cu vs.	**Co:Cu:Pb**	*0.0038*	**Mn:Hg vs.**	**Mn:Pb:Hg**	0.0379
Co:Pb vs.	**Co:Pb:Hg**	0.0228	**Ni:Hg vs.**	**Cr:Ni:Hg**	*0.0038*
Co:Hg vs.	**Co:Cr:Hg**	0.0184	**Pb:Hg vs.**[2]	**Cu:Pb:Hg**	0.0185
	Co:Pb:Hg	*0.0023*			
Cr:Cu vs.	**Cr:Cu:Pb**	0.0149			
Cr:Mn vs.	**Cr:Mn:Hg**	0.0149			

P-Value < 0.05 indicates significant difference, Italic: P < 0.01.

Cu:Pb:Hg and Cd:Pg:Hg also differs statistically when compared to the mixture of 2 metals that are contained in the 3 metal mixture, as can be seen in Table 4.3. Cu:Pb:Hg differs significantly from Cu:Hg and Pb:Hg, but not from Cu:Pb, meaning that the addition of Hg to Cu:Pb did not cause a significant increase. Cu:Pb did not however cause a more than 80% GSH depletion. Cd:Pb:Hg differs significantly from Cd:Pb and Cd:Hg, but not form Pb:Hg, indicating the addition of Cd to Pb:Hg does not cause a significant GSH depletion increase. Figure 4.8 shows these combinations as well as the effect the metals have on their own and in double combinations.

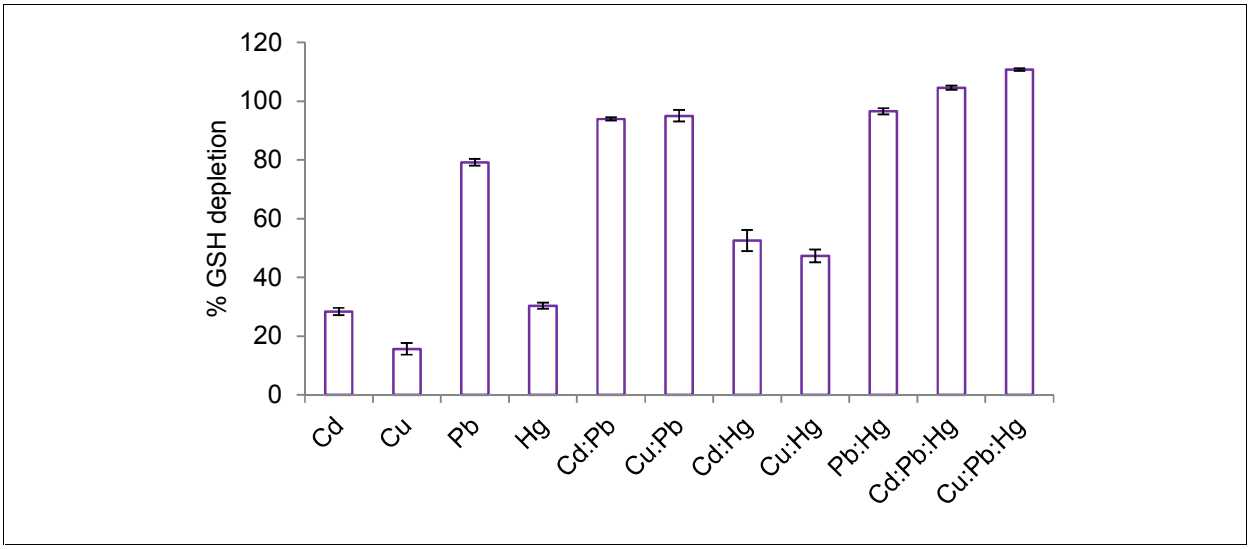

Figure 4.8: The two 3 combination mixtures which showed statistically significant difference from each single metal it contains. Data is an average of 3 independent experiments expressed as the mean ± SEM.

Agrawal *et al.* (2015) exposed male Wistar rats to Pb, Hg, and As, singularily and in combination, in their drinking water. Using the method of Ellman, the same used in this study, they also found that the combination of Pb and Hg caused significant GSH depletion in rat kidneys and -blood, possibly due to Pb and Hg binding GSH and the inhibition of glutathione reductase activity.

4.4.1.3 Synergistic, antagonistic, and additive effects of metals

The calculation of the MDR in Table 4.4 indicated that all mixtures had an additive effect. This was expected, seeing that this assay is a chemical assay. Therefore synergism of GSH depletion in biological systems may be due to the metals targeting different sites in this pathway such as the inhibition of glutathione reductase activity responsible for GSH synthesis as reported by Agrawal *et al.* (2015) as well as the binding of GSH with the pro-oxidants produced by an increase in ROS.

The best indication of GSH depletion in the human body would have been to determine it by using a biological system, e.g. cells. The prevention of GSH-auto-oxidation is important when measuring the GSH levels in biological samples. Cereser *et al.* (2001) found GSH oxidation in blood samples to be especially significant, even when cells were stored at -80ºC a rapid decrease in the amount of GSH was seen. To prevent this oxidation acid deproteinisation was done as quickly as possible in erythrocyte samples and these samples were either immediately

analysed or stored at -80ºC (Cereser *et al.* 2001). Although evaluated it was not possible to determine the effects of metals and metal combinations on GSH levels *ex vivo.* Storage of erythrocytes and the duration of each experiment would result in GSH auto-oxidation. Therefore it was not possible to determine if the observed effects was due to auto-oxidation of GSH or due to GSH depletion by the metals. Erythrocyte cellular GSH depletion could thus not be measured.

Table 4.4: GSH DEPLETION: Synergistic, antagonistic and additive effect of mixtures of metals, calculated using the MDR.

	Co	Cr	Cu*	Ni	Mn	Pb	Hg*	Co	Cr	Cu	Ni	Mn	Pb	Hg
Cd	1.037	0.777	0.903	0.907	0.809	0.873	0.894	Add	Add	Add	Add	Add	Add	Add
Co	-	1.063	1.041		0.894	1.001	1.025	-	Add	Add		Add	Add	Add
Cr	-	-	0.919	1.026	0.809	0.622	0.852			Add	Add	Add	Add	Add
Cu	-	-	-	0.916	0.617	1.001	1.027	-		-	Add	Add	Add	Add
Ni	-	-	-	-	0.610	0.7912	1.018	-		-	-	Add	Add	Add
Mn	-	-	-	-	-	0.875	0.888	-		-	-	-	Add	Add
Pb	-	-	-	-	-	-	0.882	-		-	-	-	-	Add
Cd:Co	-	0.788	1.046	1.025	0.846	0.912	0.882	-	Add	Add	Add	Add	Add	Add
Cd:Cr	-	-	0.705	0.771	0.680	0.533	0.683			Add	Add	Add	Add	Add
Cd:Cu	-	-	-	0.910	0.696	0.814	0.833	-		-	Add	Add	Add	Add
Cd:Ni	-	-	-	-	0.749	0.815	0.861	-		-	-	Add	Add	Add
Cd:Mn	-	-	-	-	-	0.803	0.729	-		-	-	-	Add	Add
Cd:Pb	-	-	-	-	-	-	0.758	-		-	-	-	-	Add
Co:Cr	-	-	0.950	1.052	0.929	0.551	0.887			Add	Add	Add	Add	Add
Co:Cu	-	-	-	1.188	0.767	1	1.150	-		-	Add	Add	Add	Add
Co:Ni	-	-	-	-	0.611	0.854	1.158	-		-	-	Add	Add	Add
Co:Mn	-	-	-	-	-	0.926	0.880	-		-	-	-	Add	Add
Co:Pb	-	-	-	-	-	-	0.931	-		-	-	-	-	Add
Cr:Cu	-	-	-	0.941	0.826	0.574	0.777				Add	Add	Add	Add
Cr:Ni	-	-	-	-	0.900	0.542	0.882					Add	Add	Add
Cr:Mn	-	-	-	-	-	0.533	0.787						Add	Add
Cr:Pb	-	-	-	-	-	-	0.559							Add
Cu:Ni	-	-	-	-	0.815	0.903	1.120	-		-	-	Add	Add	Add
Cu:Mn	-	-	-	-	-	0.894	0.888	-		-	-	-	Add	Add
Cu:Pb	-	-	-	-	-	-	0.884	-		-	-	-	-	Add
Ni:Mn	-	-	-	-	-	0.786	0.829	-		-	-	-	Add	Add
Ni:Pb	-	-	-	-	-	-	0.809	-		-	-	-	-	Add
Mn:Pb	-	-	-	-	-	-	0.823	-		-	-	-	-	Add

* - Cu and Hg at 0.05 mM, all other metals at 1 mM

4.4.2 HORAC assay

4.4.2.1 Hydroxyl radical formation of single metals

The HORAC assay was developed to test the capacity of antioxidants to protect against hydroxyl radical damage. In this assay Co (II) and H_2O_2 is used to generate hydroxyl radicals (Ou *et al.* 2002). In the current study the HORAC assay was used to determine if the investigated metals use the Fenton reaction to generate hydroxyl radicals. According to the literature found this is the first time that this assay was used for this purpose.

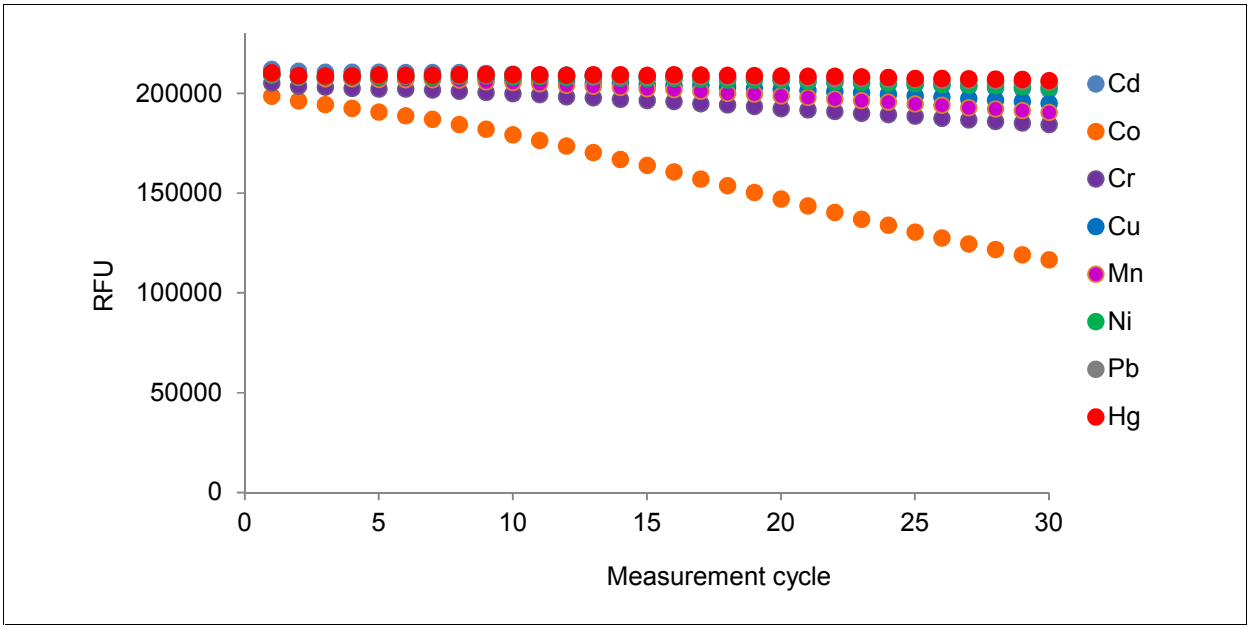

Figure 4.9: Hydroxyl radical averting assay indicating radical formation for each metal using relevant fluorescent units (RFU) – a steeper downward slope indicative of more radicals formed; Cu and Hg at 0.05 mM and Cd, Co, Cr, Mn, Ni, and Pb at 1 mM. Data is an average of 3 independent experiments.

In Figure 4.9 the steep downward slope of Co indicates hydroxyl radical formation which correlates with the assay Ou *et al.* (2002) developed. Korashy & El-Kadi (2008) measured the formation of particularly hydroxyl radicals, using the oxidation of dihydrorhodamine-123 to rhodamine, and found an increase when cells were exposed to Pb^{2+} (25 µM) and Cu^{2+} (10 µM) respectively. The results from the HORAC assay from this study correlates with the findings for Cu, but a significant measurement was not found for Pb.

The positive gradient was calculated for Cu and Hg at 0.05 mM and at 1 mM for all other metals, as shown in Figure 4.10. Han *et al.* (2007) also found that Hg causes the formation of more hydroxyl radicals in a human bronchial epithelial cell line than Cd. The metals ordered from forming the most to the least hydroxyl radicals are thus Cu > Hg > Co > Cr > Mn > Cd > Ni > Pb.

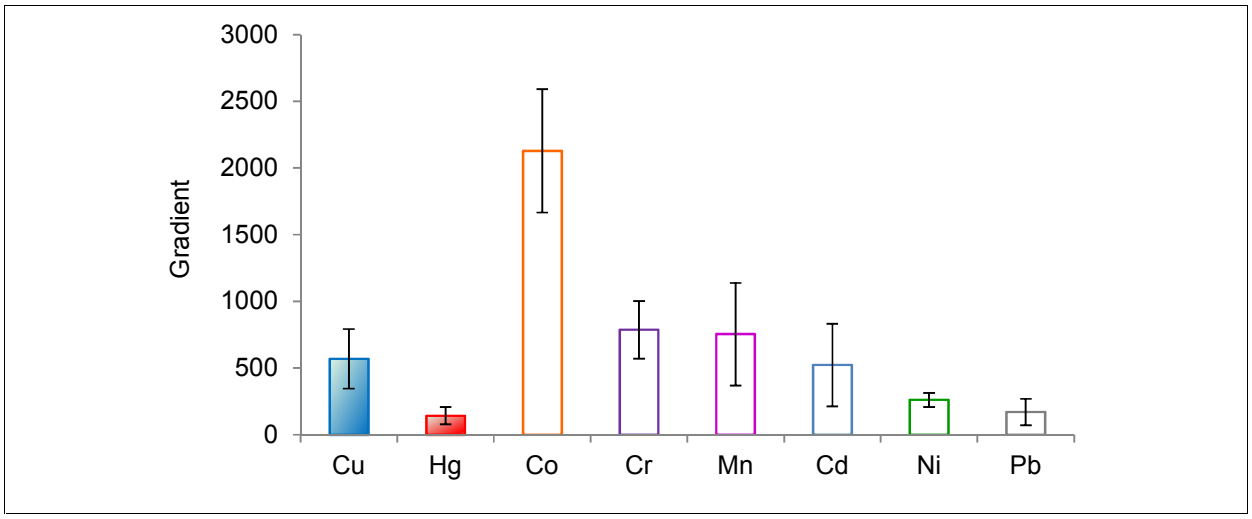

Figure 4.10: Positive gradients of hydroxyl radical averting assay indicating radical formation for each metal, from most to least – Cu and Hg at 0.05 mM and Cd, Co, Cr, Mn, Ni, and Pb at 1 mM. A bigger gradient indicative of more radicals formed; data is an average of at least 3 independent experiments ± SEM.

When comparing the gradients, calculated from the tenth to the thirtieth measurement cycle, of the single metals, calculated for all metals at 1 mM, only two significant differences are seen, as indicated in Table 4.5. The significant difference between Cu and Ni and Cu and Pb at 1 mM shows that a significantly lower amount of hydroxyl radicals were formed by Ni as well as Pb. The large SEM as seen in Figure 4.9 for some metals can be explained by the precipitation that sometimes occurs at certain temperatures and this may possibly account for the lack of significant differences observed between groups. This effect was minimised by preparing fresh metal mixtures for each experiment.

Table 4.5: HORAC ASSAY: Dunn's multiple comparisons test between single metals at 1 mM.

		P Value			P Value
Cd vs.	**Co**	> 0.9999	**Cu vs.**	**Mn**	0.5567
	Cr	> 0.9999		**Ni**	0.0425‡
	Cu	0.3700		**Pb**	*0.0085*‡
	Mn	> 0.9999		**Hg**	> 0.9999
	Ni	> 0.9999	**Mn vs.**	**Ni**	> 0.9999
	Pb	> 0.9999		**Pb**	> 0.9999
	Hg	> 0.9999		**Hg**	> 0.9999
Co vs.	**Cr**	> 0.9999	**Ni vs.**	**Pb**	> 0.9999
	Cu	> 0.9999		**Hg**	> 0.9999

	Mn	> 0.9999	**Hg**	0.4012
	Ni	> 0.9999		
	Pb	0.4546		
	Hg	> 0.9999		
Cr vs.	**Cu**	> 0.9999		
	Mn	> 0.9999		
	Ni	> 0.9999		
	Pb	> 0.9999		
	Hg	> 0.9999		

P-Value < 0.05 indicates significant difference; , Italic: P < 0.01.
Key: ‡ – significant difference

Single metals that cause both GSH depletion and the formation of hydroxyl radicals were identified and are Cd, Cr, Cu, Mn, and Hg (Table 4.6). Of these metals Cu and Hg were found to have the greatest effect. Co and Ni did not cause any GSH depletion but did catalyse the Fenton reaction resulting in the formation of hydroxyl radicals. Although some radical formation were caused by Pb, as seen in Figure 4.9, this radical formation was not significant.

Table 4.6: Single metals that caused GSH depletion and were catalysts in the Fenton reaction.

	Cd	Co	Cr	Cu	Mn	Ni	Pb	Hg
GSH depletion	√	X	√	√	√	X	√	√
Fenton reaction	√	√	√	√	√	√	X	√

Key: √ - does take part in reaction

4.4.2.2 Metal combinations causing hydroxyl radical formation

In Figure 4.11 the metal combinations with a gradient smaller than -2000 are shown. This cut-off was used as Co, with a gradient of -2128, is a known catalyst in the Fenton reaction. These combinations are presented in Figure 4.11 and Table 4.9. Only a few of these combinations do not contain Co as one of its components. These combinations are Cu:Mn, Cd:Cu:Mn, Cr:Cu:Mn, Cu:Mn:Ni, Cu:Mn:Pb, and lastly Cu:Mn:Hg. These combinations all contain the mixture of Cu and Mn, but does not differ significantly from Cu:Mn (non-significant differences not shown in Table 4.8), meaning that the addition of Cd, Cr, Ni, Pb, and Hg to Cu:Mn does not cause a significant increase in hydroxyl radical formation.

Table 4.7: HORAC ASSAY: Metal combinations for which significant differences were observed between single metals vs. double- and triple metal combinations with a gradient < -2000 (Figre 4.11) (non-significant differences not included).

		P Value			P Value
Ni vs.	**Co:Cu:Ni†**	0.0211	**Hg vs.**	**Cd:Co:Hg**	0.0342
	Cu:Mn:Ni	0.0184		**Co:Cr:Hg**	0.0362
Pb vs.	**Co:Pb**	0.0165		**Co:Cu:Hg**	0.0065
	Cd:Co:Pb	0.0246		**Co:Pb:Hg**	0.0066
	Co:Cr:Pb	0.0275		**Cu:Mn:Hg**	0.0077
	Co:Cu:Pb	0.0103			
	Co:Pb:Hg	0.0165			
	Cu:Mn:Pb	0.0407			

Key: † – antagonistic interaction

All the combinations found to differ significantly from single metals in Table 4.7 are combinations with a gradient lower than -2000. Only one of the combinations differ significantly from the gradients of two of its single metal components, namely Co:Pb:Hg. The rest of the combinations only differ significantly from one of its metal components. It is important to note that none of these combinations however has a significantly bigger gradient than that of Co. The seven combinations with the lowest gradients, as can be seen in Table 4.9, contain a mixture of Co and Cu. Co:Cr:Cu is the combination with the lowest gradient, indicating that this metal combination forms the most hydroxyl radicals. Seeing that Co, Cr, and Cu are known catalysts in the Fenton reaction according to Valko *et al.* (2005), it indicates that this assay did evaluate the formation of hydroxyl radicals using the Fenton reaction. All of the triple metal combinations found to differ statistically (Table 4.8) from a mixture of two metals they contain are combinations with gradients lower than -2000.

Table 4.8: HORAC ASSAY: Metal combinations for which significant differences were observed between double- vs. triple metal combinations with a gradient < -2000 (Figure 4.11) (non-significant differences not included).

		P Value			P Value
Cd:Cu vs.	**Cd:Co:Cu**	0.0203	**Cu:Pb vs.**	**Co:Cu:Pb**	0.0235
Cd:Pb vs.	**Cd:Co:Pb**	0.0091	**Cu:Hg vs.**	**Co:Cu:Hg**	0.0487
Cd:Hg vs.	**Cd:Co:Hg**	0.0420			

4.4.2.3 Synergistic, antagonistic, and additive effects of metals

No synergistic interactions were found, as expected, seeing that this is also a chemical assay. A few antagonistic interactions were however found for several metals, as indicated in Table 4.10 these double metal combinations were Cd:Cu, Cd:Pb, Cd:Hg, Cu:Hg, and Cr:Ni. Antagonistic effects were found in fifteen triple metal combinations as shown in Table 4.10. The exact mechanism of interaction is unknown, however a possible explanation for the antagonistic interactions found is the participation of these metals in redox reactions.

GSH depletion cannot be determined in the *ex vivo* erythrocyte model used in this study. In contrast the oxidative effects of free radical formation can be determined by measuring the radical formation (DCFH-DA assay) and the consequence thereof, lipid peroxidation, measured as mM MDA formation (TBARS assay). In Chapter 5 these effects were explored further.

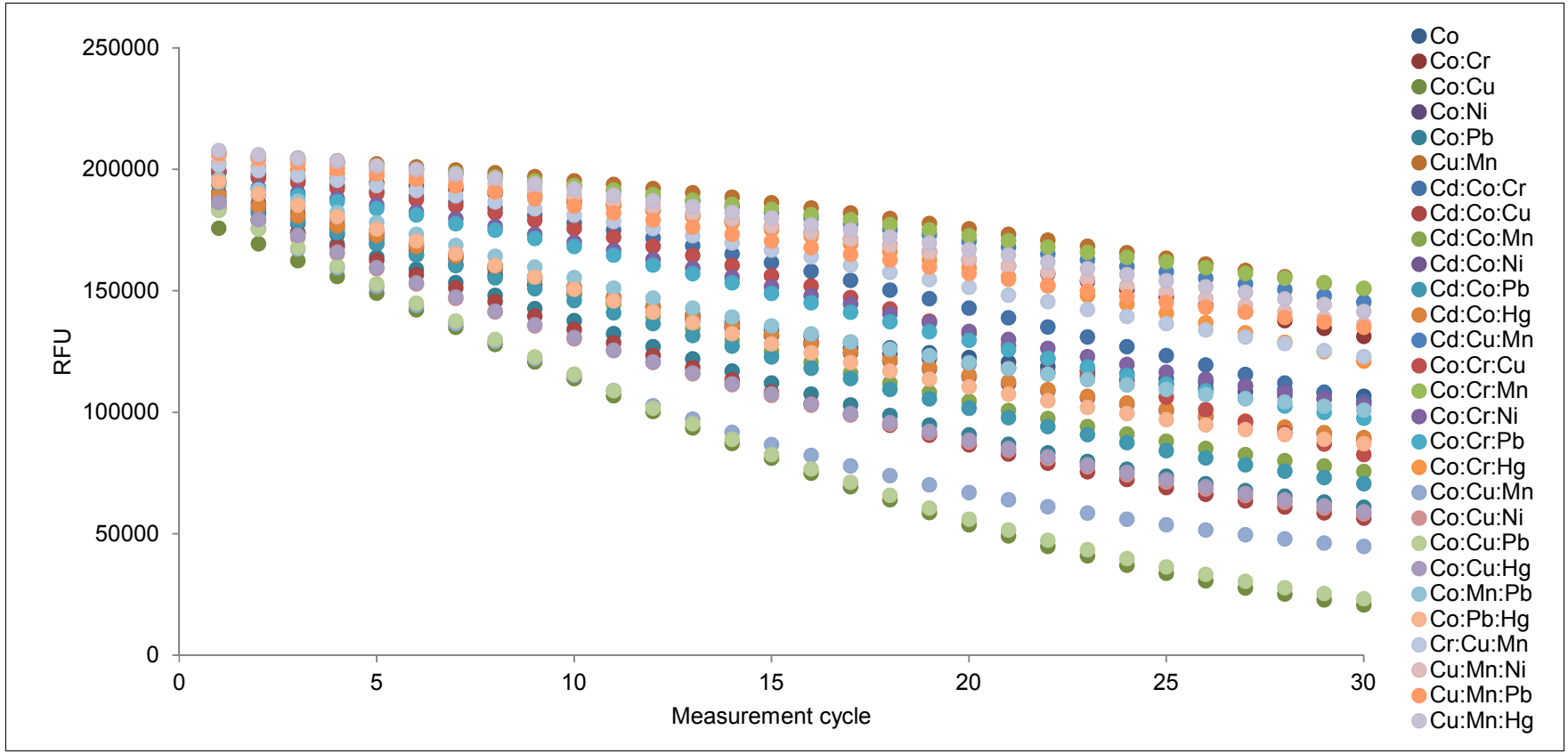

Figure 4.11: Metal combinations with a gradient lower than -2000; indicating radical formation for each metal using the hydroxyl radical averting assay.

Table 4.9: HORAC ASSAY: Ten metal combinations with lowest gradients.

Metal combination	Co:Cr:Cu	Co:Cu	Co:Cu:Pb	Co:Cu:Ni	Co:Cu:Hg	Co:Cu:Mn	Cd:Co:Cu	Co:Pb	Cd:Co:Pb	Cd:Co:Cr
Average gradient	-4807.55	-4689.74	-4625.05	-4445.52	-4369.57	-4044.84	-3896.91	-3855.16	-3794.87	-3740.71
SEM	1184.18	1246.42	875.87	1114.32	1095.60	651.90	1050.70	1005.34	1032.64	1142.41

Table 4.10: HORAC ASSAY: Synergistic, antagonistic and additive effect of mixtures of metals, calculated using the MDR.

	Co	Cr	Cu*	Ni	Mn	Pb	Hg*	Co	Cr	Cu	Ni	Mn	Pb	Hg
Cd	0.712	0.522	0.211	0.501	0.657	0.216	0.269	Add	Add	Ant	Add	Add	Ant	Ant
Co	-	0.971	1.858	0.896	0.603	1.887	0.792	-	Add	Add		Add	Add	Add
Cr	-	-	1.257	0.495	0.657	0.946	0.964			Add	Ant	Add	Add	Add
Cu	-	-	-	0.748	1.642	0.548	0.352	-		-	Add	Add	Add	Ant
Ni	-	-	-	-	0.897	0.881	0.719	-		-	-	Add	Add	Add
Mn	-	-	-	-	-	1.275	0.969	-		-	-	-	Add	Add
Pb	-	-	-	-	-	-	0.786	-		-	-	-	-	Add
Cd:Co	-	1.088	1.279	0.796	1.017	1.480	0.811	-	Add	Add	Add	Add	Add	Add
Cd:Cr	-	-	0.494	0.219	0.132	0.449	0.278			Ant	Ant	Ant	Ant	Ant
Cd:Cu	-	-	-	0.300	1.273	0.240	0.163	-		-	Ant	Add	Ant	Ant
Cd:Ni	-	-	-	-	0.533	0.232	0.333	-		-	-	Add	Ant	Ant
Cd:Mn	-	-	-	-	-	0.323	0.508	-		-	-	-	Ant	Add
Cd:Pb	-	-	-	-	-	-	0.119	-		-	-	-	-	Ant
Co:Cr	-	-	1.380	1.076	0.551	1.207	1.093			Add	Add	Add	Add	Add
Co:Cu	-	-	-	1.597	1.154	1.772	1.612	-		-	Add	Add	Add	Add
Co:Ni	-	-	-	-	0.566	0.715	1.080	-		-	-	Add	Add	Add
Co:Mn	-	-	-	-	-	0.839	0.775	-		-	-	-	Add	Add
Co:Pb	-	-	-	-	-	-	1.312	-		-	-	-	-	Add
Cr:Cu	-	-	-	0.664	1.370	0.943	1.129				Add	Add	Add	Add
Cr:Ni	-	-	-	-	0.440	0.779	0.573					Ant	Add	Add
Cr:Mn	-	-	-	-	-	0.590	0.609						Add	Add
Cr:Pb	-	-	-	-	-	-	0.769							Add
Cu:Ni	-	-	-	-	1.647	0.549	0.678	-		-	-	Add	Add	Add
Cu:Mn	-	-	-	-	-	1.712	1.618	-		-	-	-	Add	Add
Cu:Pb	-	-	-	-	-	-	0.401	-		-	-	-	-	Ant
Ni:Mn	-	-	-	-	-	0.891	0.657	-		-	-	-	Add	Add
Ni:Pb	-	-	-	-	-	-	0.364	-		-	-	-	-	Ant
Mn:Pb	-	-	-	-	-	-	0.873	-		-	-	-	-	Add

* - Cu and Hg at 0.05 mM, all other metals at 1 mM
Key: ■ – antagonistic interaction

4.5 Conclusion

Nineteen of the ninety-two evaluated metal / metal combinations caused more than 80% GSH depletion, with Cd:Pb:Hg and Cu:Pb:Hg causing the most. These two metal combinations also differed significantly from the GSH depletion caused by all three of their metal components on their own. Only additive synergism were found using this chemical assay.

Twenty-eight of the evaluated combinations had a gradient lower than -2000, indicating hydroxyl radical formation. Only six of these combinations did not contain Co, but did contain Cu and Mn. The combination with the lowest gradient was Co:Cr:Cu, which contains three metals known to be catalysts in the Fenton reaction. No synergistic interactions were found using the HORAC assay. Numerous antagonistic interactions were however found. For the double- and triple metal combinations respectively Cd:Cu and Cd:Pb:Hg showed the greatest antagonistic interaction.

Cd:Co:Pb, Cu:Mn:Pb, Co:Cr:Hg, and Co:Pb:Hg caused more than 80% GSH depletion and had a gradient of less than -2000 when evaluated using the HORAC assay.

Chapter 5: Cellular effects of metals: MDA measurement and DCFH-DA assay

5.1 Introduction

Oxidative stress is the result of reactive oxygen species (ROS) overwhelming the cellular antioxidant defence systems and altering the redox homeostasis (Eruslanov & Kusmartsev 2010).

The most common initiators for lipid peroxidation are ROS and include the singlet oxygen, triplet oxygen, hydroxyl radical and peroxyl radical (Benedet & Shibamoto 2008). Unsaturated fatty acids as well as oxygen are two major components in lipid peroxidation (Benedet & Shibamoto 2008). The lipid peroxidation in polyunsaturated fatty acids is a free radical mediated chain oxidation reaction (Benedet & Shibamoto 2008; Singh *et al*. 2011). Lipid peroxidation disrupts the structural and protective functions of cell membranes. Malondialdehyde (MDA) is a side product of enzymatic arachidonic acid oxygenation and an end product of oxidative lipid degradation (Janero 1990). It is also a well known product of the lipid peroxidation of erythrocytes and cross-link erythrocyte phospholipids and proteins (Singh *et al*. 2011). This leads to a reduction of membrane function and ultimately to erythrocyte death (Singh *et al*. 2011) and finally haemolysis.

Most metals investigated in this study have been found to have an effect on lipid peroxidation; this has been determined by the use of the TBARS (thiobarbituric acid reactive substances) assay. Although Cr(VI) is known to cause oxidative stress and through this lipid peroxidation, this study focused on Cr(III) because exposure to Cr(III) is more common than Cr(VI). Manganese is an essential metal and although at excessive concentrations it does have adverse effects, Talavera *et al.* (1999) found that it decreased the MDA levels in rat brains when rats were exposed to Mn.

Hwang *et al.* (1998) determined that Cu does cause an increase in lipid peroxidation in rat liver and plasma and that taurine protects rats from the effects of overexposure to Cu. Garoui *et al.* (2012) investigated the effect of $CoCl_2$ in 14-day old rat pups and their mothers and found a significant increase in MDA in the pups as well as the mothers after exposure. Chen *et al.* (2003) found a significant increase in MDA levels in human lymphocytes incubated with $NiCl_2$ for 1 hour. While He *et al.* (2013) found neurobehavioral changes in mice after a 3 hour exposure

to $NiCl_2$ which was accompanied by, amongst others, an increase in MDA levels. Ogunrinola (2015) as well as Triawanti *et al*. (2014) found increased MDA concentrations in rat plasma, erythrocytes, brain, and liver as well as serum when exposed to Cd.

Mercury is a toxic pollutant and is known to cause the production of reactive oxygen species and plays a key role in initiation and propagation of free radical-induced peroxidative damage (Stohs & Bagchi 1995). Hijova *et al* (2005) found increased levels of MDA as well as ascorbic acid in the plasma of rats exposed to $HgCl_2$ for 30 days. Pb-induced toxicity is known to be accompanied by oxidative stress (Kasperczyk *et al.* 2014). Pb causes the formation of ROS as well as the depletion of antioxidant enzymes and other antioxidant mechanisms, e.g. reduced glutathione (Kasperczyk *et al.* 2014). ROS can cause lipid peroxidation and this can then be measured by the measurement of MDA. Adonaylo & Oteiza (1999) found that rats exposed to Pb^{2+} as lead acetate showed signs of oxidative stress, these findings included an increase in MDA levels in the brains of these rats after 8 weeks of exposure. Pb-exposed workers have increased MDA levels, but Kasperczyk *et al.* (2014) found that an antioxidant N-acetylcysteine decreased the MDA levels caused by Pb significantly in the serum, leukocytes and erythrocytes of these workers.

The specific objectives of this chapter were to:

1. Investigate the oxidative effect of metals alone and in combinations of two and three on erythrocytes using the 2',7'-dichlorofluorescein diacetate (DCFH-DA) assay at the metal concentrations determined in the previous chapter.
2. Investigate the total oxidative effect, by measuring MDA, of metals alone and in combinations of two and three on erythrocytes using the TBARS assay at the metal concentrations determined in the previous chapter.
3. For both assays determine if metal combinations of two and three have antagonistic, additive, or synergistic interactions.

5.2 Materials

5.2.1 Reagents, equipment and disposable plasticware

In addition to the reagents used in Chapter 3, malondialdehyde tetrabutylammonium salt, hydrochloric acid (HCl), 2-Thiobarbituric acid (TBA), 2',7'-dichlorofluorescein diacetate (DCFH-DA), and 2,2'-azobis(2-amidinopropane) dihydrochloride (AAPH) were obtained from Sigma-Aldrich Company, Atlasville, SA. Trichloroacetic acid (TCA) obtained from Merck Chemicals, Modderfontein South Africa, SA was also used.

Equipment used was: a FLUOstar Omega Fluorometer from BMG LABTECH, Germany and an Ecobath water bath obtained from Labotech, SA. All other equipment, disposable laboratory ware and laboratory facilities was the same as in Chapter 3.

5.3 Methods

5.3.1 Erythrocyte collection

Erythrocytes were collected and stored as described in Section 3.3.1.

5.3.2 Preparation of metals

Metal solutions were prepared at a final concentration of 1 mM for $NiCl_2$, $CoCl_2$, $KCr(SO_4)_2$, $(CH_3COO)_2Pb$, $MnCl_2$ and at 0.05 mM for $CuSO_4$ and $HgCl_2$.

5.3.3 2',7'-Dichlorofluorescin diacetate (DCFH-DA) assay

Fluorescent probes can be used to detect oxidative stress as well as intracellular H_2O_2. One of these probes is 2',7'-dichlorofluorescein diacetate (DCFH-DA) (Kalyanaraman *et al*. 2012). DCFH-DA diffuses into cells and is hydrolysed to dichlorodihydrofluorescein (DCFH) by intracellular esterases (Blasa *et al.* 2011; Kalyanaraman *et al*. 2012). DCFH is retained in the cell and via two-electron oxidation changed to its fluorescent derivative DCF (dichlorofluorescein) which can be monitored by fluorescence-based techniques (Kalyanaraman *et al*. 2012).

DCFH does not however react with H_2O_2 directly and also reacts with other one-electron-oxidizing species e.g. the hydroxyl radical as can be seen in Figure 5.1. The reaction with DCFH-DA thus is an indication of ROS formation in a biological system.

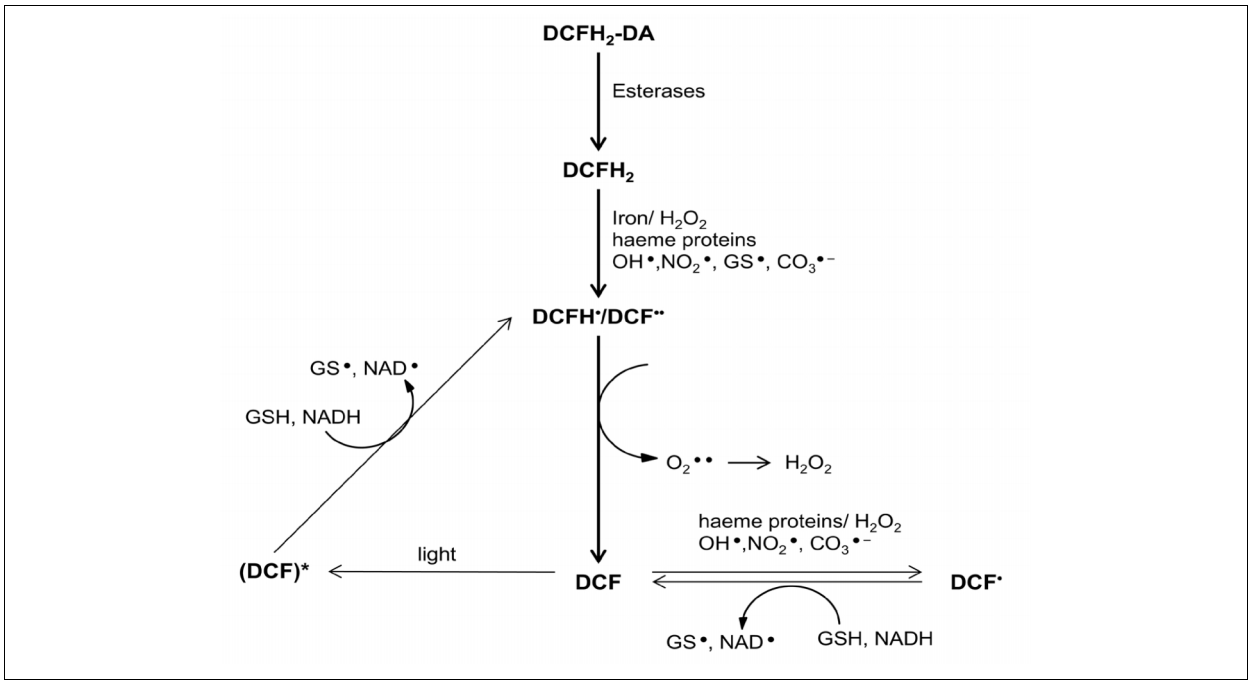

Figure 5.1: Intracellular redox chemistry of DCFH-DA (Adapted from: Kalyanaraman *et al*. 2012).

For each experiment, the erythrocyte solution was removed from the fridge and left to warm to room temperature. The solution was diluted to a 5% (v/v) dilution, using isoPBS. 60 µl of the 5% erythrocyte solution, 25 µl of each metal / metal combination, and 15 µl DCFH-DA was added to each well of a 96 well plate respectively. The change in fluorescence was read at an excitation wavelength of 485 nm and emission at 520, once every 2 min for 120 min. The control solutions were prepared as follows:

1. 0% (Blank): 60 µl 5% erythrocyte solution, 25 µl buffer, and 15 µl DCFH-DA
2. AAPH: 60 µl 5% erythrocyte solution, 25 µl, 0.4 mM, AAPH, and 15 µl DCFH-DA.

5.3.4 Thiobarbituric acid reactive substances (TBARS) assay

ROS as measured with the DCFH-DA assay causes lipid peroxidation. Malondialdehyde (MDA) is a side product of enzymatic arachidonic acid oxygenation and an end product of oxidative lipid degradation (Janero 1990). The amount of MDA formation can be quantified with the TBARS assay. The principle of this assay depends on the reactivity of thiobarbituric acid (TBA) towards MDA (Janero 1990). TBA reacts with MDA to form a red coloured product.

A standard curve of 0-100 nM of MDA, malondialdehyde tetrabutylammonium salt in isoPBS was prepared. TBA was dissolved in 0.125 M HCl with a final concentration of 0.67% (w/v). To

a 50 µl volume of MDA an equal volume of TBA was added and then the 96 well plate was left in a water bath at 80ºC for 10 min. The absorbance was then read spectrophotometrically at 532 nm.

To determine MDA formation following exposure to metals alone and in combinations the erythrocyte solution was removed from the fridge and left to warm to room temperature. A volume of 140 µl of the erythrocyte solution was pipetted into separate Eppendorf tubes and exposed to 60 µl of each of the metals/metal combinations. After exposure the samples were incubated overnight. In the morning, the samples were removed from the incubator, and centrifuged at 1201 x g for 2 minutes. Of the supernatant 150 µl of each tube was removed after which 100 µl 10% (w/v) TCA was added. Each tube was vortexed and centrifuged at 1429 x g for 2 minutes. A volume of 50 µl of the supernatant was removed and pipetted into a 96 well plate, 50 µl of the TBA solution was added to each well after which the 96 well plate was left in a water bath at 80ºC for 10 min. The absorbance was read spectrophotometrically at 532 nm. The control solution was prepared as follows:

1. 0% TBARS formation (Blank): 60 µl isoPBS added to 140 µl erythrocyte solution

5.3.6 Determination of combination effect

Metal interactions were determined using the same MDR as in the previous chapter, using the following equation:

$$\mathbf{MDR = O_v/E_v}$$

$\mathbf{O_v}$ is the observed effect value (for this Chapter either MDA concentration or calculated gradient) and $\mathbf{E_v}$ the expected additive effect value. An additive effect was indicated where $0.5 \leq MDR \leq 2$, antagonism where $MDR < 0.5$, and synergism where $MDR > 2$.

5.3.7 Data management and statistical analysis

Data for single metal exposure is an average of three experiments with each experiment done in triplicate, generating nine data points. For double and triple metal exposure data is an average of at least three single point experiments; 92 samples had to be tested making a three point experiment for all samples unattainable. The results are expressed as mean ± standard error of mean (SEM), where each point is the average of the mean of the three experiments. Data was statistically evaluated using the Dunn's multiple comparisons test (one way ANOVA), with a p-value < 0.05 indicating a significant difference between data sets. This was done using GraphPad version 6.01 for Windows, GraphPad Software, San Diego California, USA.

5.4 Results and Discussion

5.4.1 2',7'-Dichlorofluorescein diacetate (DCFH-DA) measurement

5.4.1.1 DCFH-DA measurement after exposure to single metals

The DCFH-DA assay can be used to determine if a toxin does cause oxidative stress. An increase in gradient (calculated from 10 min to 30 min) is due to increased ROS formation as shown for Cu and Mn in Figure 5.2.

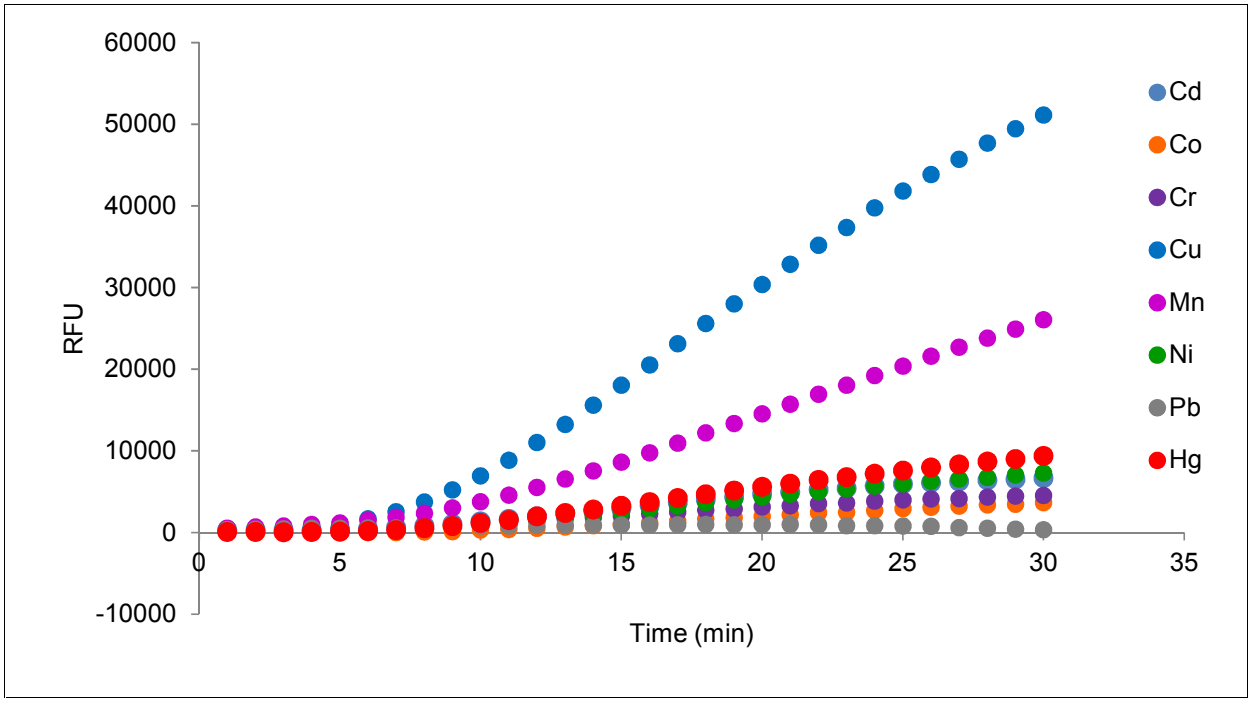

Figure 5.2: Representative experiment of DCFH-DA assay following exposure to Cd, Co, Cr, Mn, Ni, and Pb at 1 mM and Cu and Hg at 0.05 mM.

It is important to note that, again, Cu and Hg (shown in shaded columns in Figure 5.3) exposure were at a much lower concentration of 0.05 mM when compared to the 1 mM of the other metals. In Figure 5.3 the gradients of the generated curves of each metal are presented. The metals causing from most to least oxidative cellular damage were, if the ROS formation by Cu was chosen as 100%, Cu (100%) >> Hg (18.32%) > Mn (2.50%) > Ni (0.72%) > Cd (0.60%) > Cr (0.39%) > Co (0.38%) >Pb (-0.004%). These results indicate that Cu causes the most radical formation while the effects of Ni, Cd, Cr, Co and Pb are minimal. Likewise for the HORAC assay, relative to Cu, (Cu (100%) > Hg (24.7%) > Co (18.7%) > Cr (6.9%) > Mn (6.61%) > Cd (4.57%) > Ni (2.28%) > Pb (1.48%)), Cu and Hg caused the most radical formation. In the HORAC assay, radical formation was 18.7% for Co, relative to Cu, which was in contrast to 0.38% for Co, relative to Cu, for the DCFH DA assay.

The effect of Pb was less than the control (Figure 5.3). A possible explanation for this is that in the DCFH-DA assay, DCFH-DA is hydrolysed by intracellular esterases to DCFH. In a study done by Cole *et al.* (2002) it was found that lead chloride inhibited arylesterase activity by more than 50%. A consequence of this effect is that DCFH-DA is not converted to DCFH and the negative gradient is an indication of esterase inhibition by Pb. Flora *et al*. (2013) did however find an increase in DCF levels, indicating an increase in ROS, in mice blood, -liver, and -kidneys after exposing Swiss Albino mice to Pb in their drinking water.

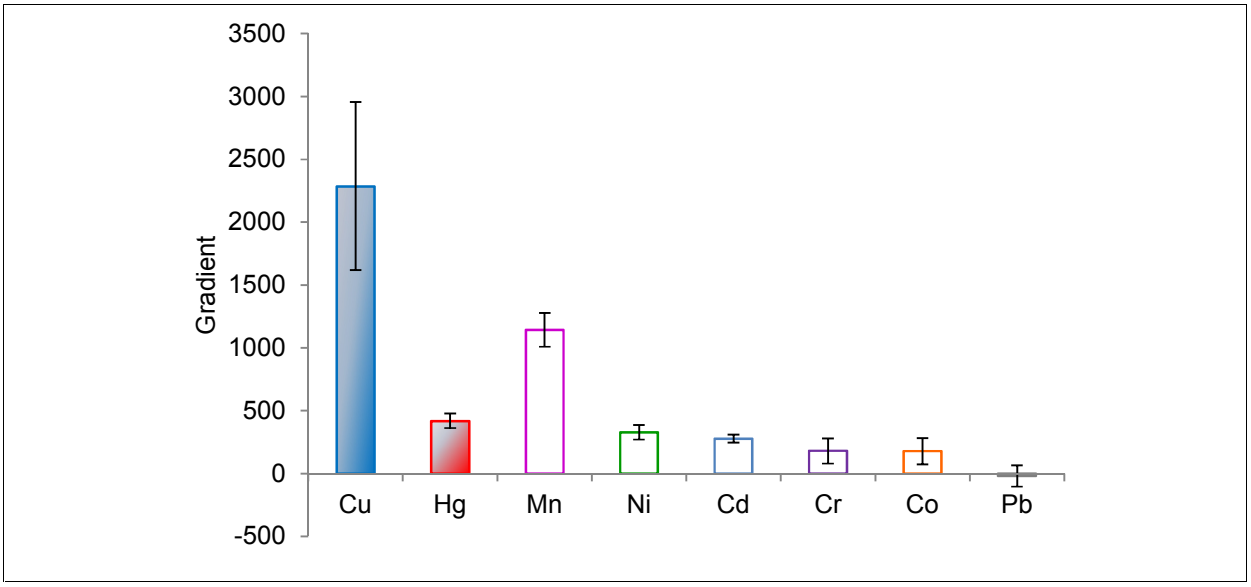

Figure 5.3: Ranking of increasing metal induced erythrocyte oxidative damage measured with the DCFH-DA assay. Data is expressed change in gradient for each metal at a concentration of 0.05 mM for Cu and Hg and 1 mM for Cd, Co, Cr, Mn, Ni, and Pb. Data is an average of at least 3 independent experiments ± SEM.

Table 5.1: DCFH-DA ASSAY: Dunn's multiple comparisons test between single metals at 1 mM.

		P Value			P Value
Cd vs.	**Co**	> 0.9999	**Cr vs.**	**Mn**	> 0.9999
	Cr	> 0.9999		**Ni**	> 0.9999
	Cu	> 0.9999		**Pb**	> 0.9999
	Mn	> 0.9999		**Hg**	0.3606
	Ni	> 0.9999	**Cu vs.**	**Mn**	> 0.9999
	Pb	> 0.9999		**Ni**	> 0.9999
	Hg	> 0.9999		**Pb**	0.0202‡
Co vs.	**Cr**	> 0.9999		**Hg**	> 0.9999
	Cu	0.2149	**Mn vs.**	**Ni**	> 0.9999
	Mn	> 0.9999		**Pb**	0.2449

	Ni	> 0.9999		**Hg**	> 0.9999
	Pb	> 0.9999	**Ni vs.**	**Pb**	> 0.9999
	Hg	0.1778		**Hg**	> 0.9999
Cr vs.	**Cu**	0.3925	**Pb vs.**	**Hg**	0.0129‡

P-Value < 0.05 indicates significant difference.
Key: ‡ – significant difference

Using Dunn's multiple comparisons test, comparing all metals at 1 mM, statistically significant differences were found between Pb and Hg and Pb and Cu (Table 5.1). Korashy & El-Kadi (2008) found a significant increase in the oxidation of DCF-DA to DCF by Hg^{2+} and Cu^{2+} but not by Pb^{2+}. In addition these researchers found that Cu^{2+} caused more oxidation than Hg^{2+}. These findings correlate with the findings in this study. According to Xie *et al.* (2007) both Ni and Cu cause radical formation while Cd does not have an effect. However, in this study no significant difference was found between Ni and Cd.

5.4.1.2 Metal combinations with a gradient of more than 4000.

Figure 5.4 shows the metal combinations with a gradient higher than 4000 when measuring ROS formation using the DCFH-DA assay. Only two double metal combinations had gradients of this magnitude and these were Cu:Ni and Cu:Mn. For the triple metal combinations these were Cd:Cu:Hg, Co:Cu:Hg, Co:Cu:Mn, Co:Cu:Ni, Cd:Cu:Mn, Mn:Ni:Hg, Cu:Ni:Hg, Cu:Mn:Pb, Cu:Mn:Ni, and Cu:Mn:Hg. All these combinations except Mn:Ni:Hg contains Cu.

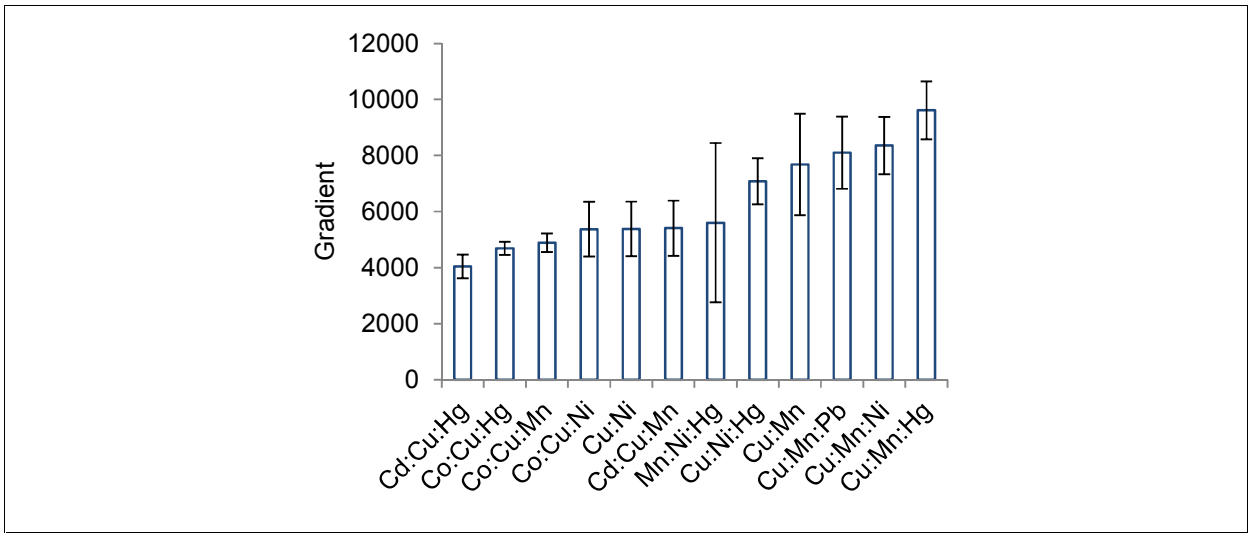

Figure 5.4: Metal combinations with a calculated gradient of more than 4000 after erythrocyte exposure to metal combinations, with a final concentration of 0.05 mM for Cu and Hg and 1 mM for Cd, Co, Cr, Mn, Ni, and Pb. Gradients shown from smallest to greatest; data is an average of at least 3 independent experiments ± SEM.

Table 5.2: DCFH-DA ASSAY: Metal combinations for which significant differences were observed between single metals vs. double- and triple metal combinations with a gradient > 4000 (Figure 5.4) (non-significant differences not included).

		P Value			P Value
Cd vs.	**Cd:Cu:Mn**	0.016	**Ni vs.**	**Cu:Mn:Ni**	0.021
	Cd:Cu:Hg	0.020		**Cu:Ni:Hg***	0.026
Co vs.	**Co:Cu:Mn**	0.024	**Pb vs.**	**Cu:Mn:Pb***	*0.0018*
	Co:Cu:Ni	0.015	**Hg vs.**	**Cu:Mn:Hg***	0.0141
	Co:Cu:Hg	0.018		**Cu:Ni:Hg***	0.0230

P-value < 0.05 indicates significant difference; Italic: P-value < 0.01.
Key: * – synergistic interaction

When comparing the combinations causing the most oxidative stress with the gradients of their single metal components, only a few significant differences were found. Cd:Cu:Mn, Cd:Cu:Hg, Co:Cu:Mn, Co:Cu:Ni, Co:Cu:Hg, Cu:Mn:Ni, Cu:Mn:Pb, and Cu:Mn:Hg differ significantly from the effect of one of the metals making up the mixtures, as can be seen in Table 5.2. Cu:Ni:Hg's gradient differs significantly from the calculated gradient of Ni as well as Hg, but does not differ significantly from that of Cu.

Table 5.3: DCFH-DA ASSAY: Metal combinations for which significant differences were observed between double- vs. triple metal combinations with a gradient > 4000 (Figure 5.4) (non-significant differences not included).

		P Value			P Value
Cd:Hg vs.	**Cd:Cu:Hg**	*0.002*	**Co:Hg vs.**	**Co:Cu:Hg**	0.046
Co:Mn vs.	**Co:Cu:Mn**	0.016	**Cu:Hg vs.**	**Cu:Mn:Hg***	*0.002*
Co:Ni vs.	**Co:Cu:Ni**	*0.009*		**Cu:Ni:Hg***	*0.009*

P-value < 0.05 indicates significant difference; Italic: P-value < 0.01.
Key: * – synergistic interaction

Cd:Cu:Hg, Co:Cu:Mn, Co:Cu:Ni, Co:Cu:Hg, Cu:Mn:Hg, Cu:Ni:Hg, and Cu:Ni:Pb differed significantly from one of the double metal combinations that it contains (refer to Table 5.3). Not one of these metal combinations with a gradient of more than 4000 differs significantly from two or three of the double metal combinations it contained. This indicates that exposure to three metals instead of two does not increase the oxidative stress caused by the metal combinations significantly.

5.4.1.3 Synergistic, antagonistic, and additive effects of metals

Synergistic interactions were found for Cu:Ni and Cu:Mn with borderline ratios of 2.058 and 2.240 respectively. Triple combinations with synergistic effects were Cu:Ni:Mn, Cu:Ni:Hg, Cu:Mn:Pb, Cu:Mn:Hg, and Ni:Mn:Hg. Of these Ni:Mn:Hg had the greatest MDR of 2.964.

Many metal combinations showed an antagonistic effect. The number of antagonistic interactions is high and for the double metal combinations are Cd:Cr, Co:Cr, Cr:Cu, Ni:Cd, Ni:Co, Ni:Cr, Mn:Cd, Mn:Co, Mn:Cr, Mn:Ni, Cd:Pb, Pb:Ni, Pb:Cr, and Hg:Cr. The strongest effect was found for the combination of Cr:Ni (MDR = -0.253), Pb:Ni (MDR = -0.032), and Cr:Cu (MDR = -0.008).

Many triple metal interactions as indicated in Table 5.4 also have an antagonistic effect. The strongest antagonistic effects were found for Co:Cr:Ni, Cd:Cr:Cu, Co:Cr:Cu, Cr:Cu:Ni, and Cr:Cu:Pb. Cr was a component in all these mixtures.

Table 5.4: DCFH-DA ASSAY: Synergistic, antagonistic and additive effect of mixtures of metals, calculated using the MDR.

	Co	Cr	Cu*	Ni	Mn	Pb	Hg*	Co	Cr	Cu	Ni	Mn	Pb	Hg
Cd	0.615	0.211	1.080	0.305	0.312	0.158	0.573	Add	Ant	Add	Ant	Ant	Ant	Add
Co	-	0.185	1.525	0.204	0.288	1.772	0.830	-	Ant	Add	Ant	Ant	Add	Add
Cr	-	-	-0.008	-0.253	0.486	0.363	0.495			Ant	Ant	Ant	Ant	Ant
Cu	-	-	-	2.058	2.240	1.364	0.570	-		-	Syn	Syn	Add	Add
Ni	-	-	-	-	0.446	-0.032	1.091	-		-	-	Ant	Ant	Add
Mn	-	-	-	-	-	0.690	1.096	-		-	-	-	Add	Add
Pb	-	-	-	-	-	-	0.897	-		-	-	-	-	Add
Cd:Co	-	1.548	0.701	0.418	0.317	1.036	0.617	-	Add	Add	Ant	Ant	Add	Add
Cd:Cr	-	-	0.061	0.324	0.341	0.407	0.453			Ant	Ant	Ant	Ant	Ant
Cd:Cu	-	-	-	0.767	1.459	0.580	1.356	-		-	Add	Add	Add	Add
Cd:Ni	-	-	-	-	0.306	0.714	0.887	-		-	-	Ant	Add	Add
Cd:Mn	-	-	-	-	-	0.460	1.012	-		-	-	-	Ant	Add
Cd:Pb	-	-	-	-	-	-	1.007	-		-	-	-	-	Add
Co:Cr	-	-	0.152	-0.036	0.426	0.331	0.400			Ant	Ant	Ant	Ant	Ant
Co:Cu	-	-	-	1.925	1.356	1.138	1.625	-		-	Add	Add	Add	Add
Co:Ni	-	-	-	-	0.346	0.748	0.850	-		-	-	Ant	Add	Add
Co:Mn	-	-	-	-	-	0.874	0.913	-		-	-	-	Add	Add
Co:Pb	-	-	-	-	-	-	1.360	-		-	-	-	-	Add
Cr:Cu	-	-	-	0.162	0.277	0.063	0.988				Ant	Ant	Ant	Add
Cr:Ni	-	-	-	-	0.236	0.377	0.370					Ant	Ant	Ant
Cr:Mn	-	-	-	-	-	0.222	0.176						Ant	Ant
Cr:Pb	-	-	-	-	-	-	0.307							Ant
Cu:Ni	-	-	-	-	2.225	1.379	2.334	-		-	-	Syn	Add	Syn
Cu:Mn	-	-	-	-	-	2.377	2.497	-		-	-	-	Syn	Syn
Cu:Pb	-	-	-	-	-	-	1.393	-		-	-	-	-	Add
Ni:Mn	-	-	-	-	-	0.479	2.964	-		-	-	-	Ant	Syn
Ni:Pb	-	-	-	-	-	-	0.987	-		-	-	-	-	Add
Mn:Pb	-	-	-	-	-	-	0.590	-		-	-	-	-	Add

* - Cu and Hg at 0.05 mM, all other metals at 1 mM

5.4.2 Lipid peroxidation - Thiobarbituric acid reactive substances assay

The TBARS assay can be used to determine the amount of MDA present in a sample. The presence of MDA can be used as an indicator for the occurrence of lipid peroxidation. With an increase in the MDA concentration a corresponding linear increase in absorbance at 532 nm with R^2 = 0.9991 (Figure 5.5) was observed.

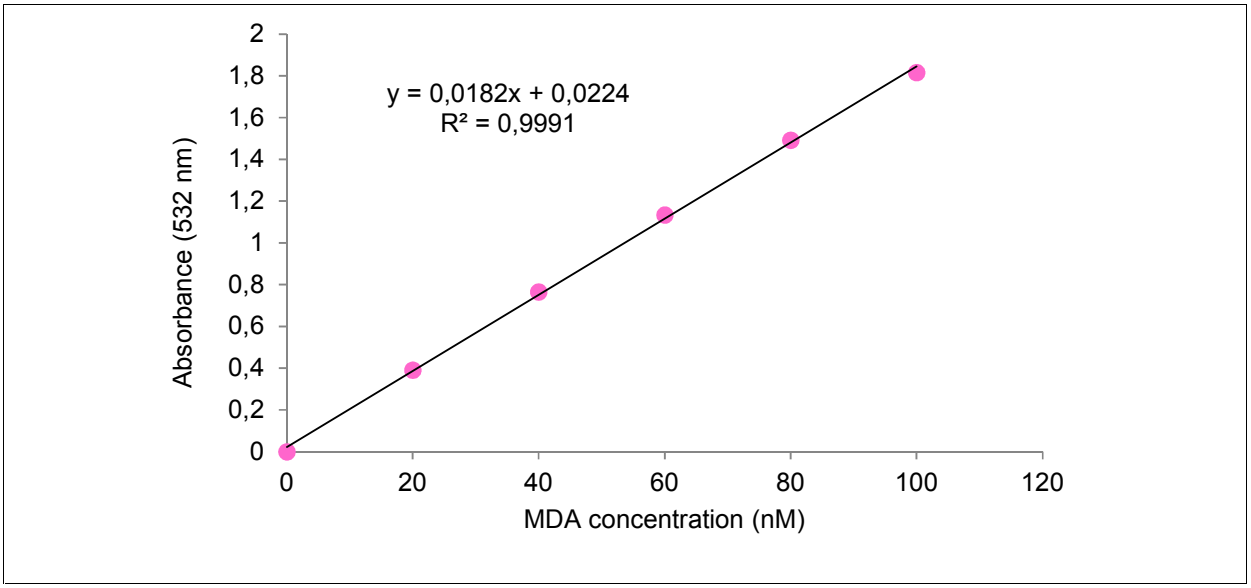

Figure 5.5: Standard curve of reduced MDA measured with TBA. Data is an average of 3 independent experiments expressed as the mean ± standard error of the mean (SEM).

Erythrocytes were exposed to 0.05 mM Hg and Cu as well as 1 mM Cd, Co, Cr, Mn, Ni, and Pb (Figure 5.6).

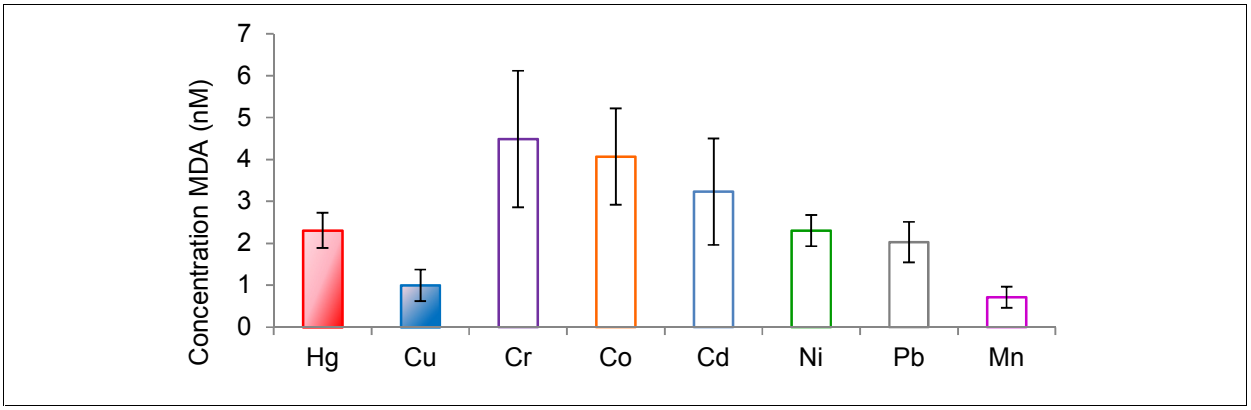

Figure 5.6: Ranking of increasing metal induced lipid peroxidation measured with the TBARS assay. Data is expressed as nM MDA for each metal at a concentration of 0.05 mM for Cu and Hg and 1 mM for Cd, Co, Cr, Mn, Ni, and Pb. Data is an average of at least 3 independent experiments expressed as the mean ± SEM.

Hg and Cu do cause MDA formation at a concentration of 0.05 mM with Cr and Co causing the most MDA formation at a concentration of 1 mM. The ranking of the metals causing from most, to least MDA to be formed is, when MDA formation by Hg at 1mM is chosen as 100%, Hg (100%) >> Cu (34%) > Cr (9.8%) > Co (8.8%) > Cd (7.21%) > Ni (5.0%) > Pb (4.4%) > Mn (1.52%). This is in contrast with the DCFH-DA assay where Cu caused the formation of the most radicals.

The measurement of MDA is a biological assay and the standard error of the mean is large due to variation between donors related to age, genetic factors, and nutritional status. For biological assays a P-value < 0.05 was used. The only statistical significant difference, when comparing metals at 1 mM, was found between Mn and Hg (Table 5.5).

Table 5.5: TBARS ASSAY: Dunn's multiple comparisons test between single metals at 1 mM.

		P Value			P Value
Cd vs.	**Co**	> 0.9999	**Cr vs.**	**Mn**	> 0.9999
	Cr	> 0.9999		**Ni**	> 0.9999
	Cu	> 0.9999		**Pb**	> 0.9999
	Mn	> 0.9999		**Hg**	> 0.9999
	Ni	> 0.9999	**Cu vs.**	**Mn**	0.0568
	Pb	> 0.9999		**Ni**	> 0.9999
	Hg	> 0.9999		**Pb**	0.7944
Co vs.	**Cr**	> 0.9999		**Hg**	> 0.9999
	Cu	> 0.9999	**Mn vs.**	**Ni**	> 0.9999
	Mn	> 0.9999		**Pb**	> 0.9999
	Ni	> 0.9999		**Hg**	0.0279*
	Pb	> 0.9999	**Ni vs.**	**Pb**	> 0.9999
	Hg	> 0.9999		**Hg**	0.5334
Cr vs.	**Cu**	> 0.9999	**Pb vs.**	**Hg**	0.3844

P-Value < 0.05 indicates significant difference.
Key: * – significant difference

The measurement of MDA after exposure to Hg, Cu, Co, Cd, Ni, and Pb correlates with studies done by Hijova *et al* (2005), Hwang *et al.* (1998), Garoui *et al.* (2012), Ogunrinola (2015), Chen *et al.* (2003) and He *et al.* (2013), Adonaylo & Oteiza (1999) and Kasperczyk *et al.* (2014). Flora *et al*. (2013) also found that Pb increased the TBARS levels in mice exposed to Pb in their drinking water. After exposure of rats to Cu, Roy *et al.* (2009) found an increase in TBARS

levels in the rats' liver tissue. Aflanie *et al*. (2015) exposed blood to increasing concentrations of Cd and Hg and found an increase in the MDA levels parallel to an increase in concentration and time. Huang *et al.* (2011) found that exposure to Mn caused a significant increase in MDA levels using the TBARS assay. Many of these studies involve animal studies where absorption, metabolism, excretion, as well as the metal half-life determine the serum levels of the specific metals. This may account for the differences observed between these studies and this *ex vivo* erythrocyte study.

Table 5.6: Single metals that caused lipid peroxidation and ROS formation.

	Cd	Co	Cr	Cu	Mn	Ni	Pb	Hg
Lipid peroxidation	√	√	√	√	√	√	√	√
ROS formation	√	√	√	√	√	√	X	√

Key: √ - does take part in reaction

In Table 5.6 the single metals that cause both lipid peroxidation as well as ROS formation were identified as Cd, Co, Cr, Cu, Mn, Ni, and Hg. Pb caused lipid peroxidation but no ROS formation when measured using the DCFH-DA assay.

5.4.2.1 Metal combinations that caused more than 10 nm malondialdehyde to form

From the ninety-two metals / metal combinations evaluated, twenty-six combinations were found to cause the formation of more than 10 nM MDA, as shown in Figure 5.7. Only two double metal combinations were found within this group, these were Cd:Ni and Ni:Hg.

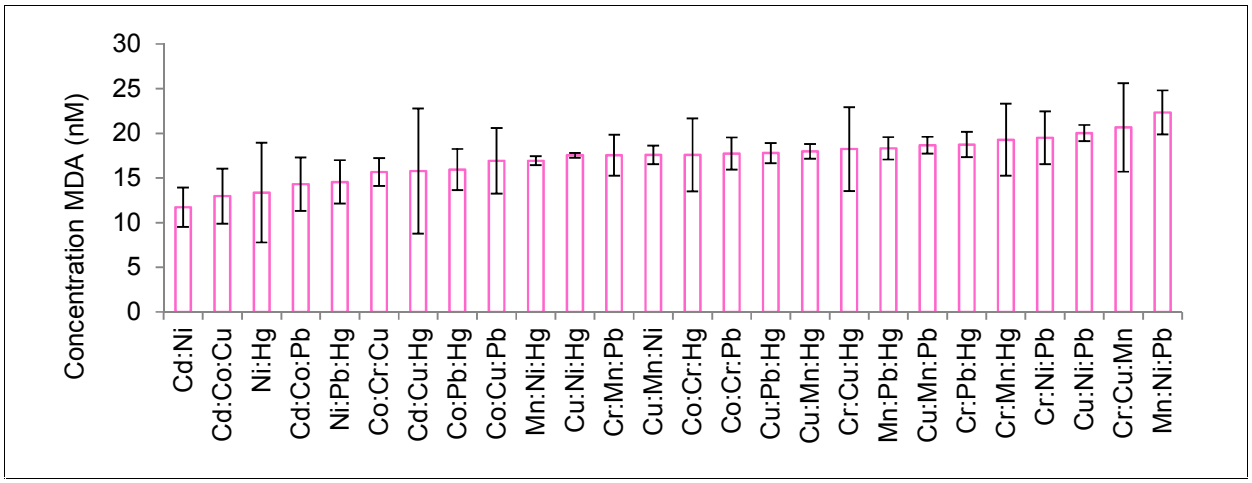

Figure 5.7: Metal combinations with more than 10 nM MDA measured in the supernatant after erythrocyte exposure, with Cu and Hg at a final concentration of 0.05 mM and Cd, Co, Cr, Mn, Ni, and Pb at 1 mM. MDA concetration shown from least to most MDA measured; data is an average of at least 3 independent experiments expressed as the mean ± SEM.

Some significant differences were seen between the metal combinations and the MDA measured after exposure to only a single metal, as indicated in Table 5.7. Cu:Mn:Ni, Cu:Mn:Hg, Mn:Pb:Hg, Cr:Pb:Hg Cu:Ni:Pb, Cr:Cu:Mn, and Mn:Ni:Pb differ significantly from the MDA formed by two of the single metal components they are made up of. However, only Cu:Mn:Pb differs significantly from the effect of all three its single metal components.

Table 5.7: TBARS ASSAY: Metal combinations for which significant differences were observed between single metals vs. double- and triple metal combinations that caused > 10 nm MDA to form (Figure 5.7) (non-significant differences not included).

		P Value			P Value
Cu vs.	**Cr:Cu:Mn‡**	0.0175	**Mn vs.**	**Cu:Mn:Pb‡**	0.0166
	Cr:Cu:Ni‡	0.0372		**Cu:Mn:Hg‡**	0.0281
	Cu:Mn:Ni‡	0.0205		**Mn:Ni:Pb‡**	*0.0047*
	Cu:Mn:Pb‡	*0.0093*		**Mn:Pb:Hg‡**	0.0257
	Cu:Mn:Hg‡	0.0142	**Pb vs.**	**Co:Cr:Pb**	0.0363
	Cu:Ni:Pb‡	*0.0024*		**Cr:Ni:Pb‡**	0.0362
	Cu:Ni:Hg‡	0.0266		**Cr:Pb:Hg‡**	0.0316
	Cu:Pb:Hg‡	0.0201		**Cu:Mn:Pb‡**	0.0293
Mn vs.	**Cr:Cu:Mn‡**	0.0272		**Cu:Ni:Pb‡**	*0.0098*
	Cr:Mn:Hg‡	0.0408		**Mn:Pb:Hg‡**	0.0355
	Cu:Mn:Ni‡	0.0367	**Hg vs.**	**Cr:Pb:Hg‡**	0.0483

P-value < 0.05 indicates significant difference; Italic: P-value < 0.01.
Key: ‡ – synergistic interaction

Quite a few of the triple metal combinations showed a significant difference from the double metal combinations contained in them. Co:Cr:Cu, Co:Cr:Hg, Cu:Mn:Hg, and Cr:Mn:Hg differed significantly from only one double metal combination as can be seen in Table 5.8. Co:Cu:Pb, Co:Cr:Pb, Mn:Pb:Hg, Cu:Mn:Pb, Cr:Pb:Hg, Cr:Ni:Pb, and Cr:Cu:Mn differs significantly from two double metal combinations. Only Cu:Ni:Pb and Mn:Ni:Pb differs significantly from all three double metal combinations contained in them. Mn:Ni:Pb is also the combination causing the formation of the most MDA.

Table 5.8: TBARS ASSAY: Metal combinations for which significant differences were observed between double- vs. triple metal combinations that caused > 10 nm MDA to form (Figure 5.7) (non-significant differences not included).

		P Value			P Value
			Cu:Ni vs.	**Cu:Ni:Pb‡**	*0.0046*
Co:Cr vs.	**Co:Cr:Pb**	*0.0094*	**Cu:Pb vs.**	**Cu:Mn:Pb‡**	0.0254
	Co:Cr:Hg	0.0235		**Cu:Ni:Pb‡**	*0.0033*
Co:Cu vs.	**Co:Cr:Cu**	0.0105	**Cu:Hg vs.**	**Cu:Mn:Hg‡**	0.0249
	Co:Cu:Pb‡	0.0174	**Mn:Ni vs.**	**Mn:Ni:Pb‡**	*0.0076*
Co:Pb vs.	**Co:Cr:Pb**	0.0194	**Mn:Pb vs.**	**Cu:Mn:Pb‡**	0.0370
	Co:Cu:Pb‡	0.0449		**Mn:Ni:Pb‡**	*0.0031*
Cr:Cu vs.	**Cr:Cu:Mn‡**	0.0195		**Mn:Pb:Hg‡**	0.0483
	Cr:Cu:Ni‡	0.0407	**Ni:Pb vs.**	**Cu:Ni:Pb‡**	0.0275
Cr:Mn vs.	**Cr:Cu:Mn‡**	0.0313		**Mn:Ni:Pb‡**	*0.0089*
	Cr:Mn:Hg‡	0.0407	**Pb:Hg vs.**	**Cr:Pb:Hg‡**	0.0344
Cr:Ni vs.	**Cr:Ni:Pb‡**	0.0126		**Mn:Pb:Hg‡**	0.0390
Cr:Pb vs.	**Cr:Ni:Pb‡**	0.0450			
	Cr:Pb:Hg‡	0.0423			

P-value < 0.05 indicates significant difference; Italic: P-value < 0.01.
Key: ‡ – synergistic interaction

5.4.2.2 Synergistic, antagonistic, and additive effects of metals

Of the twenty-eight evaluated double metal combinations, four showed synergistic interactions and five antagonistic interactions. Cu:Mn shows the strongest synergism, with a ratio of more than 4, and Cd:Cr the strongest antagonism, with a ratio of 0.259.

Two of the triple metal combinations showed an antagonistic interaction, but nineteen showed synergistic interactions. The latter were Cd:Cu:Hg, Co:Cu:Pb, Cr:Cu:Ni, Cr:Cu:Mn, Cr:Cu:Hg, Cr:Ni:Pb, Cr:Mn:Pb, Cr:Mn:Hg, Cr:Pb:Hg, Cu:Ni:Mn, Cu:Ni:Pb, Cu:Ni:Hg, Cu:Mn:Pb, Cu:Mn:Hg, Cu:Pb:Hg, Ni:Mn:Pb, Ni:Mn:Hg, Ni:Pb:Hg, and Mn:Pb:Hg. The four combinations with the highest ratios were Cu:Mn:Pb (MDR = 4.990), Cu:Mn:Hg (MDR = 4.476), Ni:Mn:Pb (MDR = 4.426), and Cu:Ni:Mn (MDR = 4.376). Common to these four combinations is the presence of Mn.

Table 5.9: TBARS ASSAY: Synergistic, antagonistic and additive effect of mixtures of metals, calculated using the MDR.

	Co	Cr	Cu*	Ni	Mn	Pb	Hg*	Co	Cr	Cu	Ni	Mn	Pb	Hg
Cd	0.794	0.259	1.023	2.120	1.110	0.607	0.306	Add	Ant	Add	Syn	Add	Add	Ant
Co	-	0.424	0.749	0.967	1.084	0.937	0.922	-	Ant	Add	Add	Add	Add	Add
Cr	-	-	0.572	0.413	1.110	0.337	0.699			Add	Ant	Add	Ant	Add
Cu	-	-	-	0.585	4.103	0.804	0.731	-		-	Add	Syn	Add	Add
Ni	-	-	-	-	2.411	1.301	2.898	-		-	-	Syn	Add	Syn
Mn	-	-	-	-	-	0.689	0.733	-		-	-	-	Add	Add
Pb	-	-	-	-	-	-	1.318	-		-	-	-	-	Add
Cd:Co	-	0.758	1.573	0.415	0.884	1.534	0.853	-	Add	Add	Ant	Add	Add	Add
Cd:Cr	-	-	0.941	0.842	0.924	0.402	0.634			Add	Add	Add	Ant	Add
Cd:Cu	-	-	-	0.778	1.475	1.010	2.412	-		-	Add	Add	Add	Syn
Cd:Ni	-	-	-	-	0.853	1.744	0.963	-		-	-	Add	Add	Add
Cd:Mn	-	-	-	-	-	1.105	1.065	-		-	-	-	Add	Add
Cd:Pb	-	-	-	-	-	-	1.658	-		-	-	-	-	Add
Co:Cr	-	-	1.640	1.332	1.466	1.676	1.620			Add	Add	Add	Add	Add
Co:Cu	-	-	-	1.372	1.963	2.385	1.551	-		-	Add	Add	Syn	Add
Co:Ni	-	-	-	-	1.776	1.285	1.466	-		-	-	Add	Add	Add
Co:Mn	-	-	-	-	-	1.818	1.947	-		-	-	-	Add	Add
Co:Pb	-	-	-	-	-	-	1.900	-		-	-	-	-	Add
Cr:Cu	-	-	-	2.241	3.098	1.932	2.339				Syn	Syn	Add	Syn
Cr:Ni	-	-	-	-	1.881	2.211	1.746					Add	Syn	Add
Cr:Mn	-	-	-	-	-	2.428	2.565						Syn	Syn
Cr:Pb	-	-	-	-	-	-	2.125							Syn
Cu:Ni	-	-	-	-	4.376	3.755	3.126	-		-	-	Syn	Syn	Syn
Cu:Mn	-	-	-	-	-	4.990	4.476	-		-	-	-	Syn	Syn
Cu:Pb	-	-	-	-	-	-	3.336	-		-	-	-	-	Syn
Ni:Mn	-	-	-	-	-	4.428	3.18	-		-	-	-	Syn	Syn
Ni:Pb	-	-	-	-	-	-	2.195	-		-	-	-	-	Syn
Mn:Pb	-	-	-	-	-	-	3.630	-		-	-	-	-	Syn

* - Cu and Hg at 0.05 mM, all other metals at 1 mM
Key: ■ – antagonistic interaction; ■ – synergistic interaction

Antagonistic effects were observed for Cr:Cd, Cr:Co, Cr:Ni, Cr:Pb and Cd:Hg with Cr being the most common metal found in these double metal combinations. Two antagonistic effects was observed for the triple metal combinations and these were for Cd:Co:Ni and Cd:Cr:Pb. Common to both combinations were Cd.

5.5 Conclusion

After exposure of erythrocytes to metals and metal combinations it was found that Cu:Ni:Pb, Cr:Cu:Mn, and Mn:Ni:Pb caused the highest levels of MDA formation. The highest synergism for the double metal combinations were found for Cu:Mn and for the triple metal combinations, Cu:Mn:Pb. Cd:Cr:Pb and Cd:Cr had the greatest antagonistic interaction for double and triple metal combinations respectively.

Using the DCFH-DA assay Cu:Mn:Ni, Cu:Mn:Pb, and Cu:Mn:Hg were shown to cause the most ROS formation in all evaluated samples. The highest synergistic effects were found for Cu:Ni and Cu:Mn, for the double metal combinations. For the triple metal combinations Ni:Mn:Hg had the greatest synergistic interaction. Co:Cr:Ni had the greatest antagonistic effect with regards to ROS formation.

Of the evaluated samples Cd:Cu:Hg, Mn:Ni:Hg, Cu:Ni:Hg, Cu:Mn:Ni, Cu:Mn:Hg, and Cu:Mn:Pb had a gradient of more than 4000 in the DCFH-DA assay and caused the formation of more than 10 nM MDA.

Chapter 6: Concluding discussion

6.1 Summary of main findings

Five assays were done to assess the toxicity as well as the oxidative effect of the ninety-two evaluated metals / metal combinations.

6.1.1 Single metals

Hg was the most toxic in the haemolysis assay. Of the metals evaluated Hg and Cu strongly bound GSH. Both metals also effectively catalysed the Fenton reaction. These effects translated to increased ROS- and MDA formation (Table 6.1).

Table 6.1: Single metals that caused lipid peroxidation and oxidative stress, as percentages of the effect of the metal with the highest measured level in each assay.

	Cd	Co	Cr	Cu	Hg	Mn	Ni	Pb
Haemolysis assay	0.21	0.43	-	0.43	**100**	0.22	0.15	0.39
Fenton reaction	4.57	18.7	6.9	**100**	24.7	6.61	2.28	1.48
ROS formation	0.6	0.38	0.39	**100**	18.3	2.5	0.72	-0.004
Lipid peroxidation	7.2	8.8	9.8	34	**100**	1.5	5.0	4.4

6.1.2 Double metal combinations

6.1.2.1 Combination effects

Using the haemolysis assay, for double metal combinations interactions were synergistic for Co:Cu, Cd:Ni, Co:Mn, and antagonistic for Ni:Pb. The metal combination with the highest MDR was Co:Mn (Table 6.2).

For GSH depletion/binding all double metal interactions were additive.

For hydroxyl radical formation no synergism was found while antagonistic interactions were found for Cd:Cu, Cd:Pb, Cd:Hg, Cu:Hg, and Cr:Ni. The lowest MDR was for Cd:Cu. Measurement of ROS formation (DCFH-DA assay) for double metal combinations revealed synergism for Cu:Ni and Cu:Mn. Many metal combinations resulted in a decrease in ROS formation. Metal combinations with the greatest antagonistic effects were Cr:Cu, Cr:Ni, and Ni:Pb. The largest antagonistic effect was found for Cr:Ni (Table 6.2).

For MDA formation synergism was found for Cd:Ni, Cu:Mn, Ni:Mn, and Ni:Hg with the highest MDR for Cu:Mn. Antagonistic effects were found for the following combinations: Cd:Cr, Co:Cr, Cr:Ni, Cr:Pb and Cd:Hg with Cd:Cr having the lowest MDR (Table 6.2).

Table 6.2: Synergistic and antagonistic effects observed for double metal combinations.

	Synergism		Antagonism	
	Combinations	**Greatest effect**	**Combinations**	**Greatest effect**
Haemolysis assay	Co:Cu, Cd:Ni, Co:Mn	**Co:Mn**	Ni:Pb	**Ni:Pb**
GSH binding	-	-	-	-
Fenton reaction	-	-	Cd:Cu, Cd:Pb, Cd:Hg, Cu:Hg, Cr:Ni	**Cd:Cu**
DCFH-DA, ROS formation	Cu:Ni, Cu:Mn	**Cu:Mn**	Many combinations, Table 5.4	**Cr:Ni**
MDA formation, lipid peroxidation	Cd:Ni, Cu:Mn, Ni:Mn, Ni:Hg	**Cu:Mn**	Cd:Cr, Co:Cr, Cd:Hg, Cr:Ni, Cr:Pb	**Cd:Cr**

Bold: Strongest synergistic or antagonistic effect

6.1.2.1 Combinations with greatest effects

The results for the haemolysis assay showed that Co:Mn and Mn:Ni had the greatest haemolytic effects (Table 6.3). Co:Mn caused the most haemolysis (37.81%), this correlates with the high synergism found for this combination.

The combinations of Pb:Hg, Cu:Pb, and Cd:Pb had the greatest effects with regards to GSH binding (Table 6.3). Pb:Hg was found to have the greatest effect with a 85.61% depletion.

Using the HORAC assay Co:Cu, with a gradient of -4689.74 and Co:Pb, with a gradient of -3855.16, caused the most hydroxyl radical formation (Table 6.3).

For MDA formation Ni:Hg (13.36 nM) and Cd:Ni (11.74 nM) had the greatest lipid peroxidation effect (Table 6.3), both of these combinations were also found to have a synergistic effect.

Table 6.3: Highest levels observed for double metal combinations.

	Combinations	**Greatest effect**
Haemolysis assay	Co:Mn, Mn:Ni, Mn:Pb, Cd:Ni, Pb:Hg	**Co:Mn,** Mn:Ni
GSH binding	Pb:Hg, Cu:Pb, Cd:Pb	**Pb:Hg**

Fenton reaction	Co:Cu, Co:Pb	**Co:Cu**
DCFH-DA, ROS formation	Cu:Mn, Cu:Ni	**Cu:Mn**
MDA formation, lipid peroxidation	Ni:Hg, Cd:Ni	**Ni:Hg**

Bold: Greatest effect

6.1.3 Triple metal combinations

6.1.3.1 Combination effects

The triple metal combination, Cd:Co:Hg, had a synergistic effect on haemolysis (Table 6.4). On haemolysis antagonistic effects were found for Cd:Cu:Ni, Cd:Cu:Mn, Cd:Cu:Pb, Cd:Ni:Mn, Ni:Mn:Pb, and Ni:Pb:Hg (Table 6.4) with the greatest antagonistic effect observed for Cd:Cu:Mn.

The ability of all triple metal combinations to bind GSH was additive.

No synergistic effects were found when triple metals were evaluated as catalysts of the Fenton reaction. Interactions were mostly antagonistic with the greatest effect observed for Cd:Pb:Hg with a ratio of 0.113.

The triple metal combinations, Cu:Ni:Mn, Cu:Ni:Hg, Cu:Mn:Pb, Ni:Mn:Hg, and Ni:Mn:Hg, caused synergism on ROS formation (Table 6.4). The greatest synergistic effect was for Ni:Mn:Hg with a ratio of 2.964. Of the numerous combinations that had an antagonistic effect, the greatest antagonistic effect was found for Co:Cr:Ni with a MDR of -0.036.

Many of the triple metal combinations caused an increase in MDA formation. This was the greatest for the following combinations: Cu:Mn:Pb, Cu:Mn:Hg, Cu:Ni:Mn, and Ni:Mn:Pb with ratios of 4.990, 4.476, 4.376, and 4.428 respectively. Antagonistic effects were found for Cd:Co:Ni and Cd:Cr:Pb, with Cd:Cr:Pb with the lowest ratio of 0.402.

Table 6.4: Synergistic and antagonistic effects observed for triple metal combinations.

	Synergism		Antagonism	
	Combinations	**Greatest effect**	**Combinations**	**Greatest effect**
Haemolysis assay	Cd:Co:Hg	**Cd:Co:Hg**	Cd:Cu:Ni, Cd:Cu:Mn, Cd:Cu:Pb, Cd:Ni:Mn, Ni:Mn:Pb, Ni:Pb:Hg	**Cd:Cu:Mn**

GSH binding	-	-	-	-
Fenton reaction	-	-	Many, Table 4.10.	**Cd:Pb:Hg**
DCFH-DA, ROS formation	Cu:Ni:Mn, Cu:Ni:Hg, Cu:Mn:Pb, Cu:Mn:Hg, Ni:Mn:Hg	**Ni:Mn:Hg**	Many Table 5.4	**Co:Cr:Ni**
MDA formation, lipid peroxidation	Many Table 5.9	**Cu:Mn:Pb,** Cu:Mn:Hg, Ni:Mn:Pb, Ni:Mn:Cu.	Cd:Co:Ni, Cd:Cr:Pb	**Cd:Co:Ni**

Bold: Strongest synergistic or antagonistic effect

6.1.3.1 Combinations with greatest effects

The triple metal combinations which caused the most haemolysis are Cd:Co:Hg, Co:Mn:Hg, Mn:Pb:Hg, Mn:Ni:Hg, and Co:Mn:Pb (Table 6.5). The triple metal combination, Cd:Co:Hg, which had the highest synergistic effect on the haemolysis assay, also caused the most haemolysis, 41.35%.

The combination of Cu:Pb:Hg caused the most depletion of GSH, 98,2%. All other combinations that showed the highest ability to bind to GSH contained Pb and Hg, as seen in Table 6.5.

Regarding hydroxyl radical formation, it was found that the combination of Co:Cr:Cu had the greatest effect. The five triple combinations which caused the most hydroxyl radicals to form contained Co and Cu, known catalysts in the Fenton reaction.

Using the DCFH-DA assay, the highest readings were found for Cu:Mn:Hg, Cu:Mn:Ni, Cu:Mn:Pb, Cu:Ni:Hg, and Mn:Ni:Hg (Table 6.5). Of these five combinations Cu:Mn:Hg caused the most ROS formation, with a gradient of 9613.08.

MDA formation was the highest for the combination Mn:Ni:Pg (22.35 nM) (Table 6.5), this combination also showed a high synergistic interaction (Table 6.4).

Table 6.5: Highest levels observed for triple metal combinations.

	Combinations	Greatest effect
Haemolysis assay	Cd:Co:Hg, Co:Mn:Hg, Mn:Pb:Hg, Mn:Ni:Hg, Co:Mn:Pb	**Cd:Co:Hg**
GSH binding	Cu:Pb:Hg, Cd:Pb:Hg, Mn:Pb:Hg,	**Cu:Pb:Hg**

	Cr:Pb:Hg, Co:Pb:Hg	
Fenton reaction	Co:Cr:Cu, Co:Cu:Pb, Co:Cu:Ni, Co:Cu:Hg, Co:Cu:Mn	**Co:Cr:Cu**
DCFH-DA, ROS formation	Cu:Mn:Hg, Cu:Mn:Ni, Cu:Mn:Pb, Cu:Ni:Hg, Mn:Ni:Hg	**Cu:Mn:Hg**
MDA formation, lipid peroxidation	Mn:Ni:Pb, Cr:Cu:Mn, Cu:Ni:Pb, Cr:Ni:Pb, Cr:Mn:Hg	**Mn:Ni:Pb**

Bold: Greatest effect

6.1.4 Evaluation of Hypotheses

6.1.4.1 Hypothesis 1

From most toxic to least toxic, with regards to the haemolysis assay, the metals are as follow: Hg >> Co > Cu > Pb > Mn > Cd > Ni. With regardsto oxidative damage, the metals can be ordered as follow: Cu >Hg >> Co > Cd > Mn > Ni > Pb.

6.1.4.2 Hypothesis 2

In all assays the predominant type of interaction was additive, while only additive interactions were found for GSH depletion. In the other assays, synergistic, additive, as well as antagonistic interactions were observed.

6.1.4.3 Hypothesis 3

Triple metal combinations had synergistic, additive as well as antagonistic interactions in all assays, except for the GSH depletion assay. Only additive interactions were found for GSH depletion. The predominant type of interaction was additive in all assays.

6.2 Limitations of the investigation

Biological systems have a high degree of variability and in this study the big standard error of means seen in the biological assays are indicative of this.

The chosen non-parametric statistical test, Dunn's multiple comparisons test, did not highlight seemingly obvious differences in data.

The *ex vivo* haemolysis assay is a useful screening method, but not a sensitive method. Due to this lack of sensitivity high concentrations of the metals, that is not physiological relevant, had to be used.

The GSH depletion- and the HORAC assay are chemical assays. These assays only give an indication of the type of effect that can be expected. These experiments do not take into account biological bioavailability and the role of absorption, distribution, metabolism, and excretion (ADME). In addition different types of tissue show variable sensitivity to metals and metal combinations. Erythrocytes, as used in this study, are only one type of differentiated cell.

6.3 Future perspectives

This study identified synergistic combinations as well as combinations showing the highest effect value, using five different assays. Future studies should focus on these combinations found, using physiological relevant concentrations in a biological system, e.g. in animal studies. Animal studies, using a homogenous animal population, will reduce the high degree of variation usually found when using human material.

Transmission electron microscopy and electron energy loss spectroscopy (Andosch *et al.* 2015) can be used to determine the target organs of the metal combinations as well as the accumulation sites of the metals in cells.

Assays measuring specific radicals formed should be used to evaluate the mechanism of the combinations more closely. GSH depletion should also be measured in a more stable biological sample, for example, the plasma of rats exposed to heavy metal combinations.

In areas with different mining and anthropogenic activities exposure to metal combinations specific to that area is found. Future studies should include the evaluation of the effects of area-specific metal combinations. These studies should include the clinical investigation of blood- and urine samples of people living in these areas. These studies should include vulnerable populations such as children, pregnant woman, and the elderly. Malnutrition also affects ADME and this may have a further adverse effect on the health of these individuals.

6.4 Conclusion

South Africa is a highly industrialised country with mining activity and energy generation from coal forming part of the economy of the country. Metal pollution thus inevitably occurs. Human exposure is however rather to metal combinations and not limited to singular metals. Synergistic metal combinations have been identified in this study. Future research is needed to determine the reaction mechanisms of these combinations to enable the formulation of appropriate preventative and safety measures.

Chapter 7: References

Aaseth J, Skaug V, Alexander J. 1984. Haemolytic activity of copper as influenced by chelating agents, albumin and chromium. Acta Pharmacologica et Toxicology. 54: 304-310.

Abdin H, Ashizawa A, Stevens Y, Llados F, Diamond G, Sage G, Citra M, Quinones A, Bosch SJ, Swarts SG. 2007. Toxicological profile for lead. U.S. Department Of Health And Human Services, Public Health Service Agency for Toxic Substances and Disease Registry.

Adonaylo VN & Oteiza PI. 1999. Lead intoxication: Antioxidant defences and oxidative damage in rat brain. Toxicology 135: 77-85.

Aflanie I, Muhyi R, Suhartono E. 2015. Effect of heavy metal on malondialdehyde and advanced oxidation protein produtcs concentration: A focus on arsenic, cadmium, and mercury. Journal of Medical and Bioengineering 4(4): 332-337.

Agrawal S, Bhatnagar P, Flora SJS. 2015. Changes in tissue oxidative stress, brain biogenic amines and acetylcholinesterase following co-exposure to lead, arsenic and mercury in rats. Food and Chemical Toxicology doi: 10.1016/j.fct.2015.10.013.

Ahamed M & Siddiqui MKJ. 2007. Low level lead exposure and oxidative stress: Current opinions. Clinica Chimica Acta 383: 57-64.

Al-Attar AM. 2011. Antioxidant effect of vitamin E treatment on some heavy metals-induced renal and testicular injuries in male mice. Saudi Journal of Biological Sciences 18: 63-72.

Al-Fartosy AJM, Awad NA, Shanan SK. 2014. Biochemical correlation between some heavy metals, malondialdehyde and total antioxidant capacity in blood of gasoline station workers. International Research Journal of Environment Sciences 3(9): 56-60.

Alves EN, Presgrave Rde F, Presgrave OA, Sabagh FP, de Freitas JC, Corrado AP. *2008.* A reassessment of the *in vitro* RBC haemolysis assay with defibrinated sheep blood for the determination of the ocular irritation potential of cosmetic products comparison with the *in vivo* Draize rabbit test. Alternatives to Laboratory Animals 36(3): 275-84.

Andosch A, Höftberger M, Lütz C, Lütz-Meindl U. 2015. Subcellular sequestration and impact of heavy metals on the ultrastructure and physiology of the multicellular freshwater alga *Desmidium swartzii.* International Journal of Molecular Sciences 16: 10389-10410.

Awofolu OR, Mbolekwa Z, Mtshemla V, Fatoki OS. 2005. Levels of trace metals in water and sediment from Tyume River and its effects on an irrigated farmland. Water SA 31(1): 87-94.

Baranowska-Bosiacka I & Hlynczak AJ. 2003. The effect of lead ions on the energy metabolism of human erythrocytes *in vitro*. Comparative Biochemistry and Physiology Part C 134: 403-416.

Barrett KE, Barman SM, Boitano S, Brooks H. 2010. Blood as a circulatory fluid and the dynamics of blood and lymph flow In: Barrett KE, Barman SM, Boitano S, Brooks H eds. Ganong's Review of Medical Physiology. Ch 32. McGraw Hill, USA.

Belden J, Gilliom R, Lydy M. 2007. How well can we predict the toxicity of pesticide mixtures to aquatic life? Integrated Environmental Assessment And Management, 3(3): 364-372.

Benedet JA & Shibamoto T. 2008. Role of transition metals, Fe(II), Cr(II), Pb(II) and Cd(II) in lipid peroxidation. Food Chemistry 107: 165-168.

Bertin G & Averbeck D. 2006. Cadmium, cellular effects, modifications of biomolecules, modulation of DNA repair and genotoxic consequences (a review). Biochimie 88: 1549-1559.

Bertinato J, Sherrard L, Plouffe LJ. 2010. Decreased erythrocyte CCS content is a biomarker of copper overload in rats. International Journal of Molecular Sciences 11: 2624-2635.

Blasa M, Angelino D, Gennari L, Ninfali P. 2011. The cellular antioxidant activity in red blood cells (CAA-RBC): A new approach to bioavailability and synergy of phytochemicals and botanical extracts. Food Chemistry 125: 685-691.

Boggs SE, McCormick TS, Lapetina EG. 1998. Glutathione levels determine apoptosis in macrophages. Biochemical and Biophysical Research Communications 247: 229-233.

Botham KM & Mayes PA. 2009. Lipids of physiologic significance In: Weitz M, Davis KJ eds. Harper's Illustrated Biochemistry. Ch15. McGraw-Hill Medical, New York.

Brandão R, Borges LP, de Oliveira R, Rocha JBT, Nogueira. 2008. Diphenyl diselenide protects against hemotological and immunological alterations induced by mercury in mice. Journal of Biochemical and Molecular Toxicology 22(5): 311-319.

Brandão R, Lara FS, Pagliosa LB, Soares FA, Rocha JBT, Noguelra CW, Farina M. 2005. Hemolytic effects of sodium selenite and mercuric chloride in human blood. Drug and Chemical Toxicology 28: 397–407.

Bull BS & Herrmann PC. 2010. Morphology of the erythron In: Lichtman MA, Kipps TJ, Seligsohn U, Kaushansky K, Prchal JT eds. Williams Hematology. Ch 29. McGraw Hill, USA.

Burger D. 2010/11. Mineral resources In: D Burger, editor. South Africa Yearbook 2010/11. 366-377.

Cai J, Chen Y, Seth S, Furukawa S, Compans RW, Jones DP. 2003. Inhibition of influenza infection by glutathione. Free Radical Biology & Medicine 34(7):928-936.

Catelas I, Petit A, Vali H, Fragiskatos C, Al Meilleur R, Zukor DJ, Antoniou J, Huk OL. 2005. Quantitative analysis of macrophage apoptosis vs. necrosis induced by cobalt and chromium ions *in vitro*. Biomaterials 26: 2441-2453.

Cedergreen N. 2014. Quantifying Synergy: A systematic review of mixture toxicity studies within environmental toxicology. PLoS ONE 9(5): e96580. doi:10.1371/journal.pone.0096580

Cereser C, Guichard J, Drai J, Bannier E, Garcia I, Boget S, Parvaz P, Revol A. 2001. Quantitaion of reduced and total glutathione at the femtomole level by high-performance liquid chromatography with fluorescence detection: application to red blood cells and cultured fibroblasts. Journal of Chromatography B 752: 123-132.

Chen C, Wang YF, Huang W, Huang Y. 2003. Nickel induces oxidative stress and genotoxicity in human lymphocytes. Toxicology and Applied Pharmacology 189: 153-159.

Chen H, Yu M, Li M, Zhao R, Zhu O, Zhou W, Lu M, Lu Y, Zheng T, Jiang J, Zhao W, Xiang K, Jia W, Liu L. 2011. Polymorphic variations in manganese superoxide dismutase (MnSOD), glutathione peroxidase-1 (GPX1), and catalase (CAT) contribute to elevated plasma triglyceride levels in Chinese patients with type 2 diabetes or diabetic cardiovascular disease. Molecular and Cellular Biochemistry. DOI 10.1007/s11010-011-1160-3.

Chtourou Y, Fetoui H, Sefi M, Trabelsi K, Barkallah M, Boudawara T, Kallel H, Zeghal N. 2010. Silymarin, a natural antioxidant, protects cerebral cortex against manganese-induced neurotoxicity in adult rats. Biometals 23: 985-996.

Číž M, Čížová H, Denev P, Kratchanova M, Slavov A, Lojek A. 2010. Different methods for control and comparison of the antioxidant properties of vegetables. Food Control 21: 518–523.

Coetzee H (compiler). 2004. An assessment of sources, pathways, mechanisms and risks of current and potential future pollution of water and sediment in gold-mining areas of the Wonderfonteinspruit catchment. WRC Report No 1214/1/06, Pretoria: 266.

Cohen G & Hochstein P. 1964. Generation of hydrogen peroxide in erythrocytes by hemolytic agents. Biochemistry 3(7): 895-900.

Cole TB, Li WF, Richter RJ, Furlong CE, Costa LG. 2002. Inhibition of paraoxonase (PON1) by heavy metals. Toxicological Sciences 66(1S): 312.

Dalle-Donne I, Rossi R, Colombo R, Giustarini D, Milzani A. 2006. Biomarkers of oxidative damage in human disease. Clinical Chemistry 52(4): 601-623.

Das KK, Das SN & Dhundasi SA. 2008. Nickel, its adverse health effects & oxidative stress. Indian Journal of Medical Research 128: 412-425.

Das KK, Gupta AD, Dhundasi SA, Patil AM, Das SN, Ambekar JG. 2007. Protective role of L-ascorbic acid on antioxidant defense system in erythrocytes of albino rats exposed to nickel sulfate. Biometals 20: 177-184.

Diakonova M, Bokoch G, Swanson JA. 2002. Dynamics of cytoskeletal proteins during Fcγ receptor-mediated phagocytosis in macrophages. Molecular Biology of the Cell 13: 402-411.

Dorsey A, Ingerman L, Swarts S. 2004. Toxicological profile for copper. U.S. Department of Health and Human Services, Public Health Service Agency for Toxic Substances and Disease Registry.

Du Preez M. 2010. Water quality and human health In: Oelofse S, Strydom W eds. A CSIR perspective on water in South Africa: 16.

Dubost NJ, Ou B, Beelman RB. 2007. Quantification of polyphenols and ergothioneine in cultivated mushrooms and correlation to total antioxidant capacity. Food Chemistry 105: 727-735.

Eisele K, Lang PA, Kempe DS, Klarl BA, Niemöller O, Wieder T, Huber SM, Duranton C, Lang F. 2006. Stimulation of erythrocyte phosphatidylserine exposure by mercury ions. Toxicology and Applied Pharmacology 210: 116-122.

Eruslanov E & Kusmartsev S. 2010. Identification of ROS using oxidized DCFDA and flow-cytometry. Methods in Molecular Biology 594: 57-72.

Evans BC, Nelson CE, Yu SS, Beavers KR, Kim AJ, Li H, Nelson HM, Giorgio TD, Duvall CL. 2013. Ex vivo red blood cell hemolysis assay for the evaluation of ph-responsive endosomolytic agents for cytosolic delivery of biomacromolecular drugs. Journal of Visualized Experiments 73(50166): 1-5.

Faroon OM, Abadin H, Keith S, Osier M, Chappell LL, Diamond G, Sage G. 2004. Toxicological profile for cobalt. U.S. Department Of Health And Human Services, Public Health Service Agency for Toxic Substances and Disease Registry: 17-86.

Faroon O, Ashizawa A, Wright S, Tucker P, Jenkins K, Ingerman L, Rudisill C. 2008. Draft toxicological profile for cadmium. U.S. Department Of Health And Human Services, Public Health Service Agency for Toxic Substances and Disease Registry: 11-173.

Fasseas MK, Mountzouris KC, Tarantilis PA, Polissiou M, Zervas G. 2008. Antioxidant activity in meat treated with oregano and sage essential oils. Food Chemistry 106(3): 1188-1194.

Fay M, Wilbur S, Abadin H, Ingerman L, Swarts SG. 2005. Toxicological profile for nickel. U.S. Department Of Health And Human Services, Public Health Service Agency for Toxic Substances and Disease Registry: 11-130.

Fawell J, Cotruvo J, Fawell JK, Giddings M, Jackson P, Magara Y, Festo Ngowi AV, Ohanian E. 2011. Cadmium in drinking-water. WHO/SDE/WSH/03.04/80/Rev/1: 6.

Flora G, Gupta D, Tiwari. 2013. Preventive efficacy of bulk and nanocurcumin against lead-induced oxidative stress in mice. Biological Trace Element Research 152: 31‑40.

Föller M. 2008. The regulation of erythrocyte survival and suicidal cell death. PhD thesis, Eberhard-Karls-Universität, Tübingen.

Gaetani GF, Ferraris AM, Rolfo M, Mangerini R, Arena S, Kirkman HN. 1996. Prodiminant role of catalase in the disposal of hydrogen peroxide within human erythrocytes. Blood 87: 1595-1599.

Gallagher PG. 2010. The red blood cell membrane and its disorders: Hereditary spherocytosis, elliptocytosis, and related diseases In: Lichtman MA, Kipps TJ, Seligsohn U, Kaushansky K, Prchal JT eds. Williams Hematology. Ch 45. McGraw Hill, USA.

Garoui EM, Fetoui H, Makni FA, Boudawara T, Zeghal N. 2011. Cobalt chloride induces hepatotoxicity in adult rats and their suckling pups. Experimental and Toxicologic Pathology 63: 9–15.

Garoui EM, Troudi A, Fetoui H, Soudani N, Boudawara T, Zeghal N. 2012. Propolis attenuates cobalt induced-nephrotoxicity in adult rats and their progeny. Experimental and Toxicologic Pathology 64: 837-846.

Girotti S, Fini F, Ferri E, Budini R, Piazzi S, Cantagalli D. 2000. Determination of superoxide dismutase in erythrocytes by a chemiluminescent assay. Talanta 51: 685-692.

Gruenberg J, Allred DR, Sherman IW. 1983. Scanning electron microscope-analysis of the protrusions (knobs) present on the surface of *Plasmodium falciparum*-infected erythrocytes. The Journal of Cell Biology 97: 795-802.

Guemouri L, Artur Y, Herbeth B, Jeandel C, Cuny G, Siest G. 1991. Biological variability of superoxide dismutase, glutathione peroxidase and catalase in blood. Clinical Chemistry 37(11): 1932-1937.

Gzik A, Keuhling M, Schneider I, Tschochner B. 2003. Heavy metal contamination of soils in a mining area in south africa and its impact on some biotic systems. Journal of Soils & Sediments 3 (1): 29-34.

Hall GW. 2007. Understanding haemolytic anaemia. Paediatrics and child health 17(8): 333-339.

Hamilton DL, Bellamy JEC, Valberg JD, Valberg LS. 1978. Zinc, cadmium and iron interactions during intestinal absorption in iron-deficient mice. Canadian Journal of Physiology and Pharmacology 56(3): 384-389.

Han SG, Castranova V, Vallyathan V. 2007. Comparative cytotoxicity of cadmium and mercury in a human bronchial epithelial cell line (BEAS-2B) and its role in oxidative stress and induction of heat shock protein 70. Journal of Toxicology and Environmental Health, Part A, 70: 852–860.

He M, Xu S, Zhang X, Wang Y, Xiong J, Zhang X, Lu Y, Zhang L, Yu Z, Zhou Z. (2013) Disturbance of aerobic metabolism accompanies neurobehavioral changes induced by nickel in mice. NeuroToxicology 38: 9-16.

Heemskerk JWM, Bevers EM, Lindhout T. 2002. Platelet activation and blood coagulation. Journal of Thrombosis and Haemostasis 88: 186-193.

Hematology. Edited by WS Beck. 1998. USA: Asco Trade Typesetting Ltd. p.606.

Hemmateenejad B, Rezaei Z, Zaeri S. 2009. Second-order calibration of excitation-emission matrix fluorescence spectra for determination of glutathione in human plasma. Talanta 79: 648-656.

Herselman JE. 2007. The concentration of selected trace metals in South African soils. PhD thesis, University of Stellenbosch, Stellenbosch.

Higdon J, Drake VJ, Drake VJ. 2010. Manganese. [Online], Available: http://lpi.oregonstate.edu/mic/minerals/manganese [Cited 2 October 2015].

Hijova E, Nistiar F, Sipulova A. 2005. Changes in ascorbic acid and malondialdehyde in rats after exposure to mercury. Bratislavske lekarske listy 106(8-9): 248-251.

Hirata Y. 2002. Manganese-induced apoptosis in PC12 cells. Neurotoxicology and Teratology 24: 639-653.

Hobbs P. 2010. Water and sustainable mining In: Oelofse S, Strydom W eds. A CSIR perspective on water in South Africa. 46-49.

Huang P, Chen C, Wang H, Li G, Jing H, Han Y, Liu N, Xiao Y, Yu Q, Liu Y, Wang P, Shi Z, Sun Z. 2011. Manganese effects in the liver following subacute or subchronic manganese chloride exposure in rats. Ecotoxicology and Environmental Safety 74: 615–622.

Horiguchi H, Oguma E, Nomoto S, Arao Y, Ikeda K, Kayama F. 2004. Acute exposure to cobalt induces transient methemoglobinuria in rats. Toxicology Letters 151: 459–466.

Horiguchi H, Oguma E, Kayama F. 2011. Cadmium induces anemia through interdependent progress of hemolysis, body iron accumulation, and insufficient erythropoietin production in rats. Toxicological Sciences 122(1): 198–210.

Hunaiti AA & Soud M. 2000. Effect of lead concentration on the level of glutathione, glutathione *S*-transferase, reductase and peroxidase in human blood. The Science of the Total Environment 248: 45-50.

Hwang DF, Wang LC, Cheng HM. 1998. Effect of taurine on toxicity of copper in rats. Food and Chemical Toxicology 36: 239-244.

Ilouno LE, Shu EN, Igbokwe GE. 1996. An improved technique for the assay of red blood cell superoxide dismutase (SOD) activity. Clinica Chimica Acta 247: 1-6.

Jadhav SH, Sarkar SN, Aggarwal M, Tripathi HC. 2007. Induction of oxidative stress in erythrocytes of male rates subchronically exposed to a mixture of eight metals found as groundwater contaminants in different parts of India. Archives of Environmental Contamination and Toxicology 52: 145-151.

Janero DR. 1990. Malondialdehyde and thiobarbituric acid reactivity as diagnostic indices of lipid peroxidation and peroxidative tissue injury. Free Radical Biology & Medicine 9: 515-540.

Jasprica I, Mornar A, Debeljak Ž, Smolčić-Bubalo A, Medić-Sarić M, Mayer L, Romić Z, Bućan K, Balog T, Sobočanec S, Šverko V. 2007. *In vivo* study of propolis supplementation effects on antioxidative status on red blood cells. Journal of Ethnopharmacology 110(3): 548-554.

Jay AWL & Rowlands S. 1975. The stages of osmotic haemolysis. The Journal of Physiology 252: 817-832.

Jiang Y, Wong JH, Pi ZF, Ng TB, Wang CR, Hou J, Chen RR, Niu HJ, Liu F. 2009. Stimulatory effect of components of rose flowers on catalytic activity and mRNA expression of superoxide dismutase and catalase in erythrocytes. Environmental Toxicology and Pharmacology 27: 396-401.

Jones DP, Mody VC, Carlson JL, Lynn MJ, Sternberg P. 2002. Redox analysis of human plasma allows separation of pro-oxidant events of aging from decline in antioxidant defenses. Free Radical Biology & Medicine 33(9): 1290-1300.

Jooste A, Marr SM, Addo-Bediako A, Luus-Powell WJ. 2015. Sharptooth catfish shows its metal: A case study of metal contamination at two impoundments in the Olifants River, Limpopo river system, South Africa. Ecotoxicology and Environmental Safety 112: 96–104.

Kalahasthi RB, Rao RHR, Murthy RBK, Kumar MK. 2006. Effect of chromium(VI) on the status of plasma lipid peroxidation and erythrocyte antioxidant enzymes in chromium plating workers. Chemico-Biological Interactions 164: 192-199.

Kalyanaraman B, Darley-Usmar V, Davies KJ, Dennery PA, Forman HJ, Grisham MB, Mann GE, Moore K, Roberts LJ, Ischiropoulos H. 2012. Measuring reactive oxygen and nitrogen

species with fluorescent probes: challenges and limitations. Free Radical Biology & Medicine 52: 1-6.

Kand'ár R, Žáková P, Lotková H, Kučera O, Červinková Z. 2007. Determination of reduced and oxidized glutathione in biological samples using liquid chromatography with fluorimetric detection. Journal of Pharmaceutical and Biomedical Analysis 43: 1382-1387.

Kanter M, Aksu B, Akpolat M, Tarladacalisir YT, Aktas C, Uysal H. 2009. Vitamin E protects against oxidative damage caused by cadmium in the blood of rats. European Journal of General Medicine 6(3): 154-160.

Kasperczyk S, Dobrakowski M, Kasperczyk A, Machnik G, Birkner E. 2014. Effect of N-acetylcysteine administration on the expression and activities of antioxidant enzymes and the malondialdehyde level in the blood of lead-exposed workers. Environemtnal Toxicology and Pharmacology 37: 638-647.

Kattlove HE & Spaet TH. 1970. The effect of chromium on platelet function in vitro. Blood 35: 659-668.

Kazi TG, Arain MB, Jamali MK, Jalbani N, Afridi HI, Sarfraz RA, Baig JA, Shah AQ. 2009. Assessment of water quality of polluted lake using multivariate statistical techniques: A case study. Ecotoxicology and Environmental Safety 72 (2009) 301– 309.

Kennely PJ & Rodwell VW. 2009. Proteins: myoglobin and hemoglobin In: Weitz M, Davis KJ eds. Harper's Illustrated Biochemistry. Ch6. McGraw-Hill Medical, New York.

Kilinç K & Rouhani R. 1992. Cobaltous ion inhibition of lipid peroxidation in biological membranes. Biochimica et Biophysics Acta 1125: 189-195.

Koçak M & Akçil E. 2006. The effects of chronic cadmium toxicity on the hemostatic system. Pathophysiology of Haemostasis and Thrombosis 35: 411-416.

Kondo T, Dale GL, Beutler E. 1980. Glutathione transport by inside-out vesicles from human erythrocytes. Proceedings of the National Academy of Sciences 77(11): 6359-6362.

Korashy HM & El-Kadi AOS. 2008. Modulation of TCDD-mediated induction of cytochrome P450 1A1 by mercury, lead and copper in human HepG2 cell line. Toxicology in Vitro 22: 154-158.

Korashy HM & El-Kadi AOS. 2008. The role of redox-sensitive transcription factors NF-κB and AP-1 in the modulation of the Cyp1a1 gene by mercury, lead, and copper. Free Radical Biology & Medicine 44: 795–806.

Kowalczyk E, Jankowski A, Niedworok J, Śmigielski J, Tyslerowicz P. 2002. Effect of long-term cadmium intoxication on selected biochemical parameters in experimental animals. Polish Journal of Environmental Studies 11(5): 599-601.

Lang KS, Lang PA, Bauer C, Duranton C, Wieder T, Huber SM, Lang F. 2005. Mechanisms of suicidal erythrocyte death. Cellular Physiology and Biochemistry 15: 195-202.

Lantin AC, Mallants A, Vermeulen J, Speybroeck N, Hoet P, Lison D. 2011. Absence of adverse effect on thyroid function and red blood cells in a population of workers exposed to cobalt compounds. Toxicology Letters 201: 42-46.

Lauwerys R & Lison D. 1994. Health risks associated with cobalt exposure – an overview. Science of The Total Environment 150(1-3): 1-6.

Lee SS, Ahn KH, Lee SJ, Sun K, Goedhart PT, Hardeman MR. 2004. Shear induced damage of red blood cells monitored by the decrease of their deformability. Korea-Australia Rheology Journal 16(3): 141-146.

Lessler MA & Walters MI. 1973. Erythrocyte osmotic fragility in the presence of lead or mercury. Procedings of the Society for Experimental Biology and Medicine 142: 548-553.

Ling X, Zhang Y, Lu Y, Huang H. 2011. Superoxide dismutase, catalase and acetylcholinesterase: biomarkers for the joint effect of cadmium, zinc and methyl parathion contamination in water. Environmental Technology 32(13): 1463-1470.

Lucaciu CM, Dragu C, Copăescu L, Morariu VV. 1997. Manganese transport through human erythrocyte membranes. An EPR study. Biochimica et Biophysica Acta 1328: 90-98.

MacDonald-Wicks LK, Wood LG, Garg ML. 2006. Methodology for the determination of biological antioxidant capacity *in vitro:* a review. Journal of the Science of Food and Agriculture 86: 2046-2056.

Mamba BB, Rietveld LC, Verberk JQJC. 2008. SA drinking water standards under the microscope. The water wheel 7(1): 24-27.

Maritim AC, Sanders RA, Watkins JB. 2003. Diabetes, oxidative stress and antioxidants: a review. Journal of Biochemical and Molecular Toxicology 17(1): 24-38.

Mathee A, Singh E, Mogotsi M, Timothy G, Maduka B, Olivier J, Ing D. 2009. Lead-based paint on playground equipment in public children's parks in Johannesburg, Tshwane and Ekurhuleni. South African Medical Journal 99: 819-821.

Monostori P, Wittmann G, Karg E, Túri S. 2009. Determination of glutathione and glutathione disulfide in biological samples: and in-depth review. Journal of Chromatography B 877: 3331-3346.

Murray RK. 2009. Red and white blood cells In: Weitz M, Davis KJ eds. Harper's Illustrated Biochemistry. Ch52. McGraw-Hill Medical, New York.

Naicker K, Cukrowska E, McCarthy TS. 2003. Acid mine drainage arising from gold mining activity in Johannesburg, South Africa and environs. Environmental Pollution 122: 29-40.

Nakayama A, Tawa R, Masuvama N, Ebara M, Fukuda H, Suzuki K, Nakajima K, Sakurai H. 2002. Disorders in blood coagulation in humans occupationally exposed to mercuric vapors. Journal of Trace Elements in Experimental Medicine 15(1): 21-29.

Ndhlala AR, Stafford GI, Finnie JF, Van Staden J. 2011. Commercial herbal preparations in Kwazulu-Natal, South Africa: The urban face of traditional medicine. South African Journal of Botany 77: 830-843.

Needleman H. 2004. Lead poisoning. Annual Review of Medicine 55: 209-222.

Nel J. 2010. Sustainable water ecosystems In: Oelofse S, Strydom W eds. A CSIR perspective on water in South Africa. 26-29.

Nemmiche S, Chabane-Sari D, Kadri M, Guiraud P. 2011. Cadmium chloride-induced oxidative stress and DNA damage in the human Jurkat T cell line is not linked to intracellular trace elements depletion. Toxicology in Vitro 25: 191-198.

Neumann C, Grünert R, Bednarski PJ. 2003. Nicotinamide adenine dinucleotide phosphate-regenerating system coupled to a glutathione-reductase microtiter method for determination of total glutathione concentrations in adherent growing cancer cell lines. Analytical Biochemistry 320: 170-178.

Nordberg GF, Gerhardsson L, Broberg K, Mumtaz M, Ruiz P, Fowler BA. 2007. Interactions in metal toxicology In: Nordberg GF, Fowler BA, Nordberg M, Friberg L eds. Handbook on the toxicology of metals. Ch 7. Elsevier, Burlington, USA.

Nordberg GF, Fowler BA, Nordberg M, Friberg L eds. 2007. Handbook on the toxicology of metals. 3rd ed. Academic Press, USA.

Oberholster P. 2010. The current status of water quality in South Africa In: Oelofse S, Strydom W eds. A CSIR perspective on water in South Africa. 8-13.

Oberholster PJ, Myburgh JG, Ashton PJ, Botha AM. 2010. Responses of phytoplankton upon exposure to a mixture of acid mine drainage and high levels of nutrient pollution in Lake Loskop, South Africa. Ecotoxicology and Environmental Safety 73: 326-335.

Oelofse S. 2010. Industry and water quality In: Oelofse S, Strydom W eds. A CSIR perspective on water in South Africa. 50-52.

Ogunrinola OO. 2015. Lipid profile and malondialdehyde concentrations in cadmium-induced rats: A study with relation to doses. MedCrave Online Journal of Toxicology 1(4): 00022. DOI: 10.15406/mojt.2015.01.00022.

Okonkwo JO & Mothiba M. 2005. Physico-chemical characteristics and pollution levels of heavymetals in the rivers in Thohoyandou, South Africa. Journal of Hydrology 308: 122–127.

O'Neal, S. & Zheng W. 2015. Manganese toxicity upon overexposure: A decade in review. Current Environmental Health Reports 2:315–328.

Oosthuizen MA, John J, Somerset V. 2010. Mercury exposure in a low-income community in South Africa. South African Medical Journal 100: 366-371.

Ou B, Hampsch-Woodill M, Flanagan J, Deemer EK, Prior RL, Huang D. 2002. Novel fluorometric assay for hydroxyl radical prevention capacity using fluorescein as the probe. Journal of Agricultural and Food Chemistry 50: 2772-2777.

Pari L & Amudha K. 2011. Hepatoprotective role of naringin on nickel-induced toxicity in male Wistar rats. European Journal of Pharmacology 650: 364-370.

Parvez S, Venkataraman C, Mukherji S. 2009. Nature and prevalence of non-additive toxic effects in industrially relevant mixtures of organic chemicals. Chemosphere 75: 1429-1439.

Patra RC, Rautray AK, Swarup D. 2011. Oxidative stress in lead and cadmium toxicity and its amelioration. Veterinary Medicine International: 1-9.

Patrick L. 2006. Lead toxicity, a review of the literature. Part I: exposure, evaluation and treatment. Alternative Medicine Review 11(1): 1-22.

Peng H, Chen W, Cheng Y, Hakuna L, Strongin R, Wang B. 2012. Thiol reactive probes and chemosensors. Sensors 12: 159077-15946.

Permenter MG, Lewis JA, Jackson DA. 2011. Exposure to nickel, chromium, or cadmium causes distinct changes in the gene expression patterns of a rat liver derived cell line. PLoS ONE 6(11): e27730.

Quintanar-Escorza MA, González-Martinez MT, Intriago-Ortega Ma del Pilar, Calderón-Salinas JV. 2010. Oxidative damage increases intracellular free calcium [Ca^{2+}] concentration in human erythrocytes incubated with lead. Toxicology in Vitro 24: 1338-1346.

Raffn E, Mikkelsen S, Altman DG, Christensen JM, Groth S. 1988. Health effects due to occupational exposure to cobalt blue dye among plate painters in a porcelain factory in Denmark. Scandinavian Journal of Work, Environment & Health 14(6): 378-384.

Ramzan M, Malik MA, Iqbal Z, Arshad N, Khan SY, Arshads M. 2011. Study of haematological indices in tannery workers exposed to chromium in Sheikhupura (Pakistan). Toxicology and Industrial Health 27(9): 857-864.

Rana SVS. 2008. Metals and apoptosis: Recent developments. Journal of Trace Elements in Medicine and Biology 22: 262-284.

Risher J & DeWoskin R. 1999. Toxicological profile for mercury. U.S. Department Of Health And Human Services, Public Health Service Agency for Toxic Substances and Disease Registry: 29-161.

Roy DN, Mandal S, Sen G, Biswas T. 2009. Superoxide anion mediated mitochondrial dysfunction leads to hepatocyte apoptosis preferentially in the periportal region during copper toxicity in rats. Chemico-Biological Interactions 182: 136–147.

Sakai T. 2000. Review Article: Biomarkers of lead exposure. Industrial Health 38: 127–142.

Sakhi AK, Russnes KM, Smeland S, Blomhoff R, Gundersen TE. 2006. Simultaneous quantification of reduced and oxidized glutathione in plasma using a two-dimensional chromatographic system with parallel porous graphitized carbon columns coupled with fluorescence and coulometric electrochemical detection. Journal of Chromatography A 1104: 179-189.

Salway JG. 2006. Free radicals, reactive oxygen species and oxidative damage In: Noyes V, Sugden M eds. Medical biochemistry at a glance. Ch 19. Blackwell Publishing Ltd, Oxford, UK.

Schäfer M & Werner S. 2008. Oxidative stress in normal and impaired wound repair. Pharmacological Research 58: 165-171.

Ścibior A, Zaporowska H, Wolińska A, Ostrowski J. 2010. Antioxidant enzyme activity and lipid peroxidation in the blood of rats co-treated with vanadium (V^{+5}) and chromium (Cr^{+3}). Cell Biology and Toxicology 26: 509-526.

Shaik IH & Mehvar R. 2006. Rapid determination of reduced and oxidized glutathione levels using a new thiol-masking reagent and the enzymatic recycling method: application to the rat liver and bile samples. Analytical and Bioanalytical Chemistry 385: 105-113.

Shaikh ZA, Vu TT, Zaman K. 1999. Oxidative stress as a mechanism of chronic cadmium-induced hepatotoxicity and renal toxicity and protection by antioxidants. Toxicology and Applied Pharmacology 154: 256-263.

Shea J, Moran T, Dehn PF. 2008. A bioassay for metals utilizing a human cell line. Toxicology in Vitro 22: 1025-1031.

Shin J, Lim K, Noh J, Bae O, Chung S, Lee M, Chung J. 2007. Lead-induced procoagulant activation of erythrocytes through phosphatidylserine exposure may lead to thrombotic diseases. Chemical Research in Toxicology 20: 38-43.

Silverthorn DU. 2007. Blood In: Human Physiology an integrated approach. Ch 16. Benjamin Cummings, San Franscisco.

Simmons SO, Fan C, Yeoman K, Wakefield J, Ramabhadran R. 2011. NRF2 oxidative stress induced by heavy metals is cell type dependent. Current Chemical Genomics 5: 1-12.

Simon HU, Haj-Yehia A, Levi-Schaffer F. 2000. Role of reactive oxygen species (ROS) in apoptosis induction. Apoptosis 5: 415-418.

Simonsen LO, Brown AM, Harbak H, Kristensen BI, Bennekou P. 2011. Cobalt uptake and binding in human red blood cells. Blood Cells, Molecules, and Diseases 46: 266-276.

Singh N & Rajini PS. 2008. Antioxidant-mediated protective effect of potato peel extract in erythrocytes against oxidative damage. Chemico-Biological Interactions 173: 97-104.

Singh R, Gautam N, Mishra A, Gupta R. 2011. Heavy metals and living systems: an overview. Indian Journal of Pharmacology 43(3): 246-253.

Smith AG, Smith AN. 1984. Effect of cobaltous chloride on aggregation of platelets from normal and afibrinogenaemic human blood. Toxicology Letter 23(3): 349-352.

Smyth SS, Whiteheart S, Italiano JE, Coller BS. 2010. Hemostasis and thrombosis In: Lichtman MA, Kipps TJ, Seligsohn U, Kaushansky K, Prchal JT eds. Williams Hematology. Ch 114. McGraw Hill, USA.

Snyder LM, Fortier NL, Trainor J, Jacobs J, Lob L, Lubin B, Chiu D, Shohet S, Mohandas N. 1985. Effect of hydrogen peroxide exposure on normal human erythrocyte deformability, morphology, surface characteristics, and spectrin-hemoglobin cross-linking. Journal of Clinical Investigation 76: 1971-1977.

Son Y, Lee JC, Hitron A, Pan J, Zhang Z, Shi X. 2010. Cadmium induces intracellular Ca^{2+} and H_2O_2-dependent apoptosis through JNK- and p53-mediated pathways in skin epidermal cell line. Toxicological Sciences 113(1): 127-137.

Stacchiotti A, Morandini F, Bettoni F, Schena I, Lavazza A, Grigolato PG, Apostoli P, Rezzani R, Aleo MF. 2009. Stress proteins and oxidative damage in a renal derived cell line exposed to inorganic mercury and lead. Toxicology 264: 215-224.

Stohs SJ & Bagchi D. 1995. Oxidative mechanisms in the toxicity of metal ions. Free Radical Biology & Medicine 18(2): 321-336.

Street RA, Kulkarni MG, Stirk WA, Southway C, Van Staden J. 2008. Variation in heavy metals and microelements in South African medicinal plants obtained from street markets. Food Additives and Contaminants: Part A 25(8): 953-960.

Swennen B, Buchet J, Stanescu D, Lison D, Lauwerys R. 1993. Epidemiological survey of workers exposed to cobalt oxides, cobalt salts and cobalt metal. British Journal of Industrial Medicine 50: 835-842.

Talavera EJ, Arcaya J, Giraldoth D, Suárez J, Bonilla E. 1999. Decrease in spontaneous motor activity and in brain lipid peroxidation in manganese and melatonin treated mice. Neurochemical Research 24(5): 705-708.

Triawanti, Sanyoto DD, Mashuri, Nur'amin H. 2014. The effect of cadmium absorption on ghrelin and malondialdehyde levels in white rats (*Rattusnorvegicus*). International Journal of Bioscience, Biochemistry and Bioinformatics 4(4): 256-260.

Valbonesi P, Ricci L, Franzellitti S, Biondi C, Fabbri E. 2008. Effects of cadmium on MAPK signalling pathways and HSP70 expression in a human trophoblast cell line. Placenta 29: 725-733.

Valko M, Morris H, Cronin MTD. 2005. Metals, toxicity and oxidative stress. Current Medicinal Chemistry 12: 1161-1208.

Van den Dobbelsteen DJ, Nobel CSI, Schlegel J, Cotgreave IA, Orrenius S, Slater AFG. 1996. Rapid and specific efflux of reduced glutathione during apoptosis induced by anti-Fas/APO-1-antibody. The Journal of Biological Chemistry 271(26): 15420-15427.

Van Papendorp DH & Claassen N. 2002. The circulatory system: the blood In: Meyer BJ, Van Papendorp DH, Meij Hs, Viljoen MV eds. Human physiology. Ch 12. Juta, Pretoria, SA.

Vorster CJ. 2002. Simplified geology and active mines South-Africa, Lesotho and Swaziland. Council for Geoscience.

Wang Z, Wang H, Xu ZM, Ji Y, Chen Y, Zhang Z, Zhang C, Meng X, Zhao M, Xu D. 2012. Cadmium-induced teratogenicity: Association with ROS-mediated endoplasmic reticulum stress in placenta. Toxicology and Applied Pharmacology 259: 236–247.

Whitfield JB, Dy V, McQuilty R, Zhu G, Heath AC, Montgomery GW, Martin NG. 2010. Genetic effects on toxic and essential elements in humans: arsenic, cadmium, copper, lead, mercury, selenium and zinc in erythrocytes. Environmental Health Perspectives 118(6): 776-782.

Wilbur S, Abadin W, Fay M, Yu D, Tencza B, Klotzbach J, James S. 2008. Draft toxicological profile for chromium. U.S. Department Of Health And Human Services, Public Health Service Agency for Toxic Substances and Disease Registry.

Williams M, Todd GD, Ronev N, Crawford J, Coles C, McClure PR, Garey JD, Citra M. 2008. Draft toxicological profile for manganese. U.S. Department Of Health And Human Services, Public Health Service Agency for Toxic Substances and Disease Registry.

Xie f, Lampi MA, Dixon G, Greenberg BM. 2007. Assessment of the toxicity of mixtures of nickel or cadmium with 9,10-phenathrenequinone to *Daphnia magna*: Impact of a reactive oxygen-mediated mechanism with different redox-active metals. Environmental Toxicology and Chemistry 26(7): 1425–1432.

Yager TR. 2008. The mineral industry of South Africa. U.S. geological survey minerals yearbook. 37.1-37.22.

Yedjou CG, Milner JN, Howard CB, Tchounwou PB. 2010. Basic apoptotic mechanisms of lead toxicity in human leukemia (H1-60) cells. International Journal of Environmental Research and Public Health 7: 2008-2017.

Yuan G, Dai S, Yin Z, Lu H, Jia R, Xu J, Song X, Li L, Shu Y, Zhao X. 2014. Toxicological assessment of combined lead and cadmium: Acute and sub-chronic toxicity study in rats. Food and Chemical Toxicology 65: 260–268.